

**POLYKETALS: A NEW DRUG DELIVERY PLATFORM FOR  
TREATING ACUTE LIVER FAILURE**

A Dissertation  
Presented to  
The Academic Faculty

by

Stephen Chen Yang

In Partial Fulfillment  
of the Requirements for the Degree  
Doctor of Philosophy in the  
Department of Biomedical Engineering

Georgia Institute of Technology  
December, 2008

**POLYKETALS: A NEW DRUG DELIVERY PLATFORM FOR  
TREATING ACUTE LIVER FAILURE**

Approved by:

Dr. Niren Murthy, Advisor  
Department of Biomedical Engineering  
*Georgia Institute of Technology and  
Emory University*

Dr. Sheldon W. May  
School of Chemistry & Biochemistry  
*Georgia Institute of Technology*

Dr. Ravi Bellamkonda  
Department of Biomedical Engineering  
*Georgia Institute of Technology and  
Emory University*

Dr. Valeria T. Milam  
School of Materials Science and  
Engineering  
*Georgia Institute of Technology*

Dr. Michael E. Davis  
Department of Biomedical Engineering  
*Georgia Institute of Technology and  
Emory University*

Date Approved: October 07, 2008

To my beautiful wife and best friend, Cindy, for her love, caring, and unconditional support

## ACKNOWLEDGEMENTS

I wish to thank my thesis advisor, Dr. Niren Murthy, for giving me the opportunity to pursue my Ph.D. study in his laboratory. Throughout my graduate studies in the field of biomaterials and drug delivery at Georgia Tech, he has provided me with many fresh and insightful ideas, interesting prospective, and constructive criticisms, all of which have benefited me greatly in becoming a scientist with the ability to critically develop, evaluate, and execute new ideas and research plans. Niren has also provided me with opportunities to collaborate with other researchers, with whom I was able to pursue various clinical applications using the materials we developed in our laboratory.

I also wish to thank all members of my research lab, past and present. Dr. Jihua Hao, Dr. Michael Heffernan, A. Rebecca Guinn, Dr. Siraj Khaja, D. Scott Wilson, Dr. Sungmun Lee, Dr. Madhuri Dasari, Dr. Dongwon Lee, Dr. Venkata Reddy Erigala, Dr. Kousik Kundu, Jay Sy, Chen-Yu Kao, Usha Kantheti, Kelly Straub, Ben Solomon, and Sydney Shaffer. Jihua worked diligently to set up the laboratory so that I could start my research; Michael and I spent five years in graduate school working side by side. His support and friendship have made my journey much more pleasant and enjoyable. Dongwon and Sungmun have provided me with much help in my research both the forms of discussions and collaborative research. They have served as my mentors from whom I have learned a great deal about how to become a successful scientist. I am particularly grateful to my undergraduate students whom I mentored: Usha, Kelly, Ben, and Sydney. They gave me an opportunity to develop as a mentor, and at the same time, greatly helped me make progress in my research projects. Usha helped with the synthesis and characterizations of polyketal copolymers, which became important parts of my Ph.D.

thesis research. Ben helped developing techniques for loading proteins in polyketal microparticles, which were later used in animal models for delivery of SOD to treat acute liver failure.

I would also like to thank our collaborators for their contributions to my thesis project. Particularly, I would like to thank Dr. Mahesh Bhide and Dr. Ian Crispe of the University of Rochester and Dr. Robert Pierce of Schering-Plough Biopharma for their contributions for the delivery of imatinib using polyketal microparticles to treat acute liver failure. I would also like to thank Dr. Michael Davis and his laboratory for their demonstrations of the biocompatibility of polyketals *in vivo*.

I would like to thank Dr. Michael Davis, Dr. Sheldon May, Dr. Valeria Milam, and Dr. Ravi Bellamkonda for serving on my thesis committee. Their advice and guidance have helped me greatly in going forward with my thesis research.

I would like to thank the TI:GER program organized by the Georgia Tech School of Management for their financial support and giving me the opportunity to participate in a training curriculum for entrepreneurship and technology commercialization. My experience there has given me a whole new perspective on technology innovation from a commercialization point of view and will certainly help me in many ways in my future career.

I am also grateful to other funding sources that made my thesis research possible. These funding sources include The Parker H. Petit Institute for Bioengineering and Bioscience, the Georgia Tech/Emory Center for the Engineering of Living Tissues, the National Science Foundation, the National Institutes of Health, a J&J/GT Health Care

Innovation Seed Grant, and a GAANN fellowship through the Center for Drug Design, Development, and Delivery (CD4).

I would like to thank all my friends from IBB and the Bioengineering program at Georgia Tech, the staff members at IBB and the BME department for their support.

I would like to thank my parents, Dr. Charles Q. Yang and Yinfeng Du for their unconditional support and encouragement over the years. I am particularly grateful to my mother for her being there and taking care of us. I would also like to thank my parents in-law, Roland and Susan Jung, and sister in-law, Laura Jung, for their continuing support of both me and my wife in pursuing our degrees. Their help has made a significant impact in our lives.

Lastly, I would like to express my deep appreciation for my wife, Cindy, for her love, caring, and unconditional support. We have gone through the journey of pursuing a Ph.D. degree together; she has always provided me with unconditional love and support in all my endeavors, both professional and personal. My five years as a graduate student has been a wonderful and enjoyable journey, largely because I spent those years with her, whom I love and adore greatly, and I am truly grateful for that.

# TABLE OF CONTENTS

	Page
ACKNOWLEDGEMENTS	iv
LIST OF TABLES	ix
LIST OF FIGURES	x
LIST OF SYMBOLS AND ABBREVIATIONS	xiii
SUMMARY	xvii
 <u>CHAPTER</u>	
1 Introduction	1
1.1 Background and Motivation	1
1.2 Research Objectives and Specific Aims	6
1.3 Review of Relevant Literature	11
2 Development of Aliphatic Polyketals that Degrade into Biocompatible Diols	18
2.1 Abstract	18
2.2 Introduction	20
2.3 Experimental Methods	26
2.4 Results	33
2.5 Discussions	45
3 Development of Polyketal Copolymers with Suitable Properties for Treating Acute Inflammatory Diseases	51
3.1 Abstract	51
3.2 Introduction	53
3.3 Experimental Methods	57
3.4 Results	62

3.5 Discussions	77
4 Development of an SOD Delivery System for Treating Acute Liver Failure	83
4.1 Abstract	83
4.2 Introduction	84
4.3 Experimental Methods	87
4.4 Results	93
4.5 Discussions	105
5 Conclusions and Future Directions	111
5.1 Conclusions	111
5.2 Future Directions	112
APPENDIX A: Experimental Protocols	117
REFERENCES	127



## LIST OF TABLES

	Page
Table 3.1. Compositions and molecular weight of polyketal copolymers synthesized.	63
Table 3.2. Polyketal copolymers composed of 1,4-cyclohexanedimethanol and 1,5-pentanediol.	79
Table 3.2. Hydrolysis half-lives of polyketal copolymers at pH 4.5 and pH 7.4 at 37 °C.	81
Table 4.1. SOD loading, encapsulation efficiency, and enzymatic activity in PK3 microparticles from S/O/W and W/O/W emulsion methods.	94

## LIST OF FIGURES

	Page
Figure 1.1. Mechanism of acute liver injury.	2
Figure 1.2. Molecular structures of PLGA, polyanhydride, and POE, which degrade into acidic byproducts.	5
Figure 1.3. Formulation of SOD-PCADK microparticles by w/o/w double emulsion.	8
Figure 1.4. PK3, a polyketal copolymer was developed to have suitable properties for drug delivery to treat ALF.	9
Figure 1.5. SOD-loaded PK3 microparticles were characterized <i>in vivo</i> .	10
Figure 2.1. Stepwise polymerization based on the acetal exchange reaction.	25
Figure 2.2. <sup>1</sup> H NMR spectrum demonstrating hydrolysis of PCADK.	29
Figure 2.3. <sup>1</sup> H NMR and GPC spectrum of PCADK.	34
Figure 2.4. <sup>1</sup> H NMR and GPC spectrum of POADK.	35
Figure 2.5. <sup>1</sup> H NMR and GPC spectrum of PPeADK.	36
Figure 2.6. Hydrolysis kinetics of PCADK and POADK.	38
Figure 2.7. Release of rhodamine B from PCADK microparticles.	39
Figure 2.8. SEM images of SOD-PCADK microparticles	40
Figure 2.9. PCADK microparticles enhance the delivery of SOD to macrophages.	41
Figure 2.10. Cell viability of TIB-186 macrophages after incubation with PCADK microparticles.	42
Figure 2.11. Inflammatory response to injected PCADK or PLGA microparticles.	43
Figure 2.12. Stability of SOD in PCADK microparticles.	44
Figure 2.13. The hydrolysis of polyketals corresponds to their hydrophobicity.	47
Figure 3.1. Synthesis of polyketal copolymers.	55
Figure 3.2. PK3, a new biomaterial for treating acute inflammatory diseases.	56
Figure 3.3. <sup>1</sup> H NMR and GPC spectrum of PK1.	64

Figure 3.4. <sup>1</sup> H NMR and GPC spectrum of PK2.	65
Figure 3.5. <sup>1</sup> H NMR and GPC spectrum of PK3.	66
Figure 3.6. <sup>1</sup> H NMR and GPC spectrum of PK4.	67
Figure 3.7. <sup>1</sup> H NMR and GPC spectrum of PK5.	68
Figure 3.8. <sup>1</sup> H NMR and GPC spectrum of PK6.	69
Figure 3.9. Hydrolysis of PK1 at 37°C.	70
Figure 3.10. Hydrolysis of PK2 at 37°C.	71
Figure 3.11. Hydrolysis of PK3 at 37°C.	71
Figure 3.12. Hydrolysis of PK4 at 37°C.	72
Figure 3.13. Hydrolysis of PK5 at 37°C.	73
Figure 3.14. Hydrolysis of PK6 at 37°C.	73
Figure 3.15. Release kinetics of rhodamine B encapsulated in PK3 microparticles.	74
Figure 3.16. SEM images of particles formulated with PK3.	75
Figure 3.17. PK3 microparticles improve the efficacy of imatinib in treating acute liver failure in mice.	76
Figure 3.18. Hydrolysis half-lives of polyketal copolymers PK1, PK2, and PK3 at pH 4.5.	79
Figure 4.1. SEM image and fluorescence microscopy image of SOD-loaded PK3 microparticles.	93
Figure 4.2. Enzymatic activities of SOD were determined by establishing a calibration curve.	95
Figure 4.3. Macrophage uptake study of SOD-loaded PK3 microparticles.	96
Figure 4.4. PK3 Microparticles enhance the delivery of SOD to macrophages.	97
Figure 4.5. Release of fluorescein from PPADK microparticles.	98
Figure 4.6. Biodistribution study using PK3 microparticles encapsulating fluorescein.	99
Figure 4.7. Biodistribution study using PK3 microparticles encapsulating pentacene.	100

- Figure 4.8. Liver histology study using hematoxylin and eosin (H&E) staining. 102
- Figure 4.9. Alanine aminotransferase (ALT) assay; liver damage was measured by the amount of ALT enzyme in the plasma. 103
- Figure 4.10. ELISA assay; the concentration of TNF- $\alpha$  in plasma collected at 24 h after the treatment of sample and LPS. 104
- Figure 5.1. Synthesis of polyketals with diols and 2,2-diethoxypropane to yield high molecular weight polymers. 113

## LIST OF ABBREVIATIONS

ABS	Absorbance
ALF	Acute liver failure
ALT	Alanine aminotransferase
APAP	Acetaminophen
APPEAQ	Amino-4-(4-phenoxyphenylethylamino) quinazoline
BSA	Bovine serum albumin
CDM	1,4-Cyclohexanedimethanol
Con A	Concavalin A
Da	Dalton
DCM	Dichloromethane
DI Water	Deionized Water
DLS	Dynamic light scattering
DMF	Dimethylformamide
DMP	2,2-Dimethoxypropane
DMP	Dimethoxypropane
DMSO	Dimethylsulfoxide
DNA	Deoxyribonucleic acid
DPI	Polydispersity index
ELISA	Enzyme-Linked ImmunoSorbent Assay
FBS	Fetal bovine serum
FITC	Fluorescein isothiocyanate

GalN	Galactosamine
GPC	Gel permeation chromatography
GRAS	Generally recognized as safe
H&E	Hematoxylin and eosin
ICU	Intensive care unit
IFN- $\gamma$	Interferon gamma
IKK	IkappaB kinase
IL	Interleukin
IP	Intraperitoneal
IV	Intravenous
LPS	Lipopolysaccharide
$M_n$	Number-average molecular weight
$M_w$	Weight-average molecular weight
MnTBAP	Manganese III tetrakis (5,10,15,20 benzoic acid)
MSDS	Material safety data sheet
NAC	N-acetyl-L-cysteine
NADPH oxidase	Nicotinamide adenine dinucleotide phosphate-oxidase
NF- $\kappa$ B	Nuclear factor-kappa B
NMR	Nuclear magnetic resonance
NMR	Nuclear magnetic resonance
OCT	Optimal cutting temperature
OLT	Orthotopic liver transplantation
PBS	Phosphate-buffered saline

PCADK	Poly(cyclohexane-1,4-diyl acetone dimethylene ketal)
PEG	Poly(ethylene glycol)
PK1	Poly(cyclohexane-1,4-diyl acetone dimethylene ketal -co-1,5-pentane-acetone dimethylene ketal) (98:2 mol %)
PK2	Poly(cyclohexane-1,4-diyl acetone dimethylene ketal -co-1,5-pentane-acetone dimethylene ketal) (92:8 mol %)
PK3	Poly(cyclohexane-1,4-diyl acetone dimethylene ketal -co-1,5-pentane-acetone dimethylene ketal) (87:13 mol %)
PK4	Poly(cyclohexane-1,4-diyl acetone dimethylene ketal-co-1,4-butane-acetone dimethylene ketal) (97:3 mol %)
PK5	Poly(cyclohexane-1,4-diyl acetone dimethylene ketal-co-1,6-hexane-acetone dimethylene ketal) (85:15 mol %)
PK6	Poly(cyclohexane-1,4-diyl acetone dimethylene ketal-co-1,8-octane-acetone dimethylene ketal) (87:13 mol %)
PKM	PK3 microparticles
PLGA	Poly(lactic acid), poly(lactic-co-glycolic acid)
PMA	Phorbol myristate acetate
POADK	Poly(1,8-octane-acetone dimethylene ketal)
POE	Polyorthoesters
PPADK	poly(1,4-phenylene-acetonedimethylene ketal)
PPeADK	Poly(1,5-pentane-acetone dimethylene ketal)
PTSA	p-Toluenesulfonic acid
PVA	Poly(vinyl alcohol)

RNA	Ribonucleic acid
ROS	Reactive oxidative species
RPM	Revolutions per minute
S/O/W	Solid-in-oil-in-water
SEM	Scanning electron microscopy/microscope
SEM	Standard error of the mean
SOD	Superoxide dismutase



## SUMMARY

Acute liver failure (ALF) is a major cause of death in the world, and effective treatments are greatly needed. Reactive oxidative species (ROS) secreted by Kupffer cells, the resident macrophage cells in the liver, plays a major role in the pathology of acute liver failure. Therefore, reducing the excessive oxidative stress in the liver caused by ROS production during an acute liver injury event provides a treatment aimed at removing an important mediator for ALF. Drug delivery vehicles that can target anti-oxidative agents such as superoxide dismutase (SOD) to Kupffer cells have great therapeutic potential for treating ALF. Microparticles, formulated from biodegradable polymers, are advantageous for treating ALF because they can passively target therapeutics to Kupffer cells. However, existing biomaterials are not suitable for the treatment of ALF because of their slow hydrolysis and acidic degradation products. The **objectives** my thesis research were (1) to develop biodegradable, biocompatible aliphatic polyketals that have suitable properties for drug delivery applications treating ALF, (2) to formulate microparticles based on polyketals that have the suitable physical and chemical characteristics for delivering SOD to the liver, and (3) to characterize and validate the efficacy of polyketal microparticles for delivery of SOD to the liver to treat ALF *in vivo*.

The first two Specific Aims of this thesis were centered around the development of a new class of biodegradable materials, termed aliphatic polyketals, which have considerable potential as drug delivery vehicles for the treatment of inflammatory diseases because of their neutral degradation products and tunable hydrolysis kinetics. The first Specific Aim demonstrates the development of an aliphatic polyketal,

poly(cyclohexane-1,4-diyl acetone dimethylene ketal) (PCADK), which degrades into biocompatible byproducts and can be used to formulate microparticle for enhanced delivery of the anti-inflammatory enzyme, SOD, to macrophages. In the second Specific Aim, we developed a family of polyketal copolymers that have tunable/rapid hydrolysis kinetics and biocompatible degradation products. In particular, a fast-hydrolyzing polyketal copolymer, termed PK3, is suitable for drug delivery to treat ALF. An anti-inflammatory drug, imatinib, was encapsulated in PK3 microparticles, which significantly enhanced the efficacy of imatinib for treating ALF. The third Specific Aim demonstrates PK3 microparticles were used to deliver SOD to the liver for treating an animal model of acute liver injury induced by the endotoxin lipopolysaccharide (LPS). Our results demonstrated that PK3 microparticles significantly improved the efficacy of SOD in treating LPS-induced acute liver damage *in vivo*, as evidenced by decreased levels of serum alanine transaminase (ALT), which corresponds to the extent of damage in the liver, and serum level of tumor necrosis factor-alpha (TNF- $\alpha$ ), which corresponds to the secretion of pro-inflammatory cytokines. The completion of this thesis research demonstrates the ability of polyketal-based drug delivery systems for treating acute inflammatory diseases and creates a potential therapy for enhancing the treatment of ALF.

# CHAPTER 1

## INTRODUCTION

### 1.1 Background and Motivation

Acute liver failure (ALF), characterized by the total loss of hepatic metabolic function, is a complex multisystem illness caused by several pathologic conditions, including bacterial infection-induced sepsis, hemorrhagic viral infections, alcohol-induced liver toxicity, hepatic ischemia/reperfusion injury, and Tylenol overdose. ALF is a devastating disease and responsible for thousands of deaths each year (Polson and Lee 2005). For instance, in the United States, septic shock accounts for 10% of hospital intensive care unit (ICU) admissions and carries a 70% mortality rate (Angus, Linde-Zwirble et al. 2001). In patients diagnosed with ALF, the level of gram negative bacteria in the blood is elevated, leading to increased levels of pro-inflammatory molecules such as reactive oxidative species (ROS) and tumor necrosis factor-alpha (TNF- $\alpha$ ) secreted by Kupffer cells, the resident macrophage cells in the liver (Figure 1.1) (Su 2002). These pro-inflammatory molecules subsequently induce massive hepatocyte necrosis, resulting in catastrophic liver injury (Decker, Lohmann-Matthes et al. 1989; Wheeler, Kono et al. 2001). Therefore, Kupffer cells play a central role in mediating inflammatory events during liver injury.

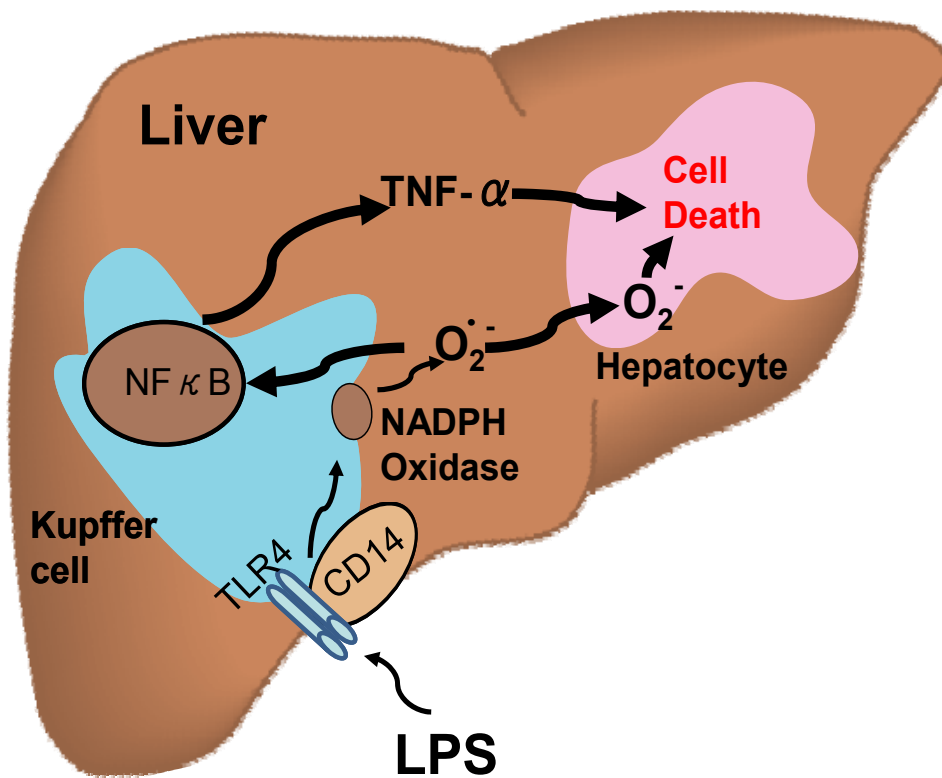


Figure 1.1 Mechanism of acute liver injury. Elevated serum gram negative bacteria activates CD14/toll-like receptor-4 (TLR4) complex to produce superoxide via NADPH oxidase. Oxidants activate NFκB, causing an increase in TNF-α production, which together with extracellular superoxide, cause hepatocyte death and liver injury.

Due to the excessive oxidative stress caused by ROS production during a liver injury event, reducing the oxidative stress provides a treatment aimed at removing an important mediator for ALF. For example, N-acetyl-L-cysteine (NAC), which acts to augment the reducing agent glutathione reserves in the body, is currently the most employed procedure for treating acute liver injury caused by acetaminophen overdose. However, there is a major limitation associated with using NAC for treating ALF.

Because there are no targeting mechanisms for NAC to accumulate in the liver, the level of NAC in the blood could be substantially high when NAC is systemically administered, which potentially causes damages to the heart and lungs by increasing the blood pressure within these organs (Palmer, Doctor et al. 2007). Another option for treating ALF is orthotopic liver transplantation (OLT), the replacement of a diseased liver with a healthy liver allograft. Even though OLT has excellent survival rate, the recipients will have to undergo immunosuppressive treatment in order to prevent organ rejection by the host. Therefore, the recipients can not effectively fight infections due to the use of immunosuppressant after a liver transplantation procedure. Another major issue associated with liver transplantation is the shortage in availability of donor organs; the majority of ALF patients die waiting for a liver transplantation (Bilir, Guinette et al. 2000). Furthermore, many patients that undergo rapid clinical deteriorations such as brain edema and multisystem organ failure are precluded from OLT. These limitations prevent OLT in becoming an effective and widespread treatment practice for ALF.

Given the limitations of current treatment options available for ALF, there is a great need for designing a new therapeutic strategy to treat ALF. Due to the critical involvement of Kupffer cells in ALF, drug delivery vehicles that can target therapeutics to Kupffer cells have great clinical potential (Fujiwara and Kobayashi 2005). A key drug delivery requirement for the treatment of acute liver failure is rapid delivery. This is because at the time of patient diagnosis, significant liver damage has already occurred, and the metabolic function of the liver is deteriorating rapidly; therefore, timely interventions that can minimize further tissue damage will greatly improve treatment (O'Grady and Schalm 1993). It has been challenging to develop clinically acceptable

drug delivery vehicles that can target therapeutics to Kupffer cells and release them rapidly. For example, liposomes are a potential delivery vehicle for treating ALF, due to their ability to target Kupffer cells (Higuchi, Kawakami et al. 2007). However, liposomes can not be freeze-dried and therefore can not be easily stored over a long period of time. In addition, most forms of liposomes are not stable in serum. These properties limit the use of liposomes for treating ALF in clinical applications. Microparticle-based drug delivery vehicles have excellent serum stability and storage properties. However, despite their promising features, microparticles have not been used extensively for the treatment of inflammatory diseases such as ALF. This is primarily because currently used biomaterials for microparticle-based drug delivery are not suitable for drug delivery applications treating acute inflammatory diseases. There are three major types of biodegradable polymers: poly(lactic-co-glycolic acid) (PLGA), polyorthoesters (POE), and polyanhydrides (Figure 1.2). These materials have been used for the development of implantable depot delivery vehicles and are being intensely investigated for many biomedical and drug delivery applications. However, PLGA, polyanhydrides, and POE have been suboptimal for the development of delivery vehicles designed to treat acute inflammatory diseases. This is partially because of their acidic degradation products, which cause inflammation and may damage fragile biotherapeutics to be delivered (Anderson and Shive 1997; Fu, Pack et al. 2000; van de Weert, Hennink et al. 2000).

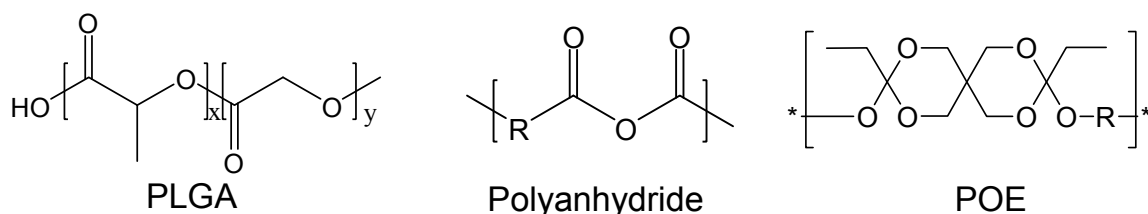


Figure 1.2. Molecular structures of PLGA, polyanhydrides, and POE, which degrade into acidic byproducts.

Microparticles formulated from the polyketal, poly(1,4-phenylene-acetonedimethylene ketal) (PPADK), represent a new drug delivery approach that has great potential for the treatment of ALF, due to their ability to be passively phagocytosed, their acid sensitivity, and their neutral degradation products (Heffernan and Murthy 2005). PPADK has ketal linkages in its backbone, which hydrolyze in proportion to the hydronium ion concentration. This acid sensitivity should enable polyketal-based microparticles to release therapeutics rapidly within the acidic environment of phagosomes (Cordes and Bull 1974; Gopferich 1996). PPADK also degrades into neutral compounds, diols and acetone, and should therefore avoid the inflammatory response associated with the acidic degradation products of polyester and polyanhydride-based biomaterials (Fu, Pack et al. 2000; Gopferich and Tessmar 2002; Kumar, Langer et al. 2002). Even though PPADK has many advantageous features for drug delivery applications, PPADK degrades into benzene dimethanol, a compound with potential toxicity, due to its aromatic ring. Therefore, there is a need to design new polyketals that degrade into biocompatible products.

## 1.2 Research Objectives and Specific Aims

Superoxide dismutase (SOD), an enzyme that scavenges superoxide, has great potential to treat ALF. SOD reduces the production of ROS from Kupffer cells, reducing inflammatory responses during an acute liver injury (Nakae, Yamamoto et al. 1990; Michael, Pumford et al. 1999; Yabe, Kobayashi et al. 2001; Jian Wu 2004). Reduced production of superoxide by Kupffer cells can also decrease the activation of the nuclear factor-kappa B (NF- $\kappa$ B), a transcription factor responsible for secretion of inflammatory cytokines, such as interleukin 12 (IL12), IL18, interferon gamma (IFN- $\gamma$ ), and TNF- $\alpha$ , from Kupffer cells, thus addressing the underlining causes of liver inflammatory responses induced by endotoxins such as lipopolysaccharide (LPS) (Ogushi, Imuro et al. 2003; Zhou, Wang et al. 2004; Liu and Malik 2006; Higuchi, Kawakami et al. 2007). Therefore, targeting SOD to Kupffer cells could significantly improve the treatment of ALF. The **objectives** my thesis research were (1) to develop biodegradable, biocompatible aliphatic polyketals that have the suitable properties for drug delivery applications treating ALF, (2) to formulate microparticles based on polyketals that have the suitable physical and chemical characteristics for delivering SOD, and (3) to characterize and validate the efficacy of polyketal microparticles for delivery of SOD to the liver to treat ALF *in vivo*. The research was based on the **central hypothesis** that: *Microparticles formulated from aliphatic polyketals will improve the treatment of acute liver failure by targeting and rapidly releasing anti-inflammatory agents such as SOD to the liver and particularly, to Kupffer cells.* The central hypothesis of this thesis research was tested by completing the following aims.



**Specific Aim 1:** Develop aliphatic polyketals, including poly(cyclohexane-1,4-diyl acetone dimethylene ketal) (PCADK), which degrade into biocompatible byproducts and can be used to formulate microparticle for enhanced delivery of SOD to macrophages.

**Hypothesis 1:** Aliphatic polyketals can be synthesized using monomers with low and known toxicity, which will degrade into byproducts with low and known toxicity.

In this Specific Aim, three aliphatic polyketals were synthesized using a step-growth polymerization, following the procedures previously developed for synthesizing PPACK (Heffernan and Murthy 2005). One of the aliphatic polyketals, PCADK, degrades into 1,4-cyclohexanedimethanol (CDM) and acetone, both of which have low and known toxicity in biological systems. The chemical structure of the aliphatic polyketals was characterized by gel permeation chromatography (GPC) and nuclear magnetic resonance (NMR) spectroscopy, and its pH-sensitive degradation was demonstrated by NMR. Using PCADK, a SOD-loaded PCADK microparticle delivery system was formulated with a water-in-oil-in-water (W/O/W) double emulsion procedure. The physical characteristics such as size and surface properties of SOD-loaded PCADK microparticles were determined by scanning electron microscopy. SOD-loaded PCADK microparticles were designed to undergo accelerated degradation and release encapsulated drugs in acidic environment of phagolysosomes upon taken up by phagocytic cells such as macrophages (Figure 1.3). The ability of PCADK microparticles to enhance the delivery of SOD to macrophages and inhibit production of ROS from these macrophages was tested in cell culture.

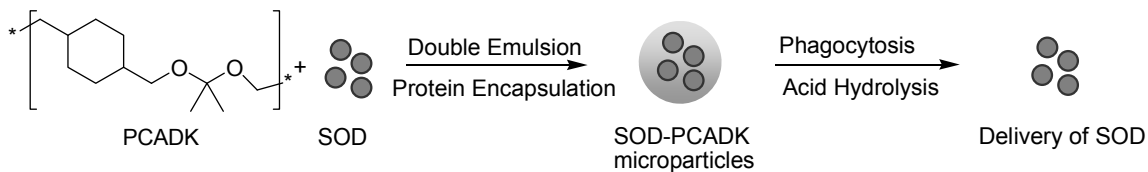


Figure 1.3. Formulation of SOD-PCADK microparticles by w/o/w double emulsion. Microparticles degrade after phagocytosis, in the acidic environment of the phagolysosome.

**Specific Aim 2:** Develop a family of polyketal copolymers that have chemical properties such as pH sensitivity, tunable/rapid hydrolysis kinetics, and biocompatible degradation products, which are suitable for drug delivery to treat acute liver failure.

**Hypothesis 2:** The hydrolysis kinetics of polyketals is governed by their hydrophilicity; therefore, a family of aliphatic polyketal copolymers with tunable hydrolysis kinetics can be synthesized by copolymerizing monomers of varying hydrophobicity.

In this Specific Aim, a family of polyketal copolymers were synthesized from two of the diols: 1,4-cyclohexanedimethanol (CDM), 1,4-butanediol, 1,5-pentanediol, 1,6-hexanediol, and 1,8-octanediol. These diols have different hydrophobicity, and therefore the resulting polyketals have varying hydrolysis kinetics. The chemical characteristics of these polyketals were characterized by GPC and NMR spectroscopy, and pH-sensitive degradation was determined by NMR. Microparticles were formulated using PK3, which was synthesized by copolymerizing 80% CDM with 20% 1,5-pentanediol. The release kinetics of PK3 microparticles were assessed by loading a fluorescent dye, rhodamine B, and measuring the accumulation of rhodamine B released into pH 4.5 and pH 7.4 buffers.

An anti-inflammatory drug, imatinib, was encapsulated in PK3 microparticles, which significantly enhanced the efficacy of imatinib for treating ALF (Figure 1.4).

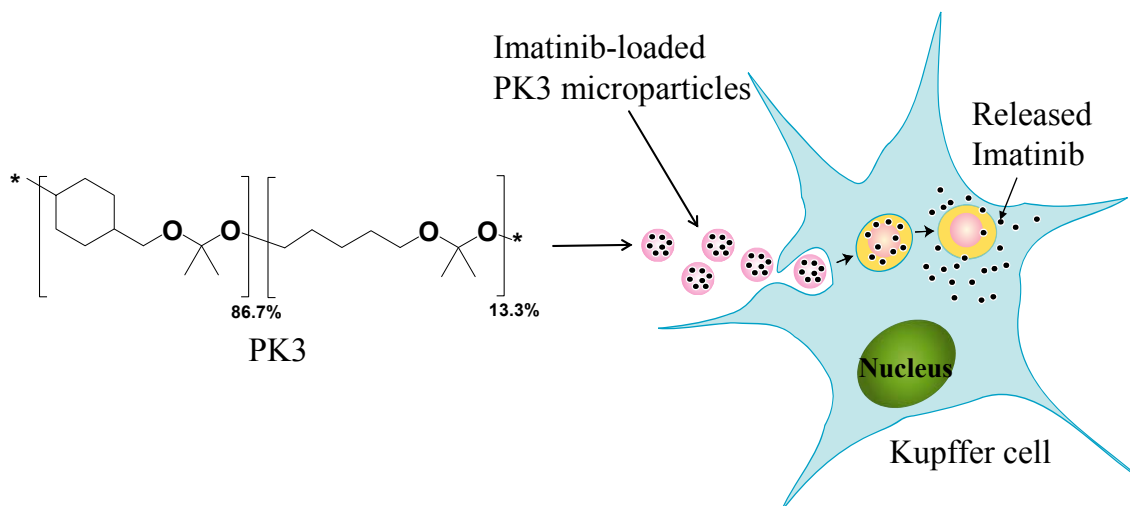


Figure 1.4. PK3, a polyketal copolymer, was developed to have suitable properties for drug delivery to treat ALF. The anti-inflammatory drug, imatinib, was encapsulated PK3 microparticles, which significantly enhance the efficacy of imatinib for treating ALF.

**Specific Aim 3:** Deliver SOD to liver, particularly Kupffer cells, using SOD-loaded PK3 microparticles to treat acute liver injury induced by the endotoxin Lipopolysaccharide (LPS) in mice.

**Hypothesis 3:** We hypothesized that SOD-loaded PK3 microparticles (1-5 microns in diameter) can deliver therapeutic levels of SOD to the liver to reduce LPS-induced liver injury by scavenging ROS secreted by Kupffer cells.

In this Specific Aim, the traditional water-in-oil-in-water (W/O/W) double emulsion method and a new technique, termed solid-in-water-in-oil (S/O/W) method, were employed to formulate SOD-loaded PK3 microparticles, which were used to deliver SOD to macrophages and release it rapidly inside the phagolysosomes. The microparticles were characterized by SEM for size and assayed for enzymatic activity of

SOD. These SOD-loaded PK3 microparticles were also tested in cell culture for their ability to be phagocytosed by macrophages. We then used these microparticles to target SOD to the liver for preventing LPS-induced liver damage *in vivo*. Damage to the liver due to LPS was characterized by three approaches (Figure 1.5). First, the morphology of the liver tissue was examined using histological techniques. Second, the degree of liver damage in mice was assessed by measuring their serum levels of alanine transaminase (ALT), which corresponds to the extent of damage in the liver. ALT is an enzyme normally present in hepatocytes. During an acute liver damage event, hepatocytes are damaged and leak ALT into the blood, dramatically rising the serum ALT level. Third, the level of inflammatory responses in the liver was assessed by measuring the serum TNF- $\alpha$  level, which corresponds to the secretion of pro-inflammatory cytokines due to activation of the transcription factor, NF $\kappa$ B.

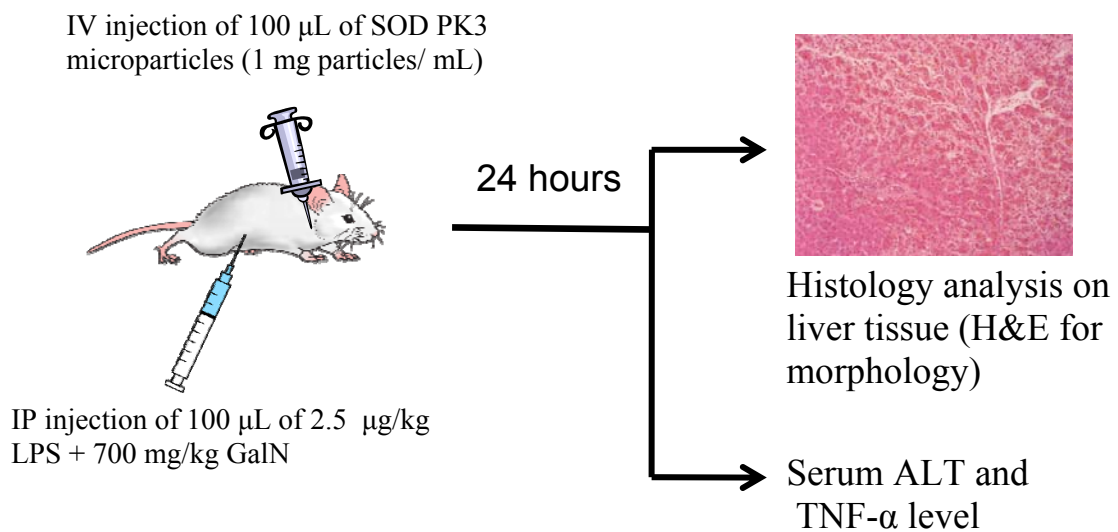


Figure 1.5. SOD-loaded PK3 microparticles were characterized *in vivo* using histology analysis with hematoxylin and eosin (H&E) stain, serum ALT measurement, and serum TNF- $\alpha$  measurement.

### 1.3 Review of Relevant Literature

#### Role of Kupffer cells in LPS-induced liver injury

Kupffer cells, the resident macrophage cells in the liver, reside primarily near the capillary bed within the liver sinusoidal spaces (Wake 1980; Decker 1990; Wheeler, Kono et al. 2001). Kupffer cells are capable of ingesting other cells and foreign particles and constitute 80% to 90% of all tissue macrophages in the body (Bilzer, Roggel et al. 2006). Therefore, Kupffer cells represent the first line of defense against foreign materials entering the liver through the portal veins (Crofton, Diesselhoff-den Dulk et al. 1978; Diesselhoff-den Dulk, Crofton et al. 1979). Kupffer cells can be activated by a variety of substances including viruses and bacteria. Phagocytosis of foreign substances by Kupffer cells leads to secretion of pro-inflammatory cytokines including TNF- $\alpha$ , interleukins, and ROS, which act as paracrine signals on hepatocytes and induce recruitment of neutrophils (Decker, Lohmann-Matthes et al. 1989; Decker 1990; Thurman 1998; Schumann, Wolf et al. 2000; Jaeschke, Gores et al. 2002; Pagliara, Carla et al. 2003; Uchikura, Wada et al. 2004; Tilg, Kaser et al. 2006). Several studies have been published demonstrating that Kupffer cells are critically involved in the inflammatory responses in the liver. For example, Adachi *et al* showed that inactivation of Kupffer cells with gadolinium chloride significantly reduced the inflammatory response and serum enzyme levels in mice undergoing alcohol-induced liver injury (Adachi, Bradford et al. 1994). In a separate study, liver toxicity due to a viral infection was significantly reduced when Kupffer cells were inactivated by gadolinium chloride treatment, as evidenced by decreased activation of NF $\kappa$ B and decreased serum level of

TNF- $\alpha$  and IL-6 (Lieber, He et al. 1997). These findings suggest that Kupffer cells play a crucial role in mediating liver injury.

### **Role of superoxide in the mechanism of liver injury**

Acute liver injury is mediated by various mediators including ROS, TNF- $\alpha$ , interleukins, and prostaglandins that are secreted by activated Kupffer cells. Of the secreted cytokines, ROS has been found to play a major role in mediating liver injury (Michael, Pumford et al. 1999; Ferret, Hammoud et al. 2001; Yabe, Kobayashi et al. 2001; Droge 2002; Hitchon and El-Gabalawy 2004; Jian Wu 2004; Kamata, Honda et al. 2005; Victor, Rocha et al. 2005). Specifically, superoxide mediates inflammatory responses in the liver in two ways. First, superoxide acts as a key signaling molecule to activate the transcription factor NF $\kappa$ B. The activation of NF- $\kappa$ B in Kupffer cells plays a central role in the development of ALF by inducing the production and secretion of inflammatory molecules such as TNF- $\alpha$ , IL-1, IFN- $\gamma$ , and IL-12, which cause extensive tissue damage in the liver and significantly contribute to necrosis of hepatocytes, eventually leading to massive liver injury (Li and Karin 1999; Pahl 1999; Hoek and Pastorino 2002; Zhou, Wang et al. 2003; Zima and Kalousova 2005; Higuchi, Kawakami et al. 2006). These cytokines regulate the phenotype of Kupffer cells themselves as well as the neighboring cells, such as hepatocytes and endothelial cells (Bilzer, Roggel et al. 2006). Second, superoxide is responsible for initiating liver damage during acute liver failure by damaging liver tissue through direct reaction of cellular lipids, proteins, and DNA, or through the generation of other ROS such as peroxynitrate (Frein, Schildknecht et al. 2005). The exact pathways for superoxide formation is not clear; however, results

from numerous studies suggest that the nicotinamide adenine dinucleotide phosphate-oxidase (NADPH oxidase) system in the Kupffer cells is a likely candidate responsible for production of superoxide from Kupffer cells. For example, Kono *et al* demonstrated that rats were protected against alcohol-induced liver injury when treated with Diphenyleneiodonium sulfate (DPI), an inhibitor of NADPH oxidase. The rats treated with DPI had lower serum ALT levels, free radical production, NFκB activation, and pro-inflammatory cytokine production as well as showed minimal pathological changes than rats that were only treated with alcohol (Kono, Rusyn et al. 2001). In another study, genetic knock-out mice deficient in a regulatory subunit of NADPH oxidase also showed a significantly reduced level of alcohol-induced acute liver injury, evidenced by decreased levels of free radical formation and inflammatory parameters such as TNF-α and NFκB (Kono, Rusyn et al. 2000). The results from these studies suggest that superoxide production from NADPH oxidase system in Kupffer cells indeed plays an important role in mediating acute liver injury. This is consistent with several *in vitro* studies which showed that LPS induced superoxide production by NADPH oxidase in cell culture via the CD14/TLR4 pathway (Sasada, Pabst et al. 1983; Landmann, Scherer et al. 1995).

### **Antioxidants are used for treating acute liver failure**

ROS plays an important role in mediating ALF; therefore, approaches that can reduce oxidative stress in the liver have great potential in treating this devastating disease. Several studies have been carried out using various anti-oxidative agents for treating liver injury. Liu *et al* demonstrated that the actions of salviainolic acid A, an

antiperoxidative component of *Saliva miltiorrhiza*, were able to reduce oxidative stress in the liver and reduce hepatocytes injury after the rat liver was insulted by CCl<sub>4</sub> (Liu, Hu et al. 2001). Mangafodipir, a MRI contrast agent with antioxidant properties, inhibited ROS production and protected hepatocytes from oxidative stresses induced by xanthine oxidase, H<sub>2</sub>O<sub>2</sub>, and UV light in cell culture. Additionally, mangafodipir could also significantly increase the survival rates and reduce ALT levels in mice (Bedda, Laurent et al. 2003). Manganese III tetrakis (5,10,15,20 benzoic acid) (MnTBAP) is a nonpeptidyl mimic of SOD and has been shown to preventively and curatively improve survival times and reduce ALF levels in APAP-intoxicated mice, whereas NAC only prevented ALF in a dose-dependent manner but was ineffective in curing ALF in mice (Ferret, Hammoud et al. 2001; Malassagne, Ferret et al. 2001). Taking together, these results suggest that antioxidants hold great promise in treating ALF by efficiently reducing ROS level in the liver.

### **SOD is effective for treating acute liver failure**

SOD is an enzyme that catalyzes the conversion of superoxide to hydrogen peroxide and has great potential for treating inflammatory diseases, such as ALF, arthritis, and sepsis, by suppressing ROS production by macrophages (Luisa Corvo, Jorge et al. 2002; Kinnula and Crapo 2003; Cuzzocrea, Thiemermann et al. 2004; Landis and Tower 2005). Cu,Zn-SOD is the major type of SOD in the liver and is subcellularly distributed in primarily lysosomes and cytosol (Okado-Matsumoto and Fridovich 2001). The normal level of Cu,Zn-SOD in the liver has been reported to be 0.58 units per milligram of protein (Ozden, Uzun et al. 2004). Numerous studies have demonstrated



that increasing SOD level in the liver has potential therapeutic effects in suppressing production of superoxide during acute liver failure. For example, studies using adenovirus containing genes for various SOD isoforms have demonstrated that SOD gene delivery protected liver from oxidative stress and resulted in reduction in free radical and pro-inflammatory cytokine levels in the liver during acute liver injury (Zwacka, Zhou et al. 1998; Wheeler, Katuna et al. 2001; Wheeler, Kono et al. 2001). Wu *et al* also demonstrated that polycationic liposome based SOD gene delivery protects mice against ROS toxicity *in vitro* and against LPS-mediated liver injury in D-galactosamine-sensitized mice (Wu, Liu et al. 2004). In another example, a study showed that genes for the cytosolic isoform of SOD delivered to the liver with an adenovirus significantly decreased transaminase release, reduced necrosis, and increased survival rates in a rat model of liver transplantation (Lehmann, Wheeler et al. 2003). Moreover, Targeted delivery of SOD to the liver has also showed promises in treating ALF. Yabe *et al* showed that mannosylated SOD targeted to non-parenchymal liver cells including Kupffer cells prevented hepatic ischemia/reperfusion injury in mice models (Yabe, Kobayashi et al. 2001).

### **Delivery systems for SOD have promises for treating inflammatory diseases**

Even though SOD has shown great promises as a therapeutic approach for treating ALF, current treatment of ALF with SOD has been ineffective, primarily due to lack of an efficient delivery system for SOD. SOD by itself is not stable in serum, having a serum half-life of only 5 minutes; therefore, the clinical application of SOD has been limited by its rapid clearance through the kidney (Valdivia, Perez et al. 2005). Covalent

modification of SOD with water-soluble and biocompatible polymers has been used as a tool for increasing the circulation time of SOD. For example, the SOD modification with poly(ethylene glycol) (PEG) was effective in decreasing the elimination rate of SOD from the blood, having a clearance half-life of 30 hours when SOD had a PEG modification extent of 54%; however, this modification does not change the organ distribution of SOD; only 1% of SOD-PEG complex was found in the liver 3 hours after intravenous injection of SOD (Nakaoka, Tabata et al. 1997). Liposome-based SOD delivery vehicles have shown promise for enhancing the delivery of SOD in animal models. Several studies have demonstrated that liposomes protected the enzymatic activities of SOD, which were then used to treat oxidative stress related diseases such as hypertension, arthritis, respiratory insufficiency, and atherosclerosis (White, Brock et al. 1994; Briscoe, Caniggia et al. 1995; Laursen, Rajagopalan et al. 1997; Luisa Corvo, Jorge et al. 2002). The use of liposome-encapsulated SOD for treating ALF has also been reported. Nakae *et al* showed that liposome-encapsulated SOD protected rats from acetaminophen-induced liver necrosis, whereas free SOD and empty liposomes had no protective effect (Nakae, Yamamoto et al. 1990). These studies demonstrated that liposomes are effective in delivering SOD to the liver; however, one major limitation of liposomes is that they suffer from problem of instability (Feng, Ruan et al. 2004). Biodegradable microspheres also have great promise for sustained and targeted delivery of proteins such as SOD (Kumar, Soppimath et al. 2006). Biodegradable materials like PLGA, alginate, and chitosan were used for preparing microspheres that can release the encapsulate SOD in a sustained fashion (Liu, Ge et al. 2003; Giovagnoli, Blasi et al. 2004; Wang, Gao et al. 2006; Celik and Akbuga 2007). However, PLGA is hydrolyzed

slowly at acidic and physiological pH condition; therefore, PLGA based delivery system for SOD is not suitable for treating ALF, which requires SOD to be released rapidly. Moreover, although PLGA-based microparticles have an excellent shelf life, well characterized degradation products, and a long history for their use in medical devices, their application for the treatment of inflammatory diseases is potentially problematic because their acidic degradation products can cause inflammation (Dailey, Jekel et al. 2006). Acid-degradable polymers, such as POE and polyacetals, hydrolyze in the acidic environment of phagolysosomes and have previously been used for intracellular drug delivery (Papisov 2001; Heller and Barr 2004; Wang, Ge et al. 2004). However, the use of POE and polyacetals for delivering SOD has not yet been reported. Polyketals are a new family of acid degradable polymers that have ketal linkages in their backbone and have several properties that make them an attractive delivery vehicle for SOD (Heffernan and Murthy 2005). Polyketals degrade into neutral compounds that may avoid the inflammatory problems associated with the acidic degradation products of polyesters, polyanhydrides, and polyorthoesters.

## **CHAPTER 2**

# **DEVELOPMENT OF ALIPHATIC POLYKETALS THAT DEGRADE INTO BIOCOMPATIBLE DIOLS**

### **2.1 Abstract**

There is currently great interest in developing biodegradable materials that can be used to deliver drugs to macrophages for treating inflammation. In this Chapter, I present three biodegradable aliphatic polyketals, which were designed to have the properties needed to treat inflammatory diseases. One particular aliphatic polyketal, poly(cyclohexane-1,4-diyl acetone dimethylene ketal) (PCADK), was designed to hydrolyze, after phagocytosis by macrophages, in the acidic environment of the phagosome and enhance the intracellular delivery of phagocytosed therapeutics. Other key attributes of PCADK for drug delivery are its well characterized degradation products and straightforward synthesis. PCADK hydrolyzes into 1,4-cyclohexanedimethanol, a compound used in food packaging, and acetone, a compound on the FDA GRAS list. PCADK was synthesized using the acetal exchange reaction between 1,4-cyclohexanedimethanol and 2,2-dimethoxypropane, and could be obtained on a multi-gram scale in one step. The hydrolysis kinetics of the ketal linkages in PCADK were measured by  $^1\text{H-NMR}$  and were determined to be pH-sensitive, having a half-life of 24.1 days at pH 4.5 and over 4 years at pH 7.4. The therapeutic enzyme superoxide dismutase (SOD), which scavenges reactive oxygen species, was encapsulated into PCADK-based microparticles using a double emulsion procedure. Cell culture experiments demonstrated that PCADK-based microparticles dramatically

improved the ability of SOD to scavenge reactive oxygen species produced by macrophages. We anticipate numerous applications of PCADK in drug delivery, based on its acid sensitivity, well characterized degradation products, and straightforward synthesis.

## 2.2 Introduction

In this chapter, I will discuss Specific Aim 1, which is to develop aliphatic polyketals, which degrades into biocompatible byproducts. Biodegradable polymers that degrade into biocompatible products have attracted much attention in the field of drug delivery and biomaterials (Tamada and Langer 1993; Freed, Vunjak-Novakovic et al. 1994; Gref, Minamitake et al. 1994; Middleton and Tipton 2000; Tansey, Ke et al. 2004). Drug delivery systems based on biodegradable polymers offer numerous advantages such as controlled rates of release, cell or tissue specific targeting, and assisting cell up-take of drugs (Heller 1984; Langer 1998; Soppimath, Aminabhavi et al. 2001; Itoh, Matsusaki et al. 2006; Kohane, Tse et al. 2006; Yih and Al-Fandi 2006). There are three major types of biodegradable polymers that have been extensively investigated for biomedical applications: PLGA, polyanhydrides, and POE. PLGA is a copolymer of glycolic acid and lactic acid and has been used in medical devices and delivery of drugs and genetic materials, due to its biocompatibility and biodegradability (Spencehauer, Vert et al. 1989; Ignatius and Claes 1996; Anderson and Shive 1997; Coombes, Tasker et al. 1997; Ando, Putnam et al. 1999; Cadee, Brouwer et al. 2001; Tamber, Johansen et al. 2005). PLGA undergoes base-catalyzed hydrolysis in the body to produce the original monomers, lactic acid and glycolic acid. By changing the ratio of lactic acid to glycolic acid, one can engineer the degradation kinetics of PLGA; however, the degradation profiles of PLGA are too slow for drug delivery applications treating acute inflammatory diseases which require fast drug release kinetics. For example, microparticles based on the fastest formulation of PLGA, had a degradation half-life of 15 days at physiological pH (Dunne, Corrigan et al. 2000). Another major disadvantage of using PLGA-based delivery system

for treating inflammatory diseases is that PLGA degrades into acid, which can cause inflammatory response itself and potentially destroy the drug loaded in the particles, due to the very acidic environment within the PLGA particles (Fu, Pack et al. 2000; van de Weert, Hennink et al. 2000). Polyanhydrides represent another major type of biodegradable polymer, which is composed of anhydride bonds, one of the most reactive functional groups available for degradation on the basis of passive hydrolysis. Therefore, the degradation of polyanhydrides is fast, usually on the order of hours to days (Rosen, Chang et al. 1983; Gopferich and Tessmar 2002). Polyanhydrides have been used for rapid delivery of drugs to the brain, bone, blood vessels, and eyes (Tamada and Langer 1992; Tabata, Gutta et al. 1993; Dang, Daviau et al. 1996; Kumar, Langer et al. 2002). Even though polyanhydrides have suitable degradation kinetics for drug delivery applications treating acute inflammatory diseases, it also degrades into diacid. Because of the fast degradation profiles of polyanhydrides, it can generate large quantity of acid in a short amount of time, which is not desirable for treating inflammation. POE has also been investigated for controlled and sustained drug delivery applications due to its biocompatible and biodegradable properties (Heller, Barr et al. 2002; van Dijkhuizen-Radersma, Hesselting et al. 2002; Heller and Barr 2004; Wang, Ge et al. 2004). However, like PLGA and polyanhydrides, POE also is not ideal for treating inflammatory diseases due to its acidic degradation products (Capancioni, Schwach-Abdellaoui et al. 2003).

Acetal and ketal based biomaterials have generated great interest in the field of drug delivery because of their neutral degradation products and pH-sensitive hydrolysis (Tomlinson, Klee et al. 2002; Jain, Standley et al. 2007). Acetals and ketals are particularly well suited for the development of acid sensitive drug delivery vehicles

because their hydrolysis is proportional to the hydronium ion concentration, making them more sensitive to pH gradients than orthoesters, esters and amides. Polyacetals hydrolyze in the acidic environment of lysosomes and phagosomes and have previously been used for intracellular drug delivery (Papisov 2001; Tomlinson, Heller et al. 2003; Sheff 2004). For example, microparticles, based on acetal linkages, have been synthesized, via free radical polymerization. These microparticles were successful in delivering proteins and antisense *in vitro* and *in vivo* to dendritic cells (Kwon, James et al. 2005). Similarly, soluble polymeric carriers containing acetal linkages, have been developed, via free radical polymerization, which can deliver peptides and antisense oligonucleotides to hepatocytes and macrophages *in vitro* (Kwon, Standley et al. 2005). However, despite their promise, the clinical impact of acetal/ketal based drug delivery vehicles has been minimal. This is partially due to synthetic problems and biocompatibility issues. Acetal/ketal based delivery vehicles are generally synthesized through free radical polymerization. Polymers synthesized via free radical polymerization have backbones composed of non-hydrolysable carbon-carbon bonds, making them difficult to excrete. Therefore synthetic strategies that can incorporate acetal/ketal linkages within the backbone of polymeric delivery vehicles are greatly needed. The polyketals are a new family of acid degradable polymers that have ketal linkages in their backbones (Hirai, Hattori et al. 1999; Heffernan and Murthy 2005). Recently, Heffernan *et al* demonstrated that the acetal exchange reaction between 2,2-dimethoxypropane and benzene-dimethanol could be used to synthesize the polymer, poly(1,4-phenylene-acetone dimethylene ketal) (PPADK). PPADK contains ketal linkages in its backbone and degrades by acid catalyzed hydrolysis in aqueous solutions into neutral compounds,



acetone and benzene dimethanol, hydrolyzing with half-lives of 35 hours at pH 5.0 and 102 hours at pH 7.4 (Heffernan and Murthy 2005). PPADK represents a new class of biodegradable polymers that are also being investigated for drug delivery, and have several unique properties that make them suitable as drug delivery vehicles for treating inflammatory diseases. First, polyketals degrade into alcohols and ketones and may avoid the inflammatory problems associated with the acidic degradation products of polyesters and polyanhydrides. This property makes polyketals particularly attractive for drug delivery applications treating inflammatory diseases. Second, polyketals undergo acid-catalyzed hydrolysis. For drug delivery systems to phagocytic cells such as macrophages, acid-sensitive polymers offer one major advantage over biodegradable polymers that are not acid-sensitive. Drug delivery systems based on acid-sensitive polymers can take advantage of the lower pH environment inside phagosomes and selectively release drugs to cells upon phagocytosis (Roux, Francis et al. 2002; Murthy, Campbell et al. 2003; Kwon, James et al. 2005; Watson, Jones et al. 2005). As discussed in Chapter 1, macrophages have the ability to take up micron-sized materials through a process known as phagocytosis and have been implicated in the generation and propagation of many types of inflammatory diseases (Thiele, Rothen-Rutishauser et al. 2001). Therefore drug delivery vehicles that can target therapeutics to macrophages have great promise. Although PPADK has several properties that make it desirable for drug delivery applications, very little is known about the toxicity of benzene dimethanol, in animals and in humans, and this will slow the clinical development of drug delivery systems based on PPADK. Therefore new polymers, which have ketal linkages in their backbone and degrade into compounds with low toxicity, would be preferable.

In this Chapter, I present three biodegradable aliphatic polyketals, PCADK, POADK, and PPeADK, which were designed to have the properties needed to treat inflammatory diseases (Figure 2.1). These aliphatic polyketals have ketal linkages in their backbone and hydrolyze in a pH sensitive manner into neutral compounds: acetone and aliphatic diols. For example, PCADK degrades into biocompatible compounds, 1,4-cyclohexanedimethanol and acetone. These polyketals also hydrolyze on the timescale of days to weeks, depending on the choice of the diols used to make the polyketals. Finally, several diols, such as 1,4-cyclohexanedimethanol, have FDA approval for human use. Acetone is also on the list of substances generally recognized as safe (GRAS). Thus these polyketals also have the potential for human use. The polyketals have several properties that make them an attractive delivery vehicle for SOD to macrophages for treating inflammatory diseases. First, polyketals degrade into neutral compounds and may avoid the inflammatory problems associated with the acidic degradation products of polyesters and polyorthoesters. Second, polyketals also have the potential to disrupt phagosomes, by degrading in the phagosome and osmotically destabilizing it. Third, the ketal linkage has excellent hydrolysis kinetics for intracellular drug delivery, hydrolyzing significantly faster at the phagosomal pH of 4.5 versus the pH 7.4 environment of the blood.

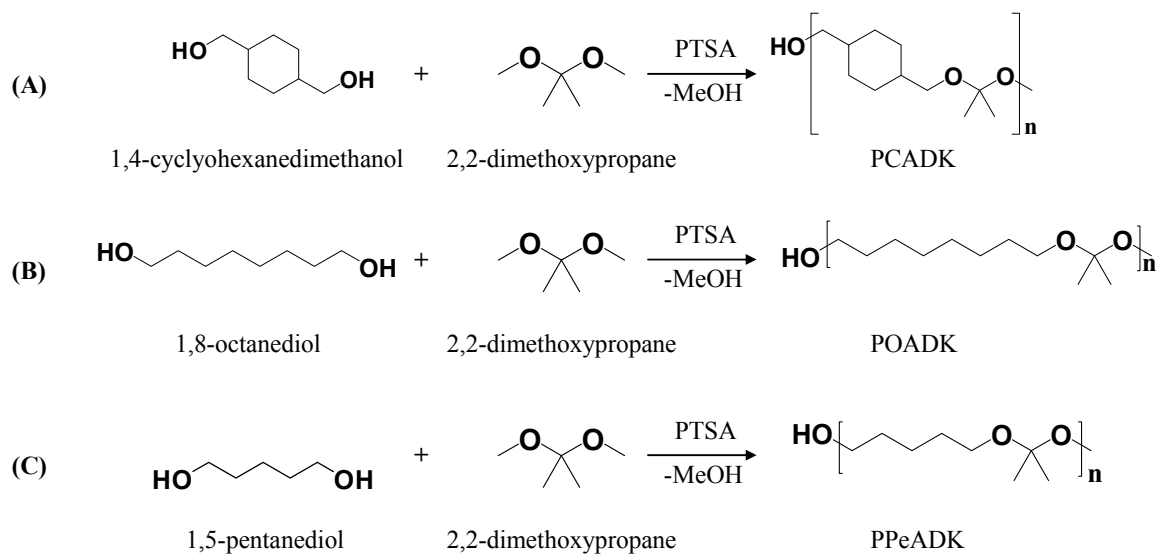


Figure 2.1. Stepwise polymerization based on the acetal exchange reaction between 1,4-cyclohexane dimethanol and 2,2-dimethoxypropane to produce PCADK. (B) Stepwise polymerization to produce poly(1,8-octane-acetone dimethylene ketal) (POADK). (C) Stepwise polymerization to produce poly(1,5-pentane-acetone dimethylene ketal) (PPeADK).

## 2.3 Experimental Methods

### Materials.

All chemicals were purchased from Sigma-Aldrich (St. Louis, MO) and were used as received unless otherwise specified. TIB-186 macrophage was obtained from the American Type Culture Collection (ATCC) (Manassas, VA).

### Synthesis of PCADK

The polyketal PCADK was synthesized in a 25 mL two-necked flask, connected to a short-path distilling head. The diol, either 1,4-cyclohexanedimethanol (1.04 g, 7.25 mmol) was dissolved in 10 mL of distilled benzene and kept at 100°C. Re-crystallized *p*-toluenesulfonic acid (5.5 mg, 0.029 mmol, Aldrich) dissolved in 550  $\mu$ L of ethyl acetate was then be added to the benzene solution. The ethyl acetate was allowed to distill off, and distilled 2,2-dimethoxypropane (900  $\mu$ L, 7.4 mmol) was added to initiate the reaction. Additional doses of 2,2-dimethoxypropane (500  $\mu$ L) and benzene (2 mL) were subsequently added to reaction every hour for 6 hours via a metering funnel to compensate for 2,2-dimethoxypropane and benzene that has been distilled off. After 8 hours, the reaction was stopped by lowering the reaction temperature to room temperature. 100  $\mu$ L triethylamine was immediately added to the reaction mixture to prevent degradation of polymer formed. Subsequently, the reaction mixture was poured in cold hexanes and stored in -20°C. After 12 hours, a white solid precipitation was collected by vacuum filter and dried under vacuum for 24 hours. Yield: 58%;  $^1\text{H}$  NMR ( $\delta$ , ppm,  $\text{CDCl}_3$ ): 3.26 – 3.18 (m, 4H,  $\text{C}_4\text{H}_8\text{CH}_2\text{O}$ ), 1.83, 1.63, 0.93 (m, 8H,  $\text{CH}_2$  from

cyclohexane, axial and equatorial), 1.32 (s, 6H, CH<sub>2</sub>OC(CH<sub>3</sub>)<sub>2</sub>OCH<sub>2</sub>); GPC: M<sub>n</sub> = 4080, PDI = 1.54.

### Synthesis of POADK

The polyketal POCDK was synthesized following the Procedures for synthesizing PCADK using 1,8-octanediol (1.06 g, 7.25 mmol) and 2,2-dimethoxypropane (900 μL, 7.4 mmol, and subsequent additions). When reaction was stopped, 50 mL of CH<sub>2</sub>Cl<sub>2</sub> was added to the reaction mixture and extracted against H<sub>2</sub>O three times. The organic phase was collected and dried with MgSO<sub>4</sub>. MgSO<sub>4</sub> solid was subsequently removed from the product mixture via a vacuum filter, and solvent was evaporated to give a viscous oil product which was then dried under vacuum for 24 hours. Yield: 83%; <sup>1</sup>H NMR (δ, ppm, CDCl<sub>3</sub>): 3.37 (t, 4H, COCH<sub>2</sub>(CH<sub>2</sub>)<sub>6</sub>CH<sub>2</sub>OC), 1.51 (t, 4H, COCH<sub>2</sub>CH<sub>2</sub>(CH<sub>2</sub>)<sub>4</sub>CH<sub>2</sub>CH<sub>2</sub>OC), 1.33 (s, 6H, CH<sub>2</sub>OC(CH<sub>3</sub>)<sub>2</sub>OCH<sub>2</sub>), 1.31 (m, 8H, COCH<sub>2</sub>CH<sub>2</sub>(CH<sub>2</sub>)<sub>4</sub>CH<sub>2</sub>CH<sub>2</sub>OC); GPC: M<sub>n</sub> = 1780, PDI = 2.24.

### Synthesis of PPeADK

The polyketal PPeCDK was synthesized following the procedure for PCADK using 1,8-pentanediol (754 mg, 7.25 mmol) and 2,2-dimethoxypropane (900 μL, 7.4 mmol, and subsequent additions). A viscous oil product was recovered following the procedures for POCDK. Yield: 78%; <sup>1</sup>H NMR (δ, ppm, CDCl<sub>3</sub>): 3.38 (t, 4H, COCH<sub>2</sub>(CH<sub>2</sub>)<sub>3</sub>CH<sub>2</sub>OC), 1.55 (t, 4H, COCH<sub>2</sub>CH<sub>2</sub>CH<sub>2</sub>CH<sub>2</sub>CH<sub>2</sub>OC), 1.33 (s, 6H, CH<sub>2</sub>OC(CH<sub>3</sub>)<sub>2</sub>OCH<sub>2</sub>), 1.32 (m, 2H, COCH<sub>2</sub>CH<sub>2</sub>CH<sub>2</sub>CH<sub>2</sub>CH<sub>2</sub>OC); GPC: M<sub>n</sub> = 1892, PDI = 2.13

### **Hydrolysis studies of PCADK, POADK, and PPeADK**

The hydrolysis of PCADK was measured by  $^1\text{H}$  NMR in buffered water at the pH values of 1.0 (100 mM HCl), 4.5 (100 mM AcOH) and 7.4 (100 mM  $\text{NaH}_2\text{PO}_4$ ) at  $37^\circ\text{C}$ . For each time point and pH, three samples were analyzed. For each sample, 20 mg of polymer (ground powder) was suspended in 1 mL of aqueous solution, at the appropriate pH, and shaken at 120 RPM and  $37^\circ\text{C}$ , using a Labline incubated shaker (Barnstead International, Dubuque, Iowa). At specific time points, the polymer samples were extracted with 1 mL of  $\text{CDCl}_3$ , and analyzed by  $^1\text{H}$  NMR, to determine the percent of ketal linkages that were hydrolyzed. Figure 2.2 describes the changes in the NMR spectrum of the polyketals, after hydrolysis of the ketal linkage. Upon hydrolysis of polyketals, the methylene group peaks were shifted from 3.2 ppm to 3.5 ppm due to conversion of acetal to hydroxyl groups as evidenced in Figure 2.2. In addition, as the polymers were hydrolyzed, the relative size of the dimethyl group (6b in Figure 1B) was progressively becoming smaller, and the peak was not present in the  $^1\text{H}$ -NMR spectrum of 1,4-cyclohexanedimethanol. The percentage of ketals hydrolyzed was defined as the ratio of peak integrals at 3.5 ppm to the total integrals of methylene peaks.

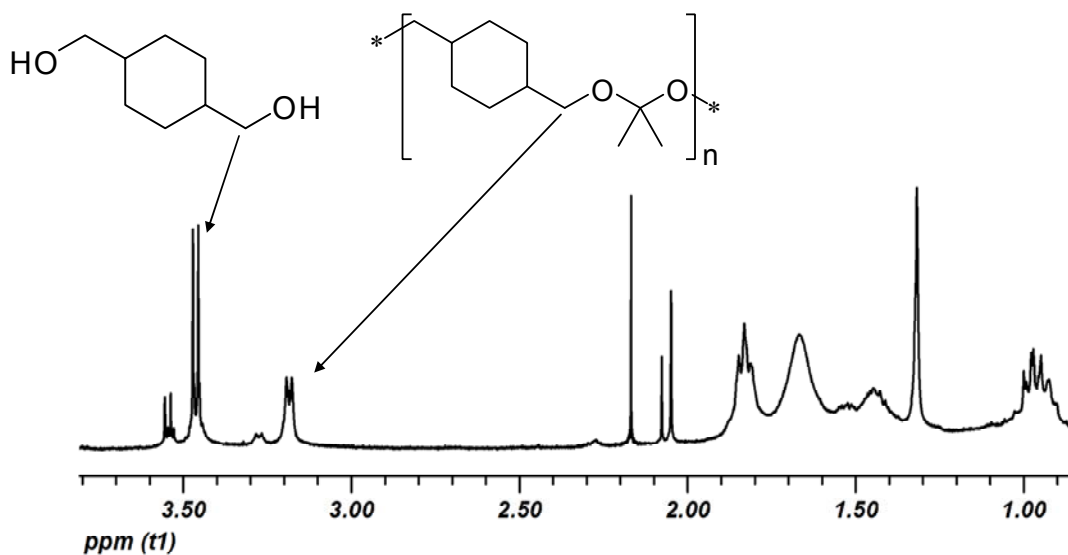


Figure 2.2.  $^1\text{H}$  NMR spectrum demonstrating hydrolysis of PCADK. The peaks for the methylene group; protons are shifted from 3.2 ppm to 3.5 ppm after hydrolysis of the ketal to a hydroxyl group.

### Formulation of microparticles with PCADK using emulsion methods

Microparticles were formulated with PCADK using an oil-in-water emulsion method. Briefly 50 mg of PCADK dissolved in 2 mL of  $\text{CHCl}_3$  (with 0.1% triethylamine) was added to 10 mL of pH 9 buffer solution (10 mM  $\text{NaHCO}_3$ ) containing various amounts of poly(vinyl alcohol) (PVA, 31–50 kDa) as the emulsifier. The particles were fabricated via two methods. (1) Sonication method: the oil-water mixture was shaken briefly and then sonicated for 2 to 3 min at 40 Watts (Branson Sonifier 250) to form a fine oil/water emulsion. (2) Homogenization method: the oil-water mixture was shaken briefly and then homogenized with a homogenizer (Fisher Scientific Powergen 500 with flat-bottom generator). For both methods, after a uniform suspension was obtained, the emulsion was stirred under for at least 3 hours to evaporate the solvent and produce a microparticle suspension. The particles were washed 3 times by removing

the supernatant following centrifugation. The particles were re-suspended and freeze-dried to give a solid powder.

### **Determination of particle size**

The size of PCADK microparticle was determined by dynamic light scattering setup (Brookhaven 90Plus particle sizer). DLS samples were prepared by taking 20  $\mu$ L of particle suspension (4mg/mL in pH 9 buffer) in 3 mL DI H<sub>2</sub>O and mixing thoroughly to obtain homogenous suspension. Each time the particle size was measured in triplicate at 25°C.

### **Scanning Electron Microscopy (SEM)**

SEM images were taken to confirm the morphology of lyophilized microparticle samples. Briefly, SEM samples were prepared by attaching lyophilized microparticles onto 12.7 mm diameter aluminum sample mounting stubs (Electron Microscopy Sciences, Hatfield, PA) using conductive double sided carbon discs (SPI Supplies, West Chester, PA). The samples were coated with a gold sputter coater (International Scientific Instruments, Prahran, Australia) for 2 minutes under argon atmosphere. The SEM samples were subsequently analyzed using a Hitachi S-800 scanning electro microscopy (Tokyo, Japan).

### **Determination of drug release profile from PCADK microparticles.**

Microparticles loaded with rhodamine B were fabricated using the same method outlined in formulation of PCADK microparticles. Briefly 50 mg of PCADK and 10 mg



of rhodamine B were dissolved in 2 mL of  $\text{CHCl}_3$ . The oil phase was then added to 10 mL of pH 9 buffer solution (10 mM  $\text{NaHCO}_3$ ) containing 10 mg of PVA. The mixture was either sonicated or homogenized, washed to remove all un-encapsulated rhodamine B, and freeze-dried to produce a solid powder. The dried particles were subsequently re-suspended in buffer with pH values of 1, 4.5, and 7.4. The suspensions were incubated under room temperature, and samples were taken out at various time points. Each sample was centrifuged down to collect the supernatant, which was analyzed using a Shimadzu RV-1700 UV-Visible spectrometer (Kyoto, Japan) or a Shimadzu RF-5301PC spectrofluorophotometer (Kyoto, Japan) with excitation wavelength of 550nm and emission wavelengths of 570 nm to 700 nm.

### **Formulation of PCAK microparticles encapsulating SOD**

An experimental protocol was developed based on procedures used to formulate SOD into PLGA-based microparticles. (Giovagnoli, Blasi et al. 2004) Briefly, a 100  $\mu\text{L}$  aqueous solution of SOD (40 mg/mL) was dispersed by homogenization (21,500 rpm, 30 sec) into 1.0 mL of methylene chloride, containing 125 mg of PCADK, generating a water-in-oil (w/o) emulsion. This w/o emulsion was then dripped into 5 mL of an 8% (w/v) aqueous polyvinyl alcohol (PVA) solution and was stirred with a homogenizer at 6,000 RPM for 5 minutes. The resulting w/o/w emulsion was then poured into 25 mL of pH 7.4 buffer, and was stirred for several hours, evaporating the methylene chloride. The resulting particles were isolated by centrifugation and freeze-dried, generating a white solid powder.

### **MTT reduction assay**

An MTT (3-(4,5-Dimethylthiazol-2-yl)-2,5-diphenyltetrazolium bromide) reduction assay was performed to measure the toxicity of PCADK microparticles. TIB-186 cells were seeded at a density of  $1 \times 10^5$  cells/well and incubated in 96-well plates for 24 hours. Cells were treated with PCADK microparticles at various particle concentrations (100 ng/mL – 1 mg/mL) and incubated for various durations (0.5 – 24 hours). Next, 20  $\mu$ L of MTT solution (5 mg/mL in PBS) was added to each well, and the cells were incubated for 2 hours. Then, 200  $\mu$ L of dimethyl sulfoxide (DMSO) was added to dissolve the resulting formazan crystals. After 10 minutes of incubation, the absorbance at 585 nm was measured using an Emax Microplate reader (Molecular Devices, Sunnyvale, CA). Percentage cell viability was calculated by comparing the absorbance of the control cells to that of PCADK microparticle-treated cells.

### **SOD activity assay**

The ability of SOD-PCADK microparticles to scavenge superoxide from macrophages was investigated in cell culture. TIB-186 macrophages ( $1 \times 10^5$  cells/well, 96 well plate) were incubated with either 0.1 mg/mL SOD-PCADK microparticles (1.14  $\mu$ g SOD in 0.1 mg microparticles), free SOD (1.14  $\mu$ g/mL SOD), or empty PCADK microparticles for 2 hours. The cells were washed 3 times and then stimulated with 0.2  $\mu$ g/mL phorbol myristate acetate (PMA) for 30 minutes. The superoxide production from these macrophages was then measured using a cytochrome c based assay, following the procedure of Voter et al. (Voter, Whitin et al. 2001).

## 2.4 Results

### Synthesis and characterization of PCADK

PCADK was synthesized using the acetal exchange reaction, on a multi-gram scale, generating polymers with a number-average molecular weight ( $M_n$ ) of approximately 4,080 Da. The acetal exchange reaction has been widely used in the field of organic synthesis for protecting primary and secondary alcohols, and therefore we hypothesized that this reaction should be capable of generating a wide variety of polymers with different properties by reacting different diols with 2,2-dimethoxypropane. An  $^1\text{H-NMR}$  spectrum and GPC spectrum are shown in Figure 2.3, confirming the chemical structure and molecular weight of PCADK.

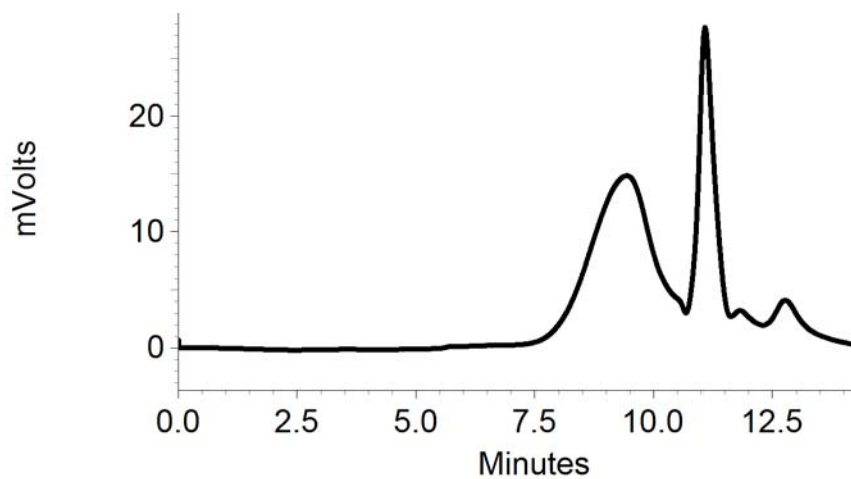
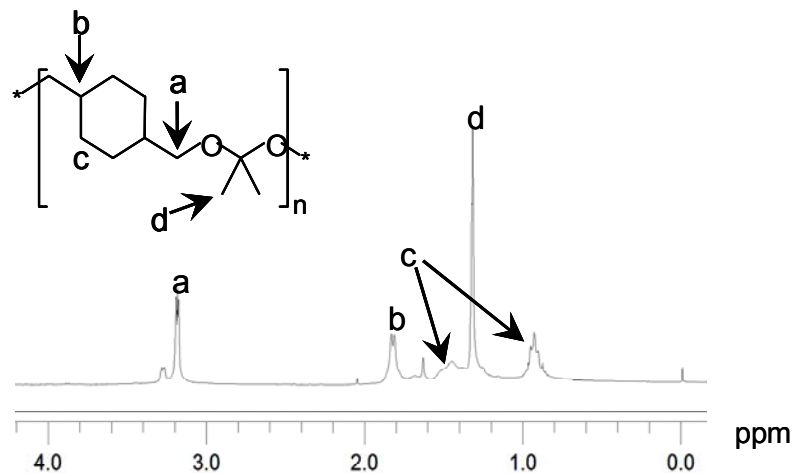


Figure 2.3. <sup>1</sup>H NMR and GPC spectrum of PCADK. (A) <sup>1</sup>H NMR spectrum of PCADK in CDCl<sub>3</sub>. (B) GPC trace of PCADK in THF, Y-axis indicates relative UV absorbance at 262 nm, M<sub>n</sub> = 4,080, polydispersity index (PDI) = 1.54.

## Synthesis of POADK

PCADK was synthesized on a multi-gram scale, generating polymers with an  $M_n$  of approximately 1,780. An  $^1\text{H}$ -NMR spectrum and GPC spectrum are shown in Figure 2.2, confirming its chemical structure and molecular weight (Figure 2.4).

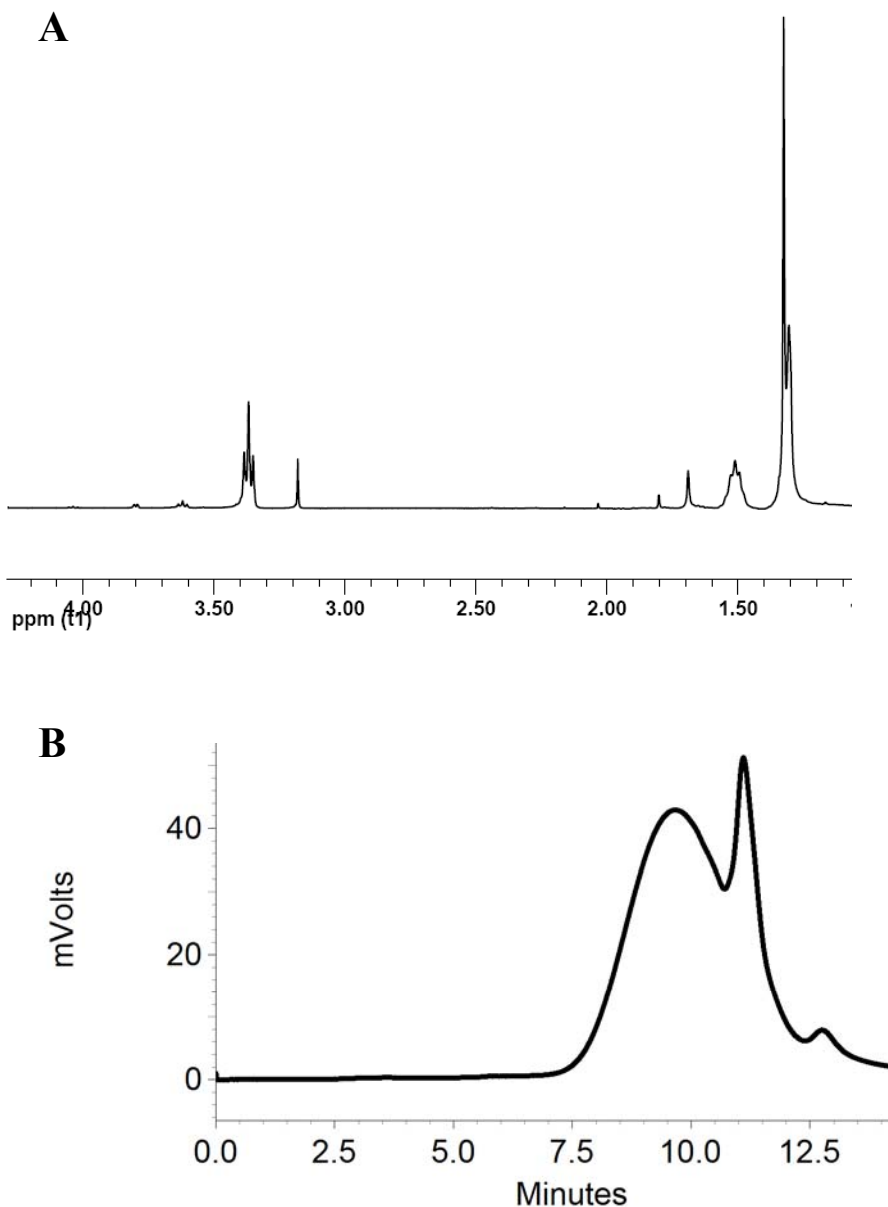


Figure 2.4.  $^1\text{H}$  NMR and GPC spectrum of POADK. (A)  $^1\text{H}$  NMR spectrum of POADK in  $\text{CDCl}_3$ . (B) GPC trace of PCADK in THF, Y-axis indicates relative UV absorbance at 262 nm,  $M_w = 1,780$ , polydispersity index (PDI) = 2.24.

## Synthesis of PPeADK

PCADK was synthesized on a multi-gram scale, generating polymers with an  $M_n$  of approximately 1,892. An  $^1\text{H}$ -NMR spectrum and GPC spectrum are shown in Figure 2.2, confirming its chemical structure and molecular weight (Figure 2.5).

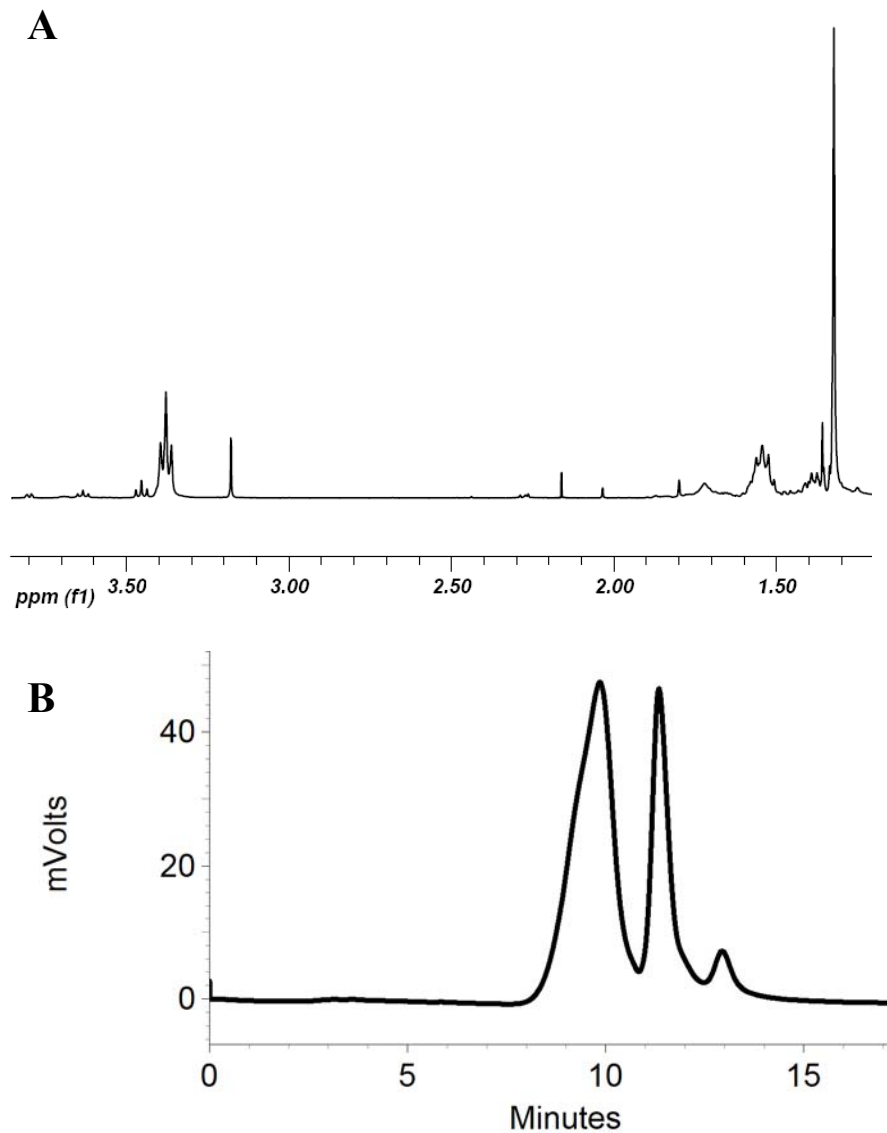


Figure 2.5.  $^1\text{H}$  NMR and GPC spectrum of PPeADK. (A)  $^1\text{H}$  NMR spectrum of POADK in  $\text{CDCl}_3$ . (B) GPC trace of PCADK in THF, Y-axis indicates relative UV absorbance at 262 nm,  $M_n = 1,892$ , polydispersity index (PDI) = 2.13.

### **Characterization of PCADK hydrolysis of PCADK**

The hydrolysis kinetics of biomaterials is key issue which determined their potential applications and toxicity. The hydrolysis kinetics of PCADK, POADK, and PPeADK were measured. Figure 2.6 demonstrates that the hydrolysis of the ketal linkages in these aliphatic polyketals is indeed pH-sensitive. For example, PCADK has a half-life of 24.1 days at pH 4.5, and an estimated half-life of over 4 years at pH 7.4. PPeADK was completely hydrolyzed in pH 4.5 and pH 7.4 within 3 hours.

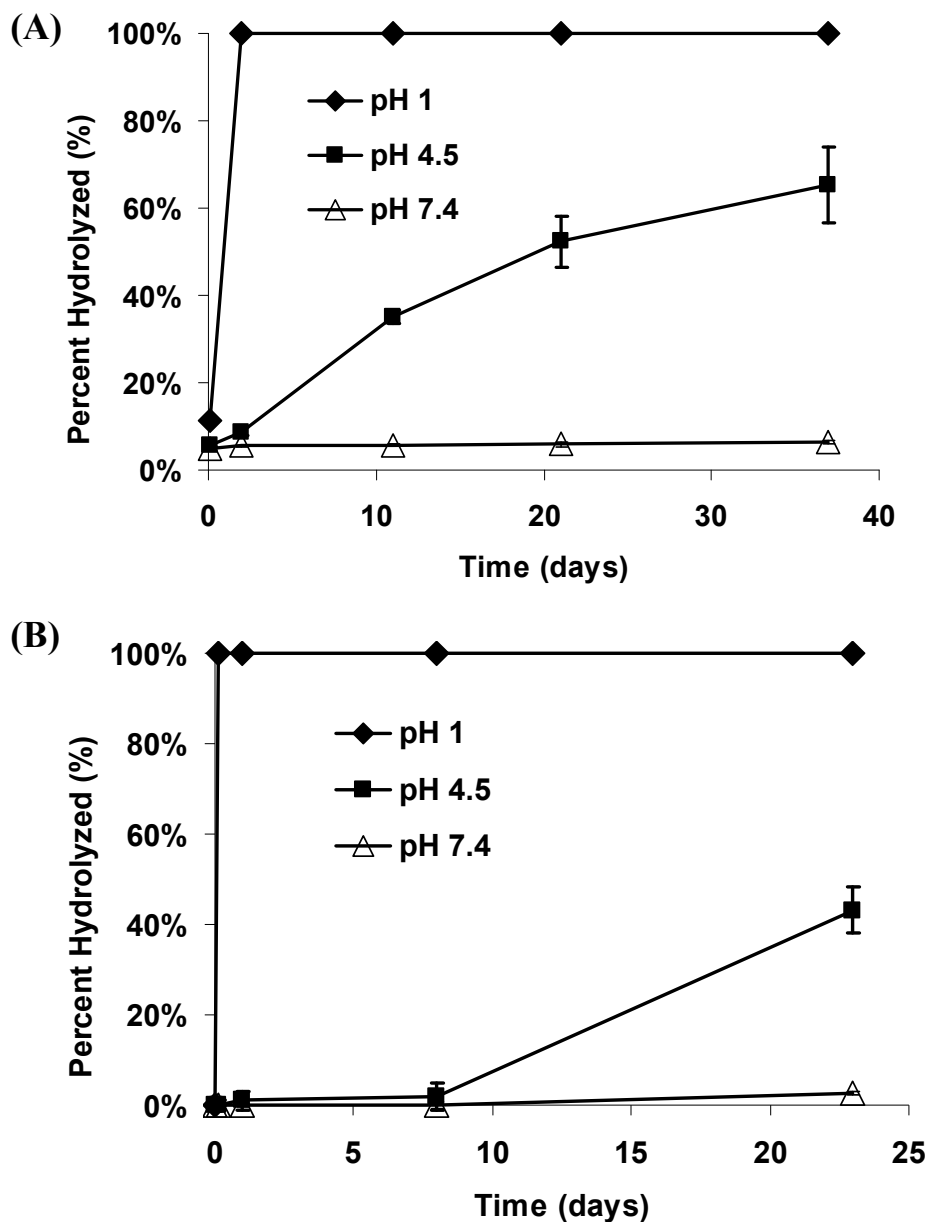


Figure 2.6. Hydrolysis kinetics of PCADK and POADK. (A) Hydrolysis of PCADK at 37°C. (B) Hydrolysis of POADK at 37°C. Data are presented as means  $\pm$  standard deviation, n = 3.

### Release of Rhodamine B from PCADK microparticles

Since the hydrolysis rate of PCADK follows a pH-dependent manner, it is reasonable to hypothesize that degradation of particles would also be pH-sensitive. Therefore the release of compounds encapsulated in the particles should also depend on



the pH of the surrounding environment. The pH-dependent drug release characteristic has many practical implications in biological systems. To further investigate the release profile of particles based on PCADK, a series of samples were prepared by re-suspending particles loaded with rhodamine B in buffers with pH values 1, 4.5, and 7.4.

The release kinetics of rhodamine B from PCADK microparticles at room temperature is shown in Figure 2.7. The particles were made by single emulsion and their diameter was approximately 5  $\mu\text{m}$  as measured by SEM. The amount of rhodamine B released was determined by measuring the fluorescence of the supernatant following centrifugation. The calculated half-lives were 1 day at pH 1.0, 5 days at pH 4.5, and greater than 15 days at pH 7.4.

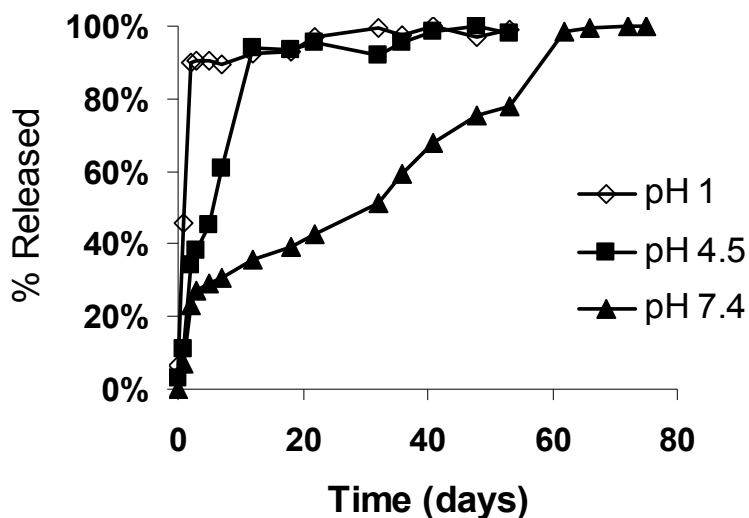


Figure 2.7. Release of rhodamine B from PCADK microparticles at room temperature.

### **Encapsulation of SOD in PCADK microparticles**

SOD was encapsulated into PCADK microparticles using a water/oil/water double emulsion procedure. An experimental protocol was developed based on procedures used to formulate SOD into PLGA-based microparticles. (Diesselhoff-den Dulk, Crofton et al. 1979; Giovagnoli, Blasi et al. 2004). The protein encapsulation efficiency of the SOD-PCADK microparticles was 36.7%, as determined by U.V. absorbance at 280 nm. An SEM image of the SOD-PCADK microparticles, shown in Figure 2.8, demonstrates that they are 3 to 15  $\mu\text{m}$  in diameter, which is suitable for both intracellular and extracellular delivery. This may be beneficial in the case of SOD delivery, because superoxide causes both intracellular toxicity and extracellular tissue damage during inflammation

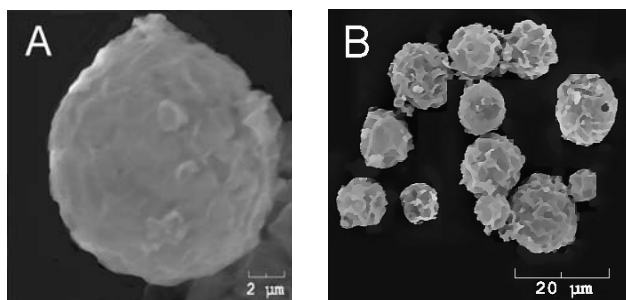


Figure 2.8. SEM images of SOD-PCADK microparticles. (A) 6,000x magnification, (B) 1,000x magnification. SEM images were taken on a Hitachi S-800.

### **Delivery of SOD-PCADK microparticles to macrophages in cell culture**

The ability of SOD-PCADK microparticles to scavenge superoxide from macrophages was investigated in cell culture. TIB-186 macrophages ( $1 \times 10^5$  cells/well, 96 well plate) were incubated with either 0.1 mg/mL SOD-PCADK microparticles (1.14  $\mu\text{g}$  SOD in 0.1 mg microparticles), free SOD (1.14  $\mu\text{g}/\text{mL}$  SOD), or empty PCADK

microparticles for 2 hours. The cells were washed 3 times and then stimulated with 0.2  $\mu\text{g/mL}$  phorbol myristate acetate (PMA) for 30 minutes. The superoxide production from these macrophages was then measured using a cytochrome c based assay, following the procedure of Voter et al. (Voter, Whitin et al. 2001). Figure 2.9 demonstrates that free SOD by itself caused very little inhibition of superoxide production, whereas SOD-PCADK microparticles caused a 60% reduction in superoxide production. Empty microparticles also reduced superoxide production by macrophages by approximately 20%. This is most likely due to the toxicity of the particles, which caused approximately 20% toxicity under these experimental conditions (0.1 mg/mL for 2 hrs) as determined by an MTT assay (Figure 2.10). These data demonstrate that PCADK microparticles significantly improved the ability of SOD to scavenge superoxide generated by macrophages.

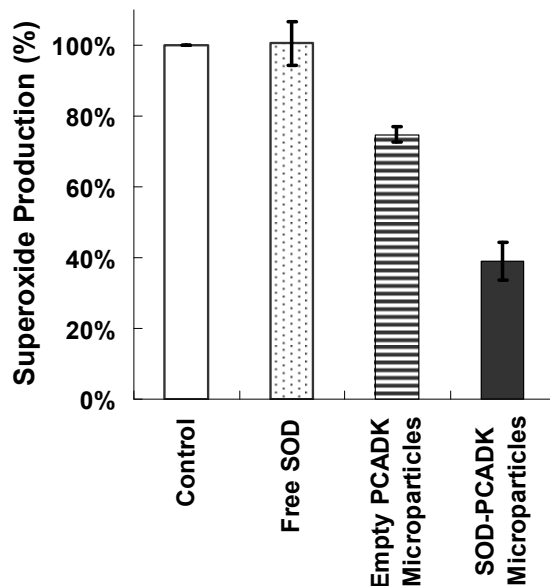


Figure 2.9. PCADK microparticles enhance the delivery of SOD to macrophages. Macrophages were incubated with either SOD-PCADK microparticles (black bar), empty PCADK microparticles (horizontal stripe), free SOD (dotted bar), and media only (white bar).  $n=3$ ,  $p<0.05$ .

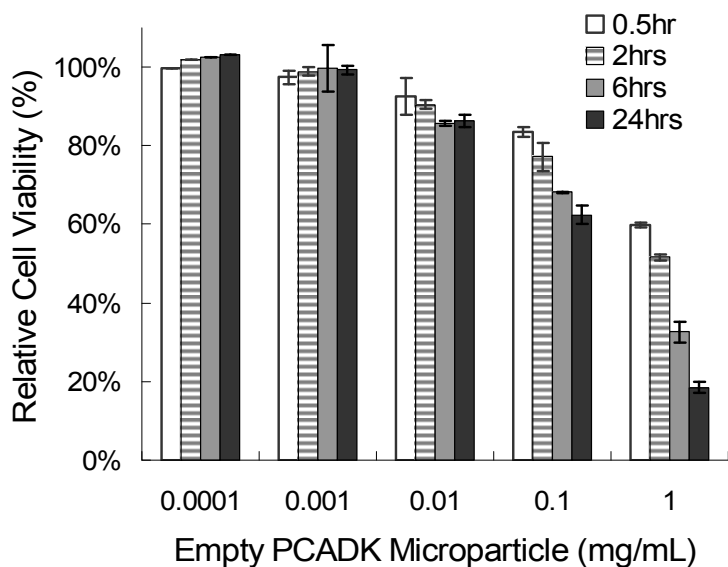


Figure 2.10. Cell viability of TIB-186 macrophages after incubation with PCADK microparticles; 0.5 h (white bar), 2 h (horizontal stripe), 6 h (gray bar), 24 h (black bar) for statistical analysis, 3 independent cell viabilities were measured for each sample.

### **Biocompatibility of polyketal**

PCADK degrades into neutral, biocompatible compounds, whereas PLGA degrades into acidic byproducts; therefore the inflammatory responses caused by PCADK microparticles should be less than PLGA microparticles. In collaboration with Dr. Michael Davis's laboratory at Emory University, the inflammatory responses caused by injection of PCADK microparticles were tested in mice. PLGA microparticles were also injected into the same mice for comparison to polyketals. We injected 200  $\mu$ L of PCADK microparticles (25 mg/mL) or PLGA of the same quantity to the leg muscle of C57BL/6J mice. The leg muscle tissues were isolated and fixed in 4% paraformaldehyde three days after the injection. Sections were stained with a fluorescently tagged anti-mouse CD 45 antibody, which is a maker for inflammatory responses. DAPI was also used to mark the presence of cells. Figure 2.11 demonstrates that PLGA elicited a

significant amount of inflammation, where as PCADK did not cause the same level of inflammatory responses as PLGA.

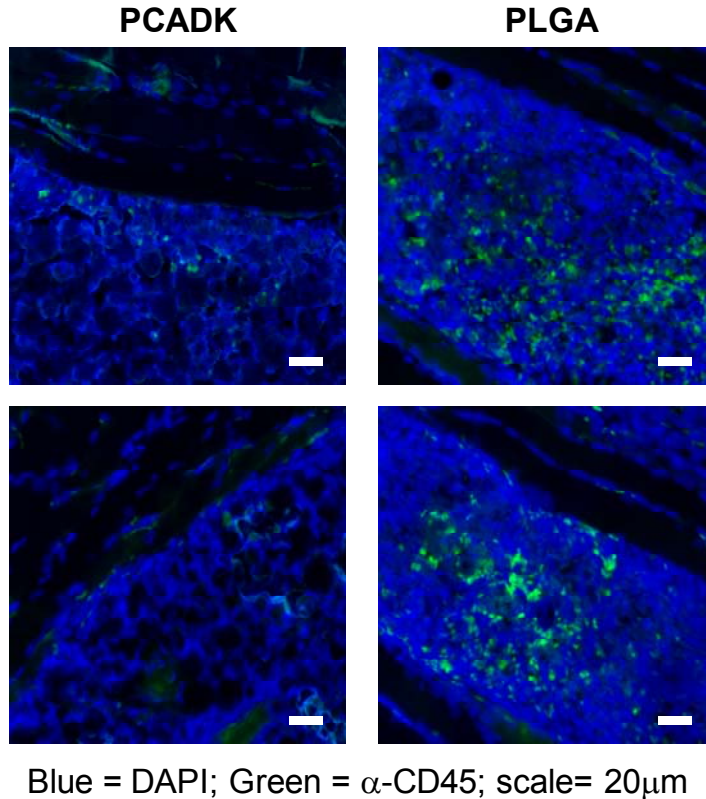


Figure 2.11. Inflammatory response to injected PCADK or PLGA microparticles. Blue = DAPI, green =  $\alpha$ -CD45, scale bar = 20  $\mu$ m.

### Stability of SOD in PCADK microparticles

The activity of SOD in PCADK microparticles was determined using an SOD assay kit (Fluka, SOD determination kit 19160, St Louis, MO), using the protocol provided in the kit. These results are presented in Figure 2.12 and demonstrate that SOD retains its activity after encapsulation within the particles (compare dark versus white

bars).

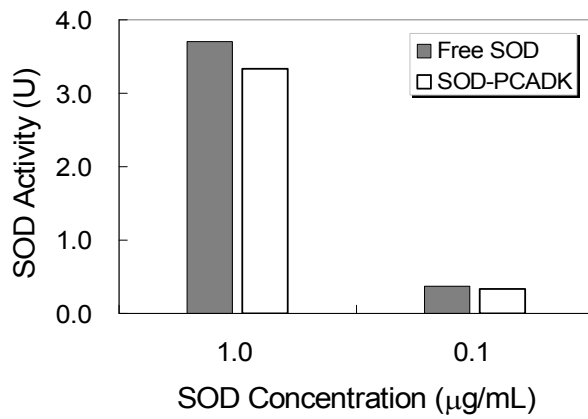


Figure 2.12. Stability of SOD in PCADK microparticles. Free SOD (white bar), SOD in PCADK microparticles (dark bar)

## 2.5 Discussions

### Synthesis of aliphatic polyketals

The synthesis of polymers, which degrade under physiologic conditions into low molecular weight compounds, has been intensely under investigation in recent years. The majority of degradable polymers are generated by ring opening polymerization, which generates ester or amide linkages. However these chemistries are not ideal for the development of drug delivery vehicles designed to target therapeutics to macrophages and treat inflammatory diseases, due to their toxic and acidic degradation products and relatively slow degradation times. In this Chapter, I demonstrate that the acetal exchange reaction can be used to synthesize a variety of aliphatic polyketals, which degrade into neutral, membrane permeable, and biocompatible compounds. A variety of primary dialcohols were used to generate polyketals with the acetal exchange reaction. For example, 1,4-cyclohexanedimethanol, 1,8-octanediol, and 1,5-pentane diol all generated polymers whose number-average molecular weight ranges from 2,000-4,000 Da. The relatively low molecular weights generated by this polymerization are attributed to the nature of step-growth polymerization employed in making these polyketals. In step growth polymerization, the stoichiometry of the reaction is a critical issue; slight deviation from the exact stoichiometry ratio of the two reactants will result in significant molecular weight decrease in the polymer synthesized. Although an equal molar ratio of diol to 2,2-dimethoxy propane was initially added in the reaction feeds, a 1:1 ratio was not possible to maintain during the polymerization process. The reason is that the polymerization was performed at 100°C, which is needed to remove methanol byproduct to drive the reaction to favor the polymer; however, this would also cause 2,2-

dimethoxypropane to distill off, which has a boiling point at 80°C. To compensate for the loss of 2,2-dimethoxypropane, additional doses of 2,2-dimethoxypropane were continuously added to the reaction throughout the polymerization. Other polymerization techniques were attempted, in which excess 2,2 dimethoxy propane was not added, at either 80°C or 100°C; in both cases no polymerization was observed, presumably due to the removal of the 2,2-dimethoxypropane. Importantly, the acetal exchange reaction could also be scaled up to a multi-gram synthesis, a 6 gram batch PCADK was synthesized with a 65% yield.

### **Hydrolysis of aliphatic polyketals**

The hydrolysis kinetics of biomaterials is key issue which determined their potential applications and toxicity. Obtaining the optimal hydrolysis kinetics for polyester based biomaterials, to suppress a phagocytosis induced inflammatory response has been challenging. Phagocytosis of PLGA causes the secretion of inflammatory cytokines due to two phenomena, (1) accumulation of PLGA within macrophages, as do all other types of non-degradable particles, because PLGA undergoes slow base-catalyzed hydrolysis, and (2) their acidic degradation products also cause macrophage toxicity and an inflammatory response. Importantly, PLGA particles which degrade rapidly could avoid the inflammatory effects of particle accumulation but may also generate a more severe inflammatory response because they are producing large quantities of acid at a rapid rate.

The polyketals have the potential to avoid the inflammatory problems of PLGA, their degradation products are acetone and diols, which are neutral and membrane





## **Biocompatibility of aliphatic polyketals**

PPADK was the first reported synthesis of polyketal, through the reaction of 2,2-dimethoxypropane and 1,4-benzenedimethanol (Heffernan and Murthy 2005). While PPADK has many of the characteristics needed for drug delivery, its degradation products have potential toxicity. PCADK, in contrast, degrades into 1,4-cyclohexanedimethanol and acetone, both of which have excellent toxicity profiles. In contrast to PPADK, PCADK degrades into acetone, a compound on the FDA GRAS (Generally Recognized As Safe) list, and 1,4-cyclohexanedimethanol, a compound with an excellent toxicity profile. According to the Material Safety Data Sheets (MSDS) for the degradation products of PCADK, the LD50 of 1,4-cyclohexanedimethanol is 3,200 mg/kg for an oral dosage in rats. In addition, 1,4-cyclohexanedimethanol is a commonly used food packaging material and has approval for human consumption as an indirect food additive (Food Contact Notification (FCN) No. 000087). 1,4-cyclohexanedimethanol is rapidly excreted from the blood, can diffuse through biological membranes, and is generally not metabolized by biological enzymes. For example, DiVencenzo et al. fed mice 400 mg/kg 1,4-cyclohexanedimethanol and observed that over 95% of the ingested dose was excreted unaltered after 2 days, 0.03% was respired as CO<sub>2</sub>, and 0.4% remained in the carcass after 48 hours (DiVincenzo and Ziegler 1980). They also observed that the half life of 1,4-cyclohexanedimethanol was 13 minutes. The major metabolic product of this compound is 4-hydroxymethyl-cyclohexanecarboxylic acid. The excellent toxicity profile of 1,4-cyclohexanedimethanol makes it an ideal candidate to be used in synthesizing biodegradable polymers.

## **Microparticle Formation with PCADK**

The polymer PCADK was chosen for further investigation for its ability to form microparticles and its biocompatible degradation products 1,4-cyclohexanedimethanol, which has been used extensively in the food packing industry. Microparticles based on PCADK were fabricated using a single emulsion method. The size of these microparticles was 300-500 nm in diameter via sonication emulsification and 4-6  $\mu\text{m}$  in diameter via homogenization emulsification. Particles with 300-500 nm size range are suitable for phagocytosis by macrophages and antigen presenting cells. On the other hand, when homogenization was used to form the emulsion, the size of the particles were significantly larger as compared to particles formed from sonication procedures. This indicates that an important factor controlling the size of the particles is the method of emulsification. Hence we speculate that by controlling the type and intensity of the emulsification procedure, the size of particles can be manipulated to obtain particles with sizes suitable for various biological applications.

## **SOD delivery with PCADK microparticles**

As discussed in Chapter 1, ROS produced by macrophages plays a central role in mediating inflammatory diseases, such as acute liver failure, arthritis, and sepsis (Droge 2002; Hitchon and El-Gabalawy 2004; Kamata, Honda et al. 2005; Victor, Rocha et al. 2005). SOD is an enzyme that scavenges reactive oxygen species and has the potential to treat inflammatory diseases by suppressing ROS production by macrophages. Unfortunately, clinical trials with free SOD have been ineffective, due to its membrane impermeability, and SOD delivery vehicles are therefore being investigated. Polymeric

microparticles, based on PLGA and polycaprolactone, are also being investigated for the delivery of SOD (Liu, Ge et al. 2003; Giovagnoli, Blasi et al. 2004; Giovagnoli, Luca et al. 2005). Although polyester-based microparticles have an excellent shelf-life and well characterized degradation products, their application for the treatment of inflammatory diseases is potentially problematic because their acidic degradation products can cause inflammation (Dailey, Jekel et al. 2006). Polymeric microparticles based on acid degradable polymers also have the potential to enhance the delivery of SOD to macrophages. In our studies, SOD was encapsulated into PCADK-based microparticles via a double emulsion procedure. Cell culture experiments with macrophages demonstrated that these microparticles dramatically improved the ability of SOD to scavenge superoxide produced by macrophages. Based on our results, we anticipate widespread interest in PCADK for drug delivery, based on its acid sensitivity, well characterized degradation products, and ease of synthesis.

# **CHAPTER 3**

## **DEVELOPMENT OF POLYKETAL COPOLYMERS WITH SUITABLE PROPERTIES FOR TREATING ACUTE INFLAMMATORY DISEASES**

### **3.1 Abstract**

Acute inflammatory diseases are a major cause of death in the world, and effective treatments are greatly needed. Macrophages play a central role in mediating acute inflammatory diseases; therefore, there is currently great interest in developing drug delivery vehicles that can target therapeutics to macrophages. Microparticles formulated from aliphatic polyketals have great potential to enhance the treatment of acute inflammatory diseases, due to their ability to passively target therapeutics to macrophages, their acid sensitivity, and their biocompatible degradation products. However, existing aliphatic polyketals are unsuitable for treating acute inflammatory diseases because they require weeks to hydrolyze, and strategies for accelerating their hydrolysis kinetics are greatly needed. In this Chapter, I demonstrate that the hydrolysis kinetics of aliphatic polyketals can be accelerated by increasing their hydrophilic/hydrophobic balance. Aliphatic polyketals of varying hydrophobicity were synthesized, via the acetal exchange reaction, and their hydrolysis kinetics were investigated at the pH values of 4.5 and 7.4. A polyketal termed PK3 was developed, which had the hydrolysis kinetics suitable for treating acute inflammatory diseases. PK3 has a hydrolysis half-life of 2 days at pH 4.5, but requires several weeks to hydrolyze at pH 7.4. Microparticles were formulated with PK3, which encapsulated the anti-

inflammatory drug, imatinib. *In vivo* experiments demonstrated that PK3 microparticles were able to significantly improve the efficacy of imatinib in treating acute liver failure. We anticipate that aliphatic polyketals will have numerous applications for the treatment of acute inflammatory diseases, given their pH sensitivity, tunable hydrolysis kinetics, and biocompatible degradation products.

### 3.2 Introduction

Acute inflammatory diseases such as acute lung injury and acute liver failure cause millions of death each year, and effective treatments are greatly needed (Hudson and Steinberg 1999; Angus, Linde-Zwirble et al. 2001). Pro-inflammatory cytokines secreted by macrophages play a central role in mediating acute inflammatory diseases, and drug delivery vehicles that can target therapeutics to macrophages have great clinical potential (Goodman, Pugin et al. 2003). A key drug delivery requirement for the treatment of many acute inflammatory diseases is fast release of drugs to diseased organs, within several hours. This is because at the time of patient diagnosis, significant tissue damage has already occurred, and organ function is rapidly deteriorating (O'Grady and Schalm 1993). It has been challenging to develop clinically acceptable drug delivery vehicles that can target therapeutics to macrophages and release them rapidly. Liposomes are a potential delivery vehicle for treating acute inflammatory diseases, due to their ability to target macrophages (Higuchi, Kawakami et al. 2007). However, their serum instability and poor storage properties have slowed their progress in clinical trials. Microparticles, based on biodegradable polymers, also have potential to enhance the treatment of acute inflammatory diseases. Microparticles can be freeze-dried, have an excellent shelf-life, and can also passively target therapeutics to macrophages (Zender, Hutker et al. 2003; Wullaert, van Loo et al. 2007). However, currently used biomaterials for drug delivery are predominantly based on polyesters, which are potentially problematic for treating acute inflammatory diseases because of their slow hydrolysis kinetics and acidic degradation products, which themselves frequently cause inflammation (Anderson and Shive 1997; Fu, Pack et al. 2000).

Microparticles formulated from polyketals are a new drug delivery vehicle, which degrade into neutral compounds comprised of acetone and diols, and should therefore avoid the inflammatory problems associated with polyester-based materials (Fu, Pack et al. 2000; Gopferich and Tessmar 2002; Kumar, Langer et al. 2002; Heffernan and Murthy 2005; Lee, Yang et al. 2007). At present, only two polyketals have been synthesized for drug delivery, poly-(1,4-phenyleneacetone dimethylene ketal) (PPADK) and poly(cyclohexane-1,4-diyl acetone dimethylene ketal) (PCADK) (Heffernan and Murthy 2005; Lee, Yang et al. 2007). PPADK has excellent hydrolysis kinetics for treating acute inflammatory diseases, having a half-life of 35 hours at pH 5.0, but degrades into benzene dimethanol, a compound with potential toxicity, due to its aromatic ring. PCADK is an aliphatic polyketal, which degrades into acetone and 1,4-cyclohexanedimethanol, both of which have excellent biocompatibility. However, PCADK has a hydrolysis half-life of 24 days at pH 4.5, which is too slow for applications involving the treatment of acute inflammatory diseases, and therefore strategies that can accelerate its hydrolysis kinetics are greatly needed.

In this Chapter, I demonstrate that the hydrolysis kinetics of PCADK derived aliphatic polyketals could be accelerated by increasing their hydrophilic/hydrophobic balance. Using this principle, we were able to generate a family of polyketal copolymer with tunable hydrolysis kinetics (Figure 3.1).



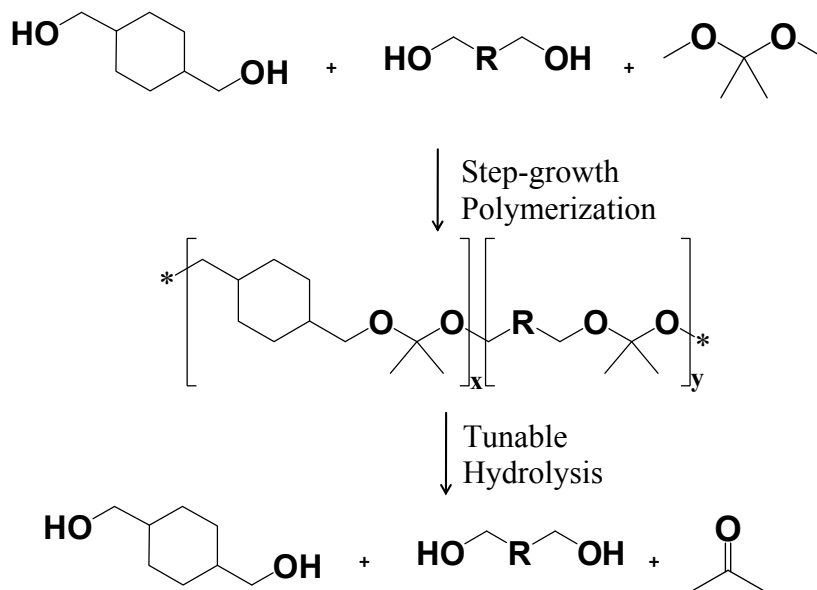


Figure 3.1. Synthesis of polyketal copolymers from 1,4-cyclohexanedimethanol, a second diol, and 2,2-dimethoxypropane. Hydrolysis kinetics of polyketals can be controlled by manipulating the hydrophilicity of the polyketals through copolymerizing 1,4-cyclohexanedimethanol with a more hydrophilic diol.

One particular polyketal copolymer, PK3, had a hydrolysis half-life of 2 days at pH 4.5 but several weeks at pH 7.4. Microparticles formulated from PK3 should therefore be suitable for treating acute inflammatory diseases because they should hydrolyze and release therapeutics rapidly in the phagolysosomes of macrophages, but remain stable at physiological pH. PK3 was used to generate microparticles 1-5 microns in size, which encapsulated the NF $\kappa$ B inhibitor imatinib, using a solvent evaporation procedure. The therapeutic efficacy of these PK3-imatinib microparticles was investigated in mice, using a Conavalin A (Con A) model of acute liver failure (Figure 3.2). The results from these experiments demonstrate that imatinib-loaded PK3 microparticles significantly enhanced the therapeutic efficacy of imatinib, presumably due to their accumulation in Kupffer cells.

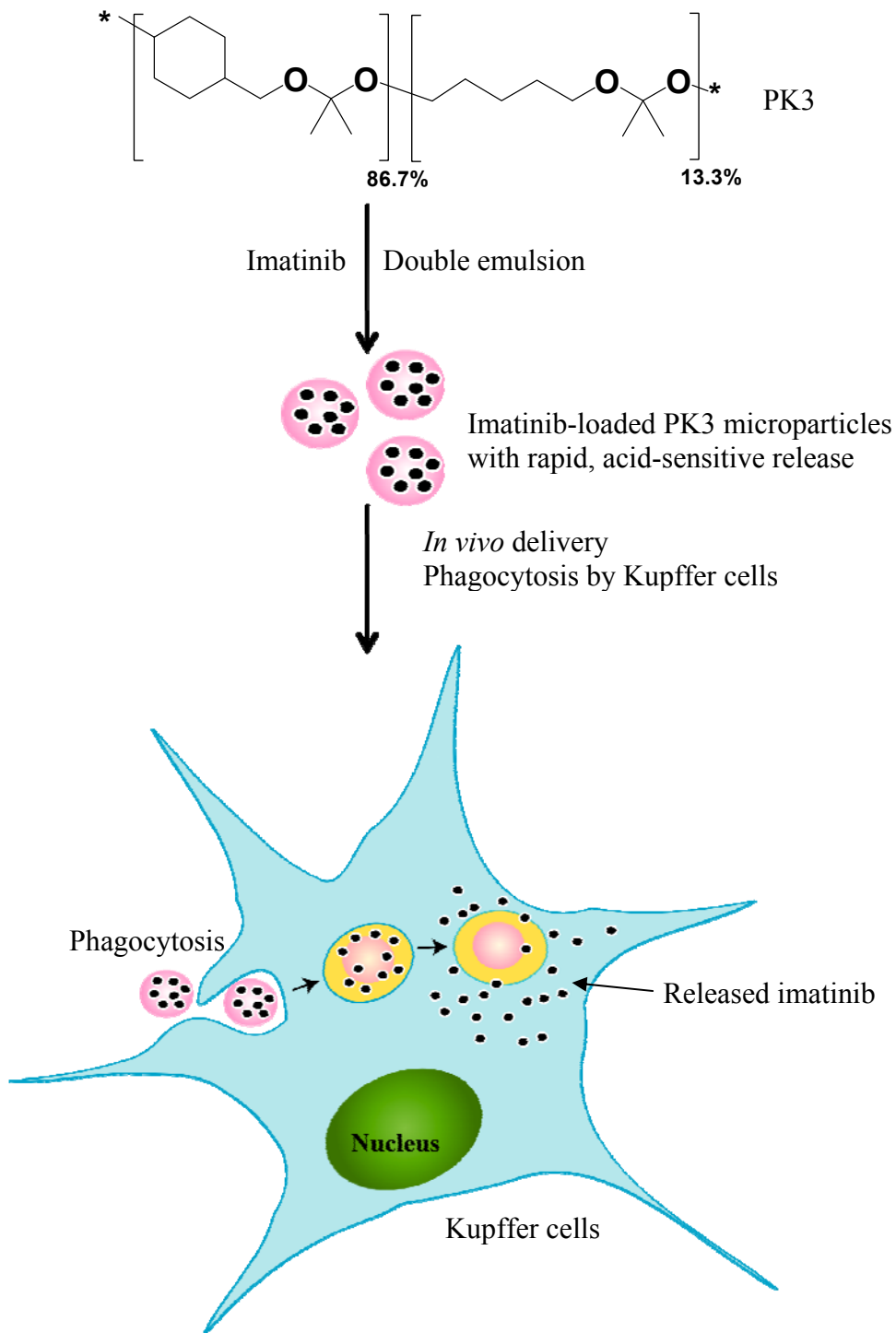


Figure 3.2. PK3, a new biomaterial for treating acute inflammatory diseases. PK3 is a new polyketal copolymer, which hydrolyzes rapidly at the acidic pH of the macrophage phagosome. PK3 is designed to deliver therapeutics to liver macrophages and enhance the treatment of acute liver failure. PK3 microparticles were capable of enhancing the delivery of imatinib in mice suffering from acute liver failure.

### 3.3 Experimental Methods

#### Materials.

All chemicals were purchased from Sigma-Aldrich (St. Louis, MO) and were used as received unless otherwise specified. Benzene and 2,2-dimethoxypropane were purified by distillation. Imatinib was a gift from Novartis.

#### Animals.

Male C57/BL6 mice were purchased from Jackson Laboratory (Bar Harbor, ME). All animal experiments were approved by the Institutional Animal Care and Use Committee (IACUC) of the University of Rochester Medical Center.

#### Synthesis of polyketal copolymers.

Polyketal copolymers were synthesized in a 25 mL two-necked flask, connected to a short-path distilling head. The diols, 1,4-cyclohexanedimethanol (1.04 g, 7.25 mmol) and, either 1,4-butanediol, 1,5-pentanediol, 1,6-hexanediol, or 1,8-octanediol were dissolved in 20 mL of distilled benzene and kept at 100 °C. Re-crystallized *p*-toluenesulfonic acid (5.5 mg, 0.029 mmol) was dissolved in ethyl acetate (500 µL) and added to the benzene solution. The ethyl acetate was distilled off, and the polymerization reaction was initiated by the addition of 2,2-dimethoxypropane (equal molar to the two diols combined). Additional doses of 2,2-dimethoxypropane (500 µL) and benzene (2 mL) were subsequently added to the reaction, every hour for six hours, via a metering funnel, to compensate for 2,2-dimethoxypropane and benzene that had distilled off. After 24 hours, the reaction was stopped with triethylamine (100 µL). The copolymers were

isolated by precipitation into cold hexanes and analyzed by  $^1\text{H}$ -NMR and GPC. In general the resulting polymers had number average molecular weights between 2000 to 3000 Da. Table 1 lists the compositions and molecular weights of the polyketal copolymers synthesized.  $^1\text{H}$  NMR spectra were obtained from a Varian Mercury VX 400 MHz NMR spectrometer (Palo Alto, CA) using  $\text{CDCl}_3$  as the solvent. PK1  $^1\text{H}$  NMR (400 MHz,  $\text{CDCl}_3$ ,  $\delta$ ): 3.4 – 3.18 (m, 4H,  $\text{CH}_2$ ), 1.66 (s, 1.9H, CH), 1.85 – 0.93 (m, 8H,  $\text{CH}_2$ ), and 1.32 (s, 6H,  $\text{CH}_3$ ); PK2  $^1\text{H}$  NMR (400 MHz,  $\text{CDCl}_3$ ,  $\delta$ ): 3.4 – 3.18 (m, 4H,  $\text{CH}_2$ ), 1.66 (s, 1.8H, CH), 1.85 – 0.93 (m, 8H,  $\text{CH}_2$ ), and 1.32 (s, 6H,  $\text{CH}_3$ ); PK3  $^1\text{H}$  NMR (400 MHz,  $\text{CDCl}_3$ ,  $\delta$ ): 3.4 – 3.18 (m, 4H,  $\text{CH}_2$ ), 1.64 (s, 1.7H, CH), 1.85 – 0.93 (m, 8.2H,  $\text{CH}_2$ ), and 1.32 (s, 6H,  $\text{CH}_3$ ); PK4  $^1\text{H}$  NMR (400 MHz,  $\text{CDCl}_3$ ,  $\delta$ ): 3.4 – 3.18 (m, 4H,  $\text{CH}_2$ ), 1.68 (s, 2H, CH), 1.85 – 0.93 (m, 8H,  $\text{CH}_2$ ), and 1.32 (s, 6H,  $\text{CH}_3$ ); PK5  $^1\text{H}$  NMR (400 MHz,  $\text{CDCl}_3$ ,  $\delta$ ): 3.4 – 3.18 (m, 4H,  $\text{CH}_2$ ), 1.67 (s, 1.8H, CH), 1.85 – 0.93 (m, 8H,  $\text{CH}_2$ ), and 1.32 (s, 6H,  $\text{CH}_3$ ); PK6  $^1\text{H}$  NMR (400 MHz,  $\text{CDCl}_3$ ,  $\delta$ ): 3.4 – 3.18 (m, 4H,  $\text{CH}_2$ ), 1.68 (s, 1.8H, CH), 1.85 – 0.93 (m, 8H,  $\text{CH}_2$ ), and 1.32 (s, 6H,  $\text{CH}_3$ ).

### **Gel permeation chromatography.**

The molecular weights of the polyketal copolymers were determined by gel permeation chromatography (GPC) using a Shimadzu system (Kyoto, Japan) equipped with a UV detector. Tetrahydrofuran was used as the mobile phase at a flow rate of 1 mL/min. Polystyrene standards (Peak Mw = 1060, 2970, and 10680) from Polymer Laboratories (Amherst, MA) were used to establish a molecular weight calibration curve.

### **Hydrolysis of polyketal copolymers.**

The hydrolysis of the polyketal copolymers was measured according to the procedures of Lee *et al* (Lee, Yang et al. 2007). Briefly polymer samples (20 mg) were placed in buffered water (1 mL) at the pH values of 4.5 (100 mM AcOH) and 7.4 (100 mM Na<sub>2</sub>HPO<sub>4</sub>) at 37 °C. The polymer samples were mixed by gentle shaking, and at specific time points, were extracted into CDCl<sub>3</sub> (1 mL). The CDCl<sub>3</sub> phase was isolated and analyzed by <sup>1</sup>H NMR, to determine the percent hydrolysis.

### **Release kinetics of rhodamine B from PK3 microparticles.**

Rhodamine B was encapsulated in PK3 microparticles using single emulsion procedures. Rhodamine B-loaded PK3 microparticles (10 mg) were suspended in pH 4.5 and pH 7.4 buffer solutions (10 mL). The suspensions were kept at 37°C under gentle shaking. At specific time points, the suspensions (100 µL) were centrifuged at 10,000 x g for 2 minutes to remove unhydrolyzed particles. The supernatant (3 µL) was then diluted in pH 7.4 buffer (3 mL), which was then analyzed by a Shimadzu spectrofluorophotometer (Kyoto, Japan) to quantify the relative concentration of rhodamine B released from the PK3 microparticles (excitation wavelength = 556 nm, emission wavelength = 573 nm).

### **Formulation of imatinib-loaded PK3 microparticles.**

Imatinib-loaded microparticles were formulated from PK3 using a modified water/oil/water emulsion method. Briefly, PK3 (100mg) was dissolved in dichloromethane (1 mL), and in a separate vial imatinib (40 mg) was dissolved in

deionized (DI) water (400  $\mu$ L). The aqueous solution of imatinib was mixed with the PK3 solution, and sonicated for 60 seconds (Misonix Incorporated, Farmigdale, NY). The sonicated mixture was then immersed in liquid nitrogen for 15 seconds, and a 5% w/w PVA solution (pH 7.45, 12 mL) was added to it. This mixture was homogenized for 120 seconds with a Powergen 500 homogenizer (Fisher Scientific, Waltham, MA), and then transferred to a beaker containing 1% w/w PVA (pH 7.4, 40 mL). This solution was stirred for 3 hours with a magnetic stir bar to evaporate the organic solvent. The particles were isolated by centrifuging at 10,000 x g for 15 min, washed twice with PBS buffer (15 mL) and freeze-dried.

#### **Scanning Electron Microscopy (SEM).**

SEM images were taken to analyze the morphology of the polyketal microparticles. Briefly, SEM samples were prepared by attaching lyophilized particles onto 12.7 mm diameter aluminum sample mounting stubs (Electron Microscopy Sciences, Hatifield, PA), using conductive double sided carbon discs (SPI Supplies, West Chester, PA). The samples were coated with a gold sputter coater (International Scientific Instruments, Prahran, Australia) for 2 minutes under an argon atmosphere. The SEM samples were subsequently analyzed using a Hitachi S-800 scanning electron microscope (Tokyo, Japan).

#### **Determination of imatinib loading in PK3 microparticles.**

The loading of imatinib in PK3 microparticles was determined by Ultraviolet-visible (UV-Vis) spectrometry. A calibration curve for imatinib was established at 268

nm, with a Shimadzu UV-1700 spectrometer (Kyoto, Japan) in pH 7.4 buffer. Imatinib-loaded PK3 particles were dissolved in a small amount of methylene chloride, and the imatinib was extracted into pH 7.4 buffer (100 mM Na<sub>2</sub>HPO<sub>4</sub>). The absorbance of both the aqueous and organic phase was measured to verify that all the imatinib was partitioned into the aqueous phase. The concentration of imatinib loaded into the PK3 microparticles was determined against the established calibration curve as mentioned above.

#### **Treatment of acute liver failure in mice with imatinib-loaded PK3 microparticles**

Male C57/BL6 mice, 6-8 weeks old, were used in these studies. Appropriate doses of imatinib-PK3 particles (containing between 5 µg/kg to 500 µg/kg of imatinib), or an equal quantity of free imatinib, was suspended/dissolved in PBS (200 µL) and was injected intravenously using a 26 G5/8 sterilized needle. One hour later Con A (15 mg/kg), dissolved in PBS (200 µL), was injected into the intraperitoneal cavity using a 26 G5/8 sterilized needle. Between 4 and 8 mice were used per experimental group. The mice were euthanized 8 hours after the Con A injection, by cervical dislocation. Blood was then withdrawn from the heart using a 26 G5/8 sterilized needle, and kept at 4°C overnight. The serum was isolated by centrifuging at 600 x g for 10 minutes and sent to the core facility at the University of Rochester for measurement of ALT levels.

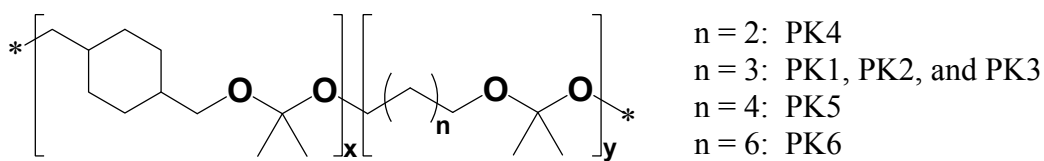
### 3.4 Results

#### **Characterizations of polyketal copolymers.**

Six polyketal copolymers were synthesized (PK1 – PK6, Table 3.1) by copolymerizing 1,4-cyclohexanedimethanol with either 1,4-butanediol, 1,5-pentanediol, 1,6-hexanediol, or 1,8-octanediol. The hydrophilicity of these diols is different from that of 1,4-cyclohexanedimethanol ( $\log P = 1.46$ ), as evidenced by their respective  $\log P$  values. The synthesis of all the polyketal copolymers reported in this Chapter was accomplished using the acetal exchange reaction, and could be performed on a multi-gram scale with yields of 50 – 60%. In general, the introduction of diols other than 1,4-cyclohexanedimethanol did not cause any complications in the synthesis, and procedures developed for the synthesis of PCADK were suitable for the synthesis of all the copolymers. Importantly, all the polyketal copolymers synthesized were solid, and therefore have the potential for formulation into microparticles.



Table 3.1. Compositions and molecular weight of polyketal copolymers synthesized.



Polymer ID	Polymer composition		M <sub>n</sub>	PDI*
	Monomer diol A (x)	Monomer diol 2 (y)		
PK1	1,4-cyclohexanedimethanol (98.03%)	1,5-pentanediol (1.93%)	2149	1.742
PK2	1,4-cyclohexanedimethanol (92.46%)	1,5-pentanediol (7.56%)	2530	1.629
PK3	1,4-cyclohexanedimethanol (86.70%)	1,5-pentanediol (13.30%)	2596	1.432
PK4	1,4-cyclohexanedimethanol (96.75%)	1,4-butanediol (3.25%)	2637	1.553
PK5	1,4-cyclohexanedimethanol (85.32%)	1,6-hexanediol (14.68%)	2122	1.538
PK6	1,4-cyclohexanedimethanol (87.31%)	1,8-octanediol (12.69%)	2181	1.786

\* PDI: polydispersity index.

Polyketal copolymers were characterized by <sup>1</sup>H-NMR and GPC. As a representative example, the <sup>1</sup>H-NMR and GPC of PK3 are shown in Figure 3.5. The ratio of 1,5-pentanediol to 1,4-cyclohexanedimethanol was obtained by taking the ratio of areas under the peaks a and b, respectively.

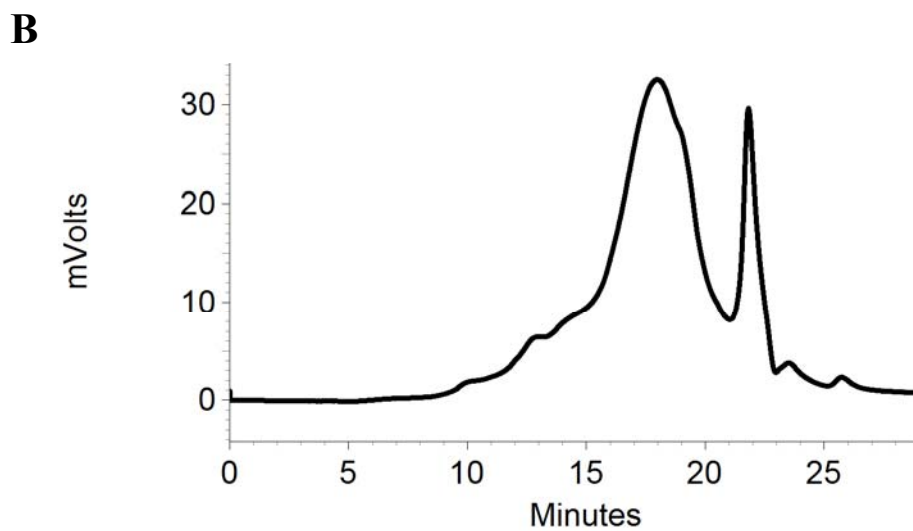
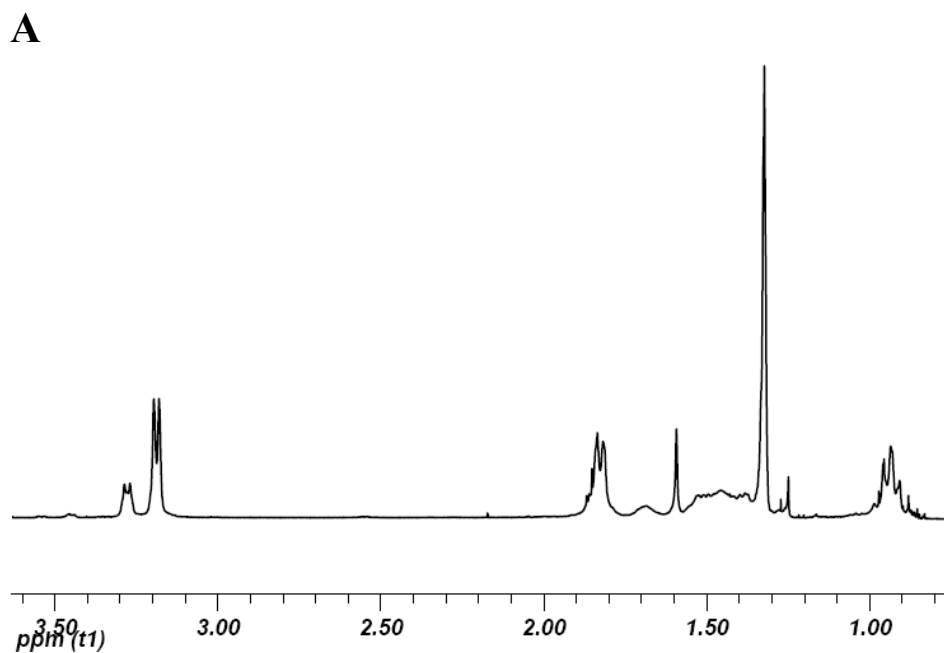


Figure 3.3.  $^1\text{H}$  NMR and GPC spectrum of PK1. (A)  $^1\text{H}$  NMR spectrum of PK1 in  $\text{CDCl}_3$ . (B) GPC trace of PK1 in THF, Y-axis indicates relative UV absorbance at 262 nm,  $M_n = 2,149$ , polydispersity index (PDI) = 1.74.

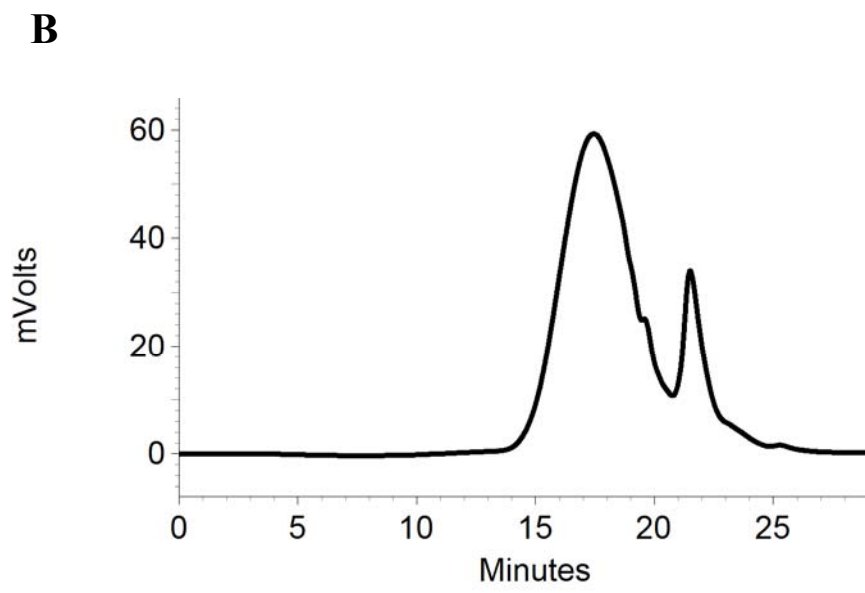
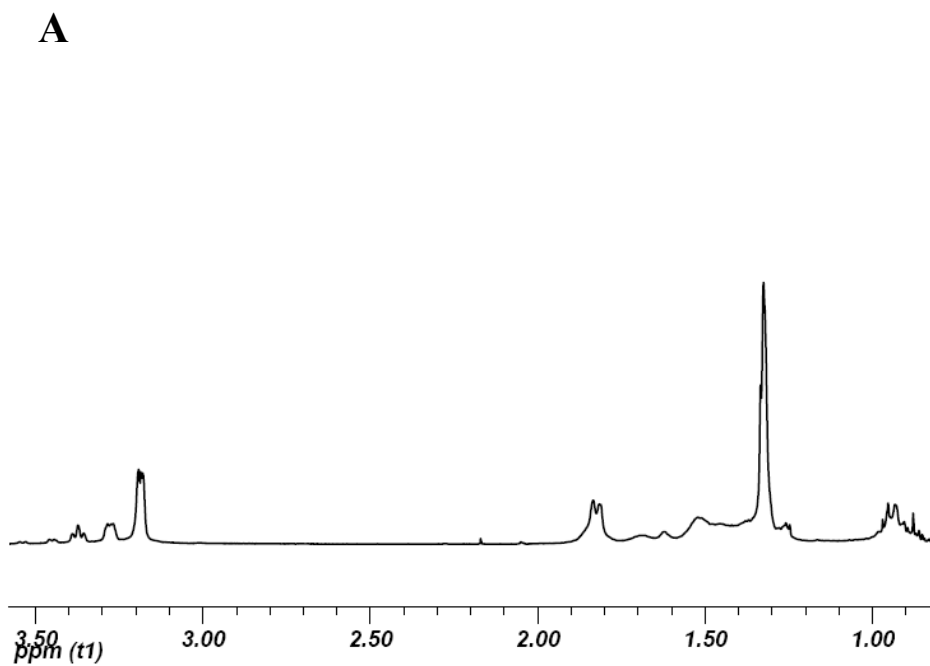


Figure 3.4. (A)  $^1\text{H}$  NMR spectrum of PK2 in  $\text{CDCl}_3$ . (B) GPC trace of PK2 in THF, Y-axis indicates relative UV absorbance at 262 nm,  $M_n = 2,530$ , PDI = 1.63.

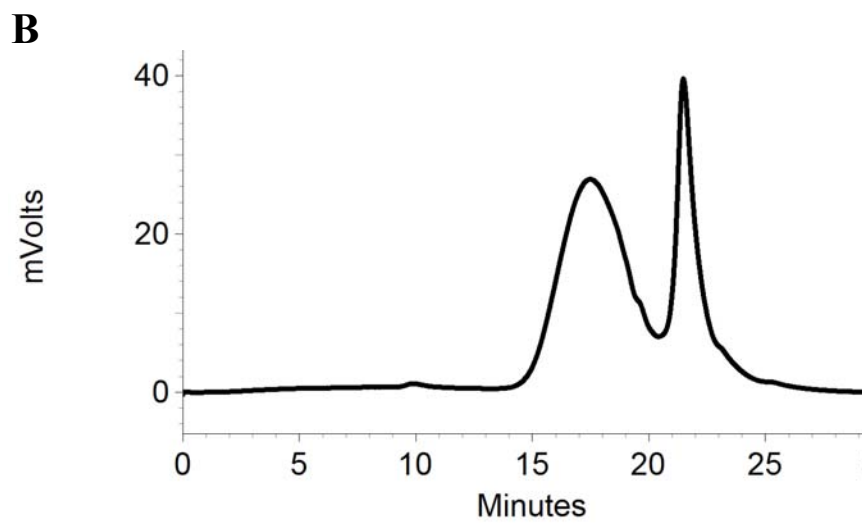
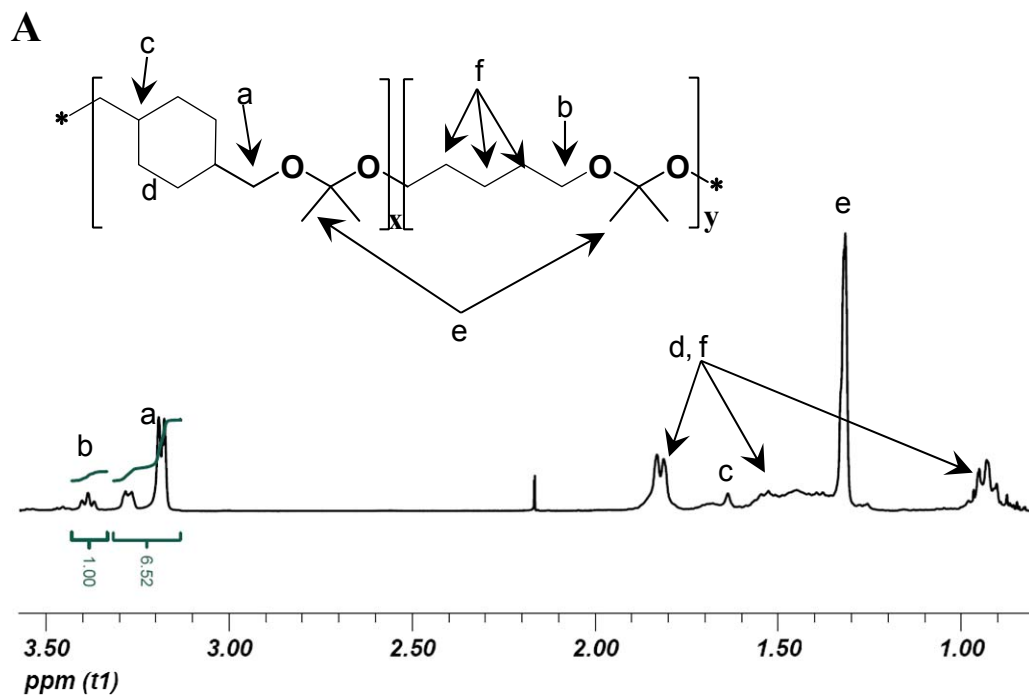


Figure 3.5. (A)  $^1\text{H}$  NMR spectrum of PK3 in  $\text{CDCl}_3$ . (B) GPC trace of PK3 in THF, Y-axis indicates relative UV absorbance at 262 nm,  $M_n = 2,596$ , PDI = 1.43.

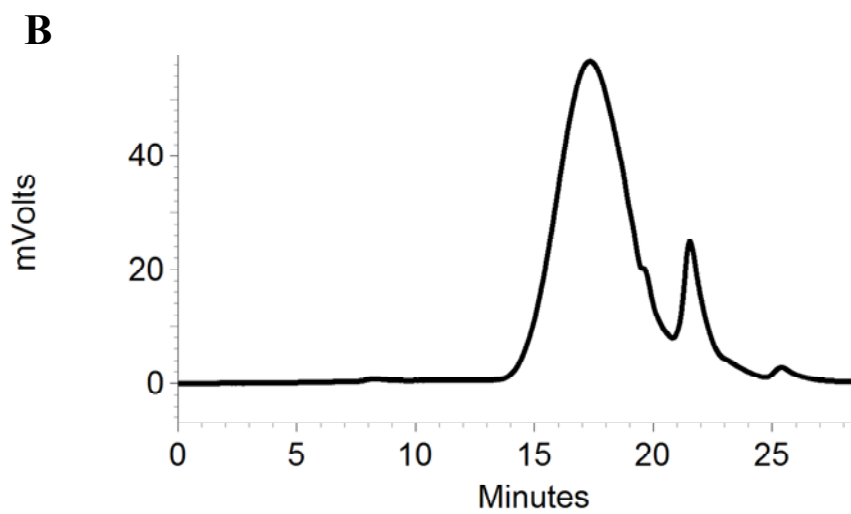
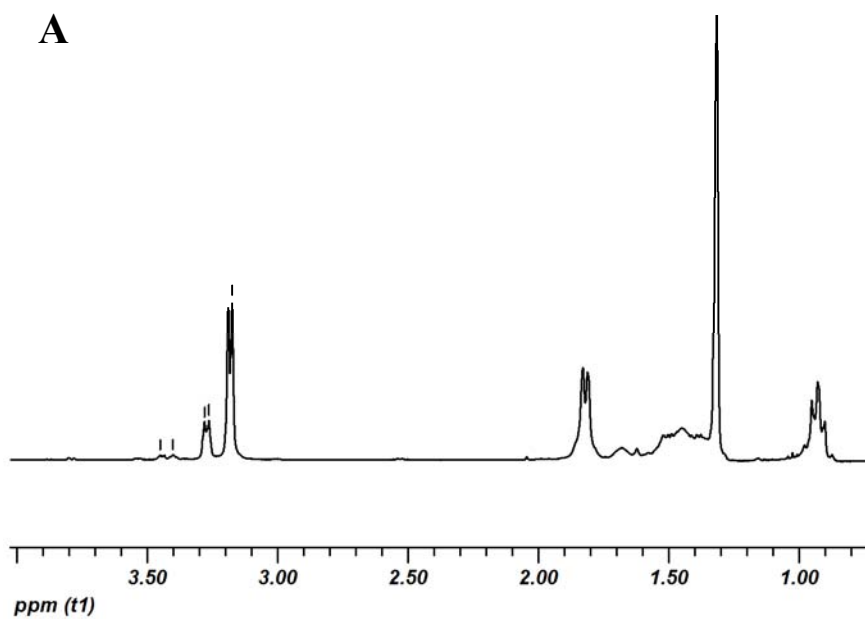


Figure 3.6. (A)  $^1\text{H}$  NMR spectrum of PK4 in  $\text{CDCl}_3$ . (B) GPC trace of PK4 in THF, Y-axis indicates relative UV absorbance at 262 nm,  $M_n = 2,637$ , PDI = 1.55.

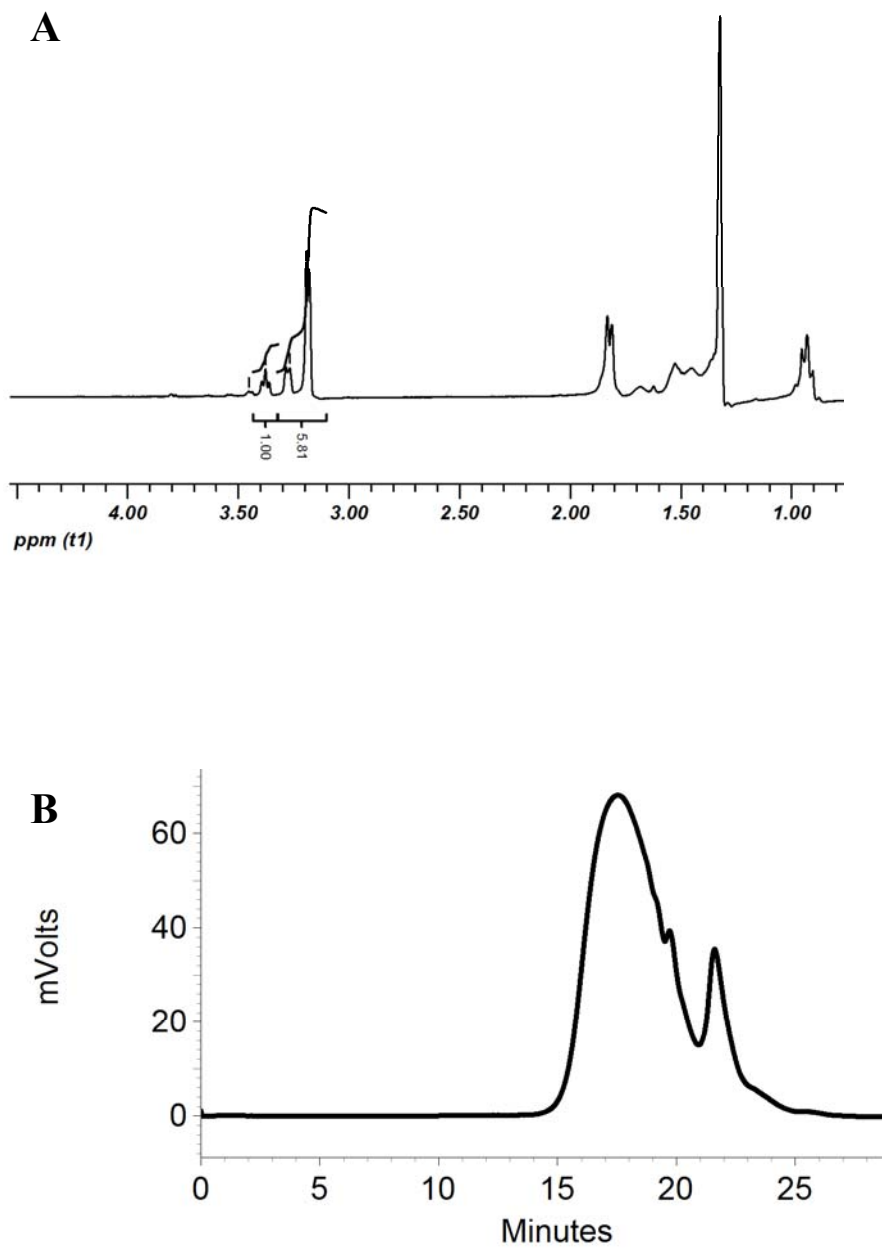


Figure 3.7. (A)  $^1\text{H}$  NMR spectrum of PK5 in  $\text{CDCl}_3$ . (B) GPC trace of PK5 in THF, Y-axis indicates relative UV absorbance at 262 nm,  $M_n = 2,122$ , PDI = 1.54.

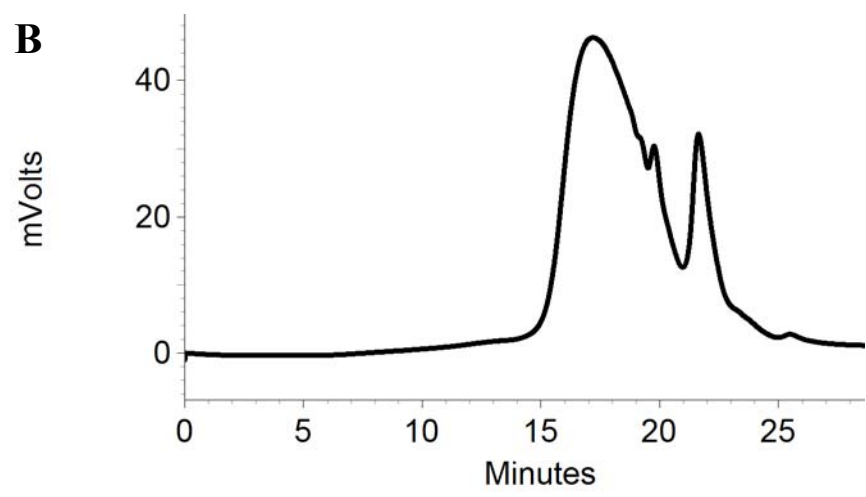
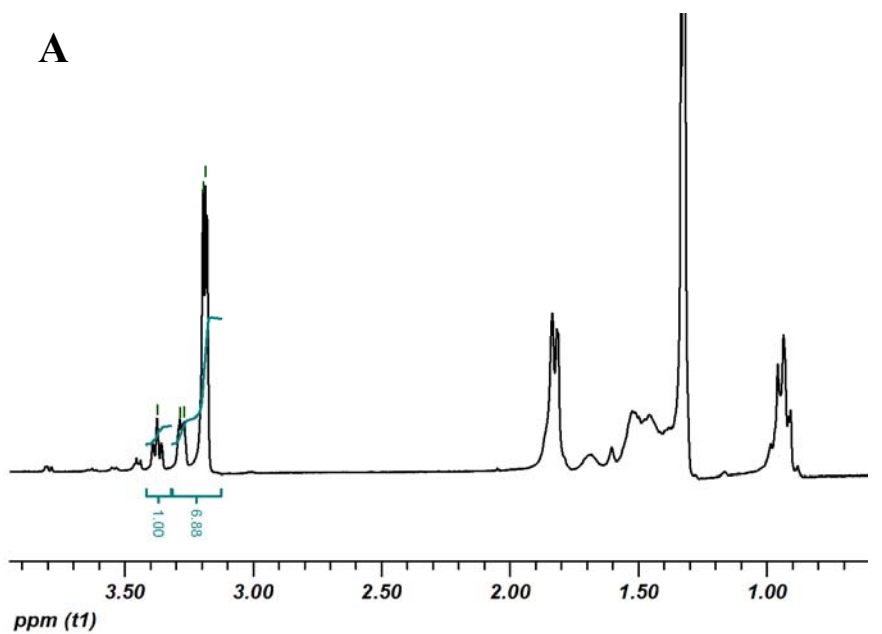


Figure 3.8. (A)  $^1\text{H}$  NMR spectrum of PK6 in  $\text{CDCl}_3$ . (B) GPC trace of PK6 in THF, Y-axis indicates relative UV absorbance at 262 nm,  $M_n = 2,181$ , PDI = 1.79.

### Acid-sensitive degradation of copolymers PK1 – PK6

The hydrolysis kinetics of PK1 to PK6 was measured at the pH values of 4.5 and 7.4 to determine their behavior in the acidic environment of phagolysosomes and in the blood. Figure 3.9 – 3.14 demonstrate that all the polyketal copolymers (PK1 – PK6) undergo acid-catalyzed hydrolysis.

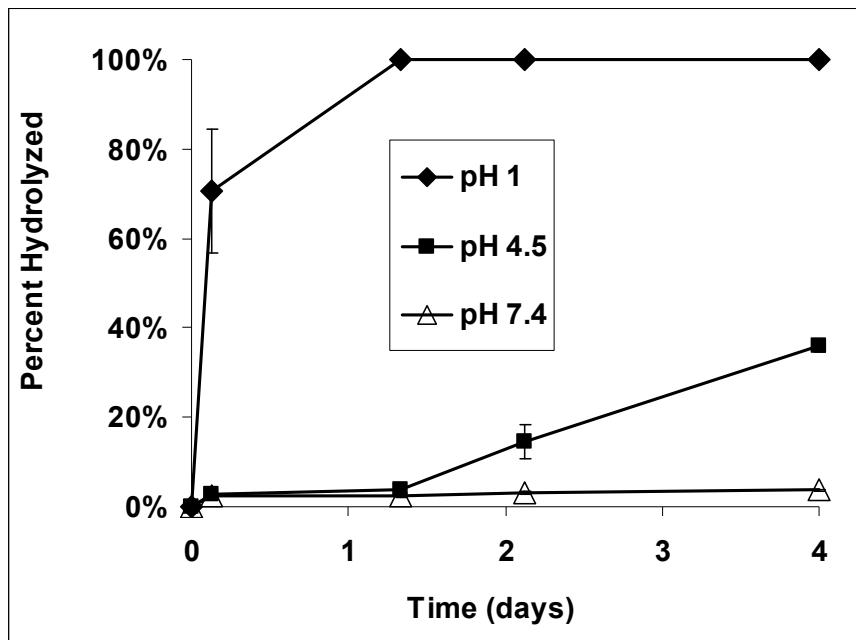


Figure 3.9. Hydrolysis of PK1 at 37°C. Data are presented as means  $\pm$  standard deviation,  $n = 3$ .



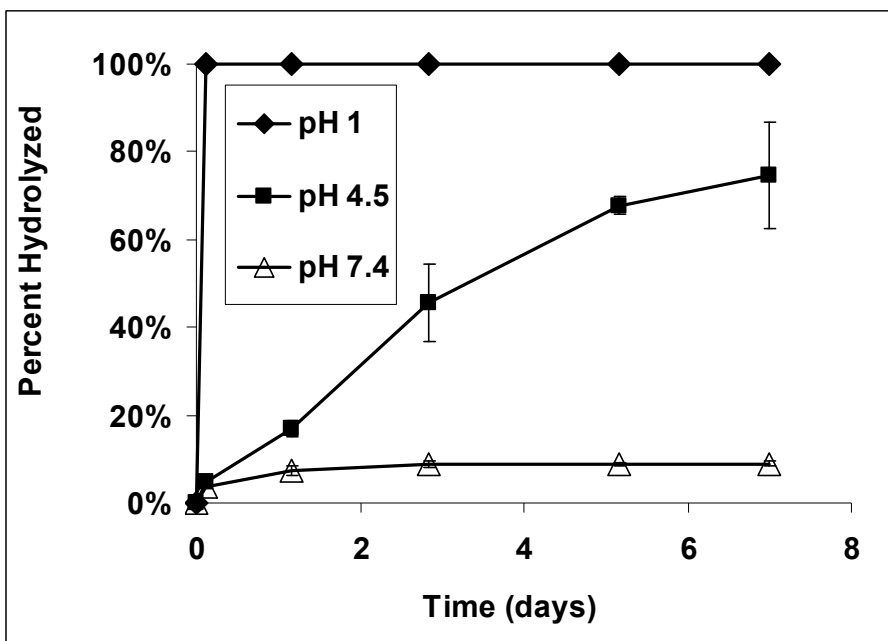


Figure 3.10. Hydrolysis of PK2 at 37°C. Data are presented as means  $\pm$  standard deviation, n = 3.

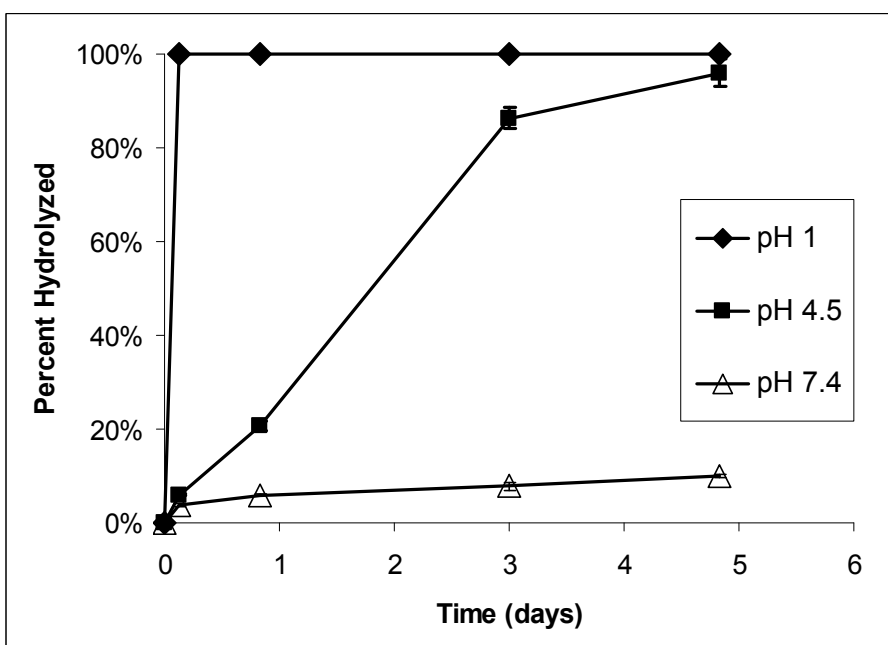


Figure 3.11. Hydrolysis of PK3 at 37°C. Data are presented as means  $\pm$  standard deviation, n = 3.

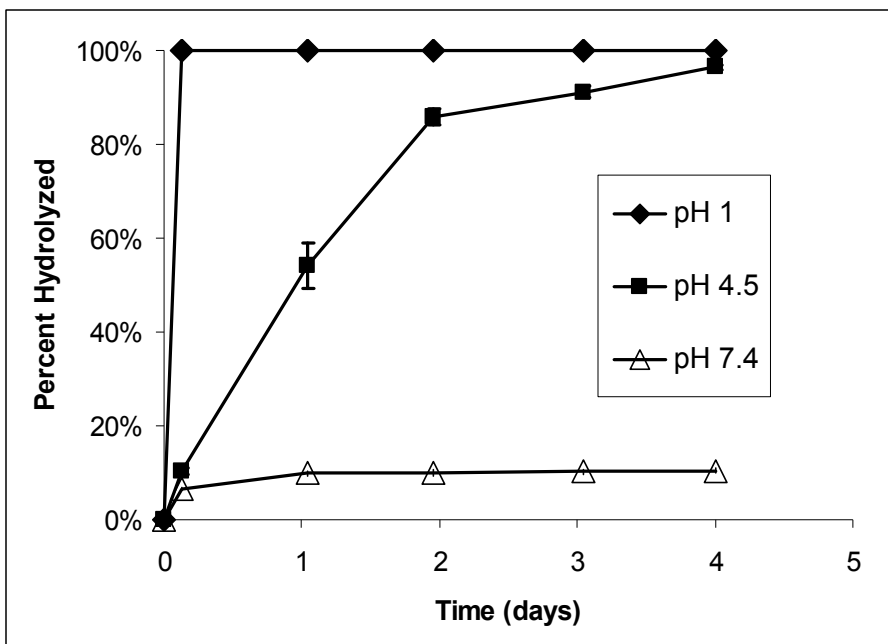


Figure 3.12. Hydrolysis of PK4 at 37°C. Data are presented as means  $\pm$  standard deviation, n = 3.

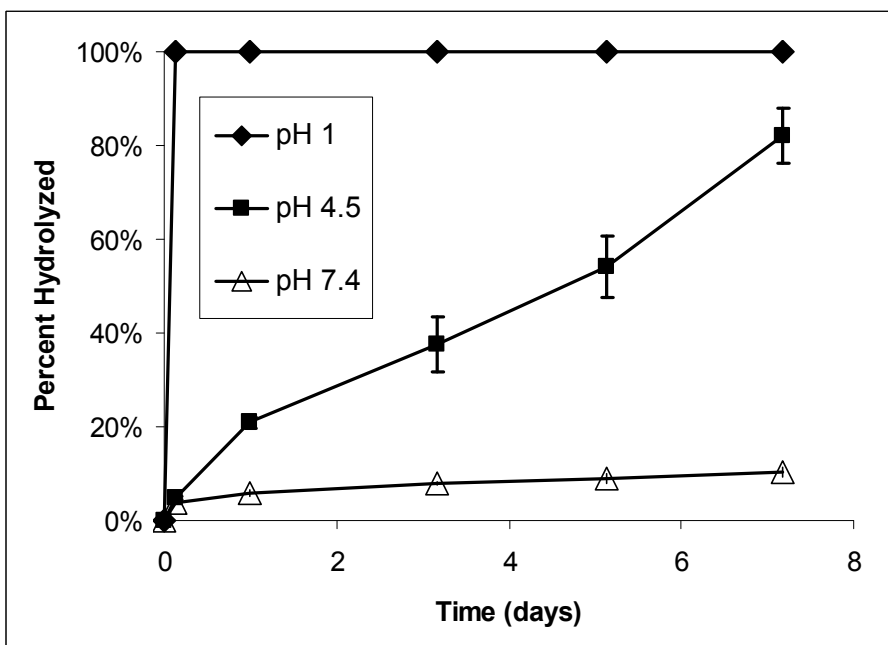


Figure 3.13. Hydrolysis of PK5 at 37°C. Data are presented as means  $\pm$  standard deviation, n = 3.

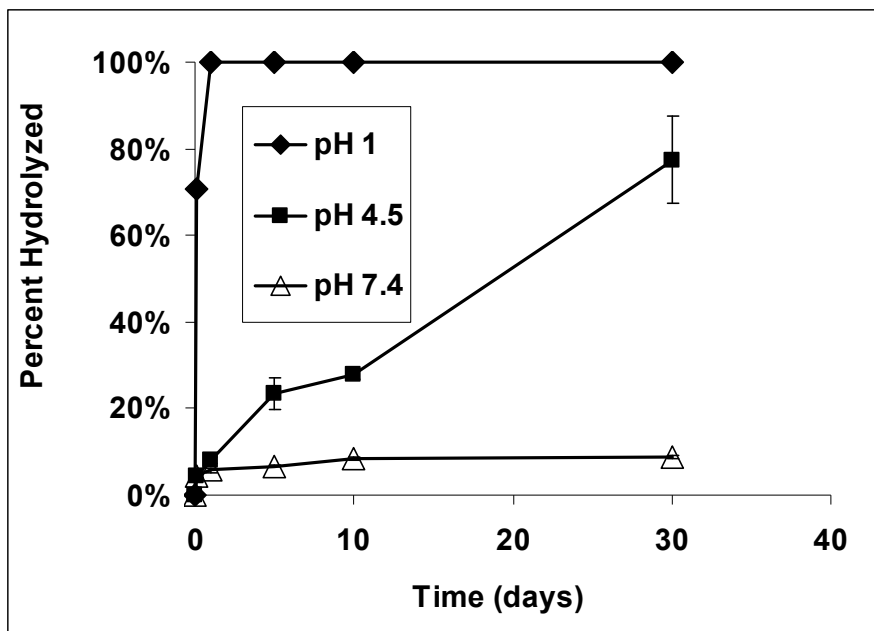


Figure 3.14. Hydrolysis of PK6 at 37°C. Data are presented as means  $\pm$  standard deviation,  $n = 3$ .

### Drug release kinetics from PK3 microparticles

In order to determine whether or not PK3 microparticles would have suitable drug-release kinetics for treating acute inflammatory diseases, a release study was conducted on PK3 microparticles which encapsulated the fluorescent dye, rhodamine B. Figure 3.15 demonstrates that the release half-lives of rhodamine B from PK3 microparticles are approximately 6 hours at pH 4.5 and 40 hours at pH 7.4, which are suitable for treating acute liver failure. The drug-release kinetics of PK3 microparticles is 20 times faster than that of PCADK microparticles, which had a release half-lives of 5 days at pH 4.5 and over 15 days at pH 7.4.

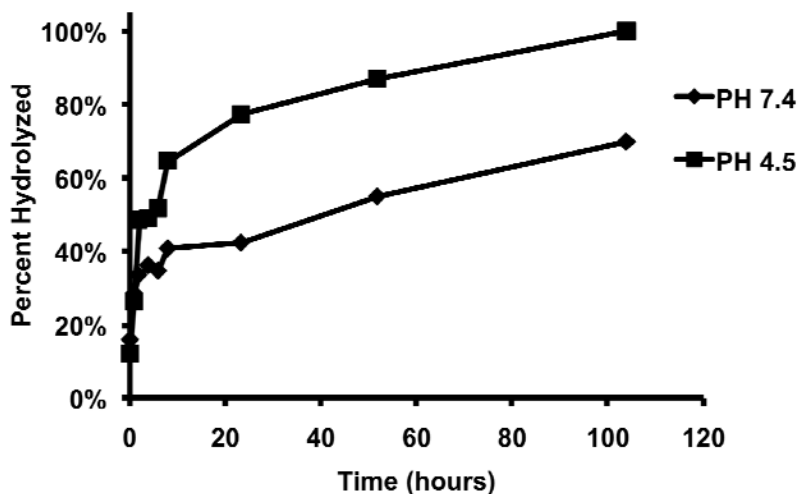


Figure 3.15. Release kinetics of rhodamine B encapsulated in PK3 microparticles.

### Formulation of PK3 microparticles encapsulating imatinib

Microparticles were formulated from PK3, using a solvent evaporation procedure. Figure 3.16 demonstrates that the size range of PK3 microparticles is between 1 to 5 microns, which is suitable for phagocytosis by macrophages. Imatinib, an anti-inflammatory drug that inhibits the activation of NF $\kappa$ B, was encapsulated into PK3 microparticles through double emulsion procedures. These microparticles were approximately 1.5 microns in size on average, as determined by SEM and DLS, which is suitable for delivering drugs to phagocytic cells such as Kupffer cells. The loading of imatinib in PK3 microparticles was determined to be  $0.90 \pm 0.10$   $\mu$ g imatinib per 1 mg of particles ( $n = 3$ ), suggesting that the encapsulation efficiency of imatinib in PK3 microparticles was approximately 0.32%.

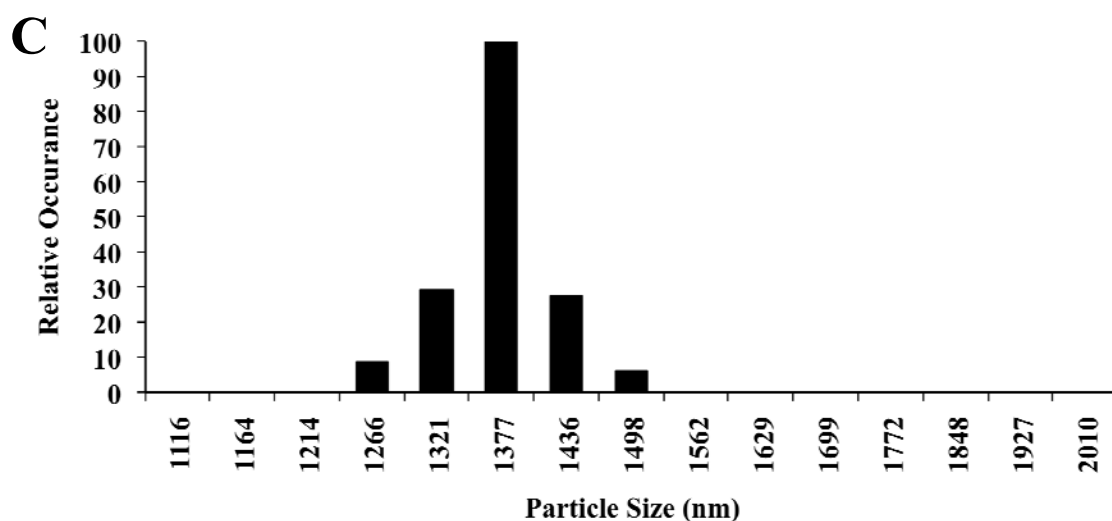
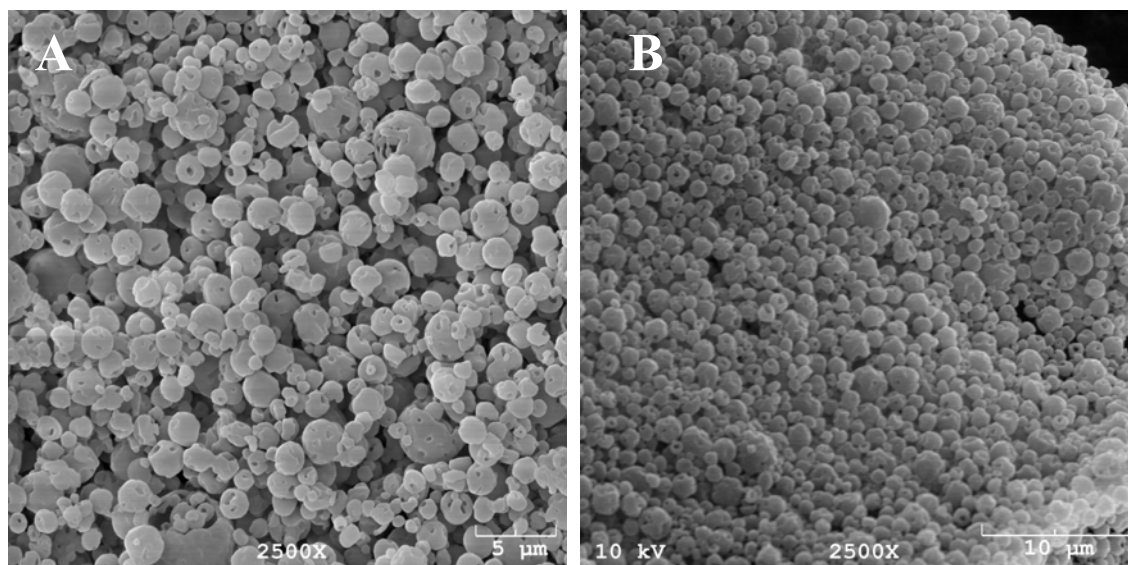


Figure 3.16. SEM images of particles formulated with PK3. (A) SEM image of empty particles formulated via double emulsion. (B) SEM images of imatinib-loaded PK3 microparticles formulated via double emulsion. (C) Size Distribution of imatinib-loaded PK3 microparticles as determined by dynamic light scattering (DLS).

The ability of PK3 microparticles to enhance the delivery of imatinib was investigated in mice suffering from Con A-induced acute liver failure. Mice were injected with either imatinib in solution (0.1  $\mu\text{g}$  to 10  $\mu\text{g}$  of imatinib dissolved in 200  $\mu\text{L}$

of saline) or an equivalent amount of imatinib loaded in PK3 microparticles (0.11 mg to 11 mg of imatinib-loaded PK3 microparticles suspended in 200  $\mu$ L of saline). Acute liver failure was subsequently induced by an intraperitoneal injection of Con A. The severity of liver injury in these mice was determined by measuring the alanine aminotransaminase (ALT) level in their blood, which is a clinical surrogate marker for hepatocyte injury. Figure 3.17 demonstrates that PK3 microparticles enhanced the treatment efficacy of imatinib in preventing Con A-induced liver damage.

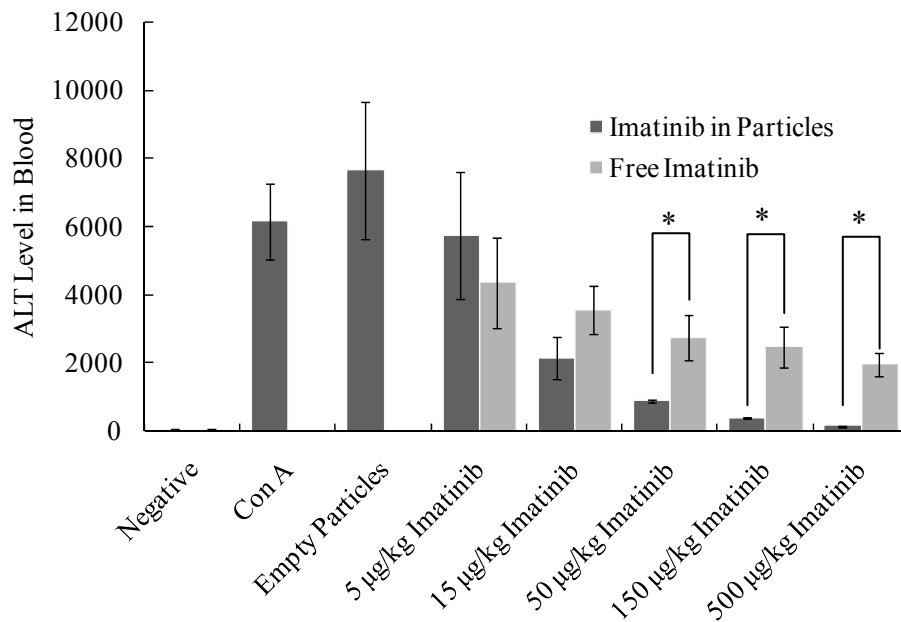


Figure 3.17. PK3 microparticles improve the efficacy of imatinib in treating acute liver failure in mice. Mice were injected intravenously with either imatinib or imatinib in PK3 microparticles, acute liver failure was then induced by intraperitoneal injection of Con A (15 mg/kg). 8 hours later, ALT levels in the blood were analyzed. \* indicates statistical significance (Student's t test,  $P < 0.05$ ,  $n = 4$  to 8).

### 3.5 Discussion

#### Tunable hydrolysis of polyketal copolymers

There is currently great interest in developing microparticle-based delivery vehicles that have the biocompatibility and hydrolysis kinetics needed to treat acute inflammatory diseases. Microparticles formulated from the aliphatic polyketal PCADK have excellent biocompatibility and degrade under the acidic conditions of the phagolysosome. However, the slow hydrolysis kinetics of PCADK makes it unsuitable for treating acute inflammatory diseases, and therefore strategies for accelerating its hydrolysis kinetics are greatly needed. We previously hypothesized that the slow hydrolysis kinetics of PCADK were due to its hydrophobicity, making the diffusion of water into the polymer matrix the rate-limiting step in ketal hydrolysis (Lee, Yang et al. 2007). This hypothesis was based on the fact that the hydrolysis half-life of a water-soluble dimethylacetone-based ketal is only 2 minutes at pH 5.0, which is 3 to 4 orders of magnitude faster than the hydrolysis of the ketal linkages in PCADK (Kwon, Standley et al. 2005). Additionally, the hydrolysis kinetics of other water insoluble polymers, such as polyanhydrides, also scale with their hydrophobicity (Gopferich and Tessmar 2002). In this Chapter, the role of hydrophobicity in governing the hydrolysis kinetics of polyketals was investigated. This was accomplished by synthesizing polyketal copolymers of varying hydrophobicity, and measuring their hydrolysis kinetics.

Six polyketal copolymers were synthesized in this Chapter (PK1 – PK6, Table 3.1), by copolymerizing 1,4-cyclohexanedimethanol with either 1,4-butanediol, 1,5-pentanediol, 1,6-hexanediol, or 1,8-octanediol. The hydrophobicity of these diols is different from that of 1,4-cyclohexanedimethanol ( $\log P = 1.46$ , where  $P = \text{water/octanol}$

partition coefficient), as evidenced by their respective log P values (Table 3.3). The synthesis of all the polyketal copolymers reported in this study was accomplished using the acetal exchange reaction, and was performed on a multi-gram scale with yields of 50 – 60% (Figure 3.1). In general, the introduction of additional diols other than 1,4-cyclohexanedimethanol did not cause any synthetic complications, and procedures developed for the synthesis of PCADK were suitable for the synthesis of all the copolymers. Importantly, all the polyketal copolymers reported in Table 3.1 were solid, and therefore have the potential for formulation into microparticles.

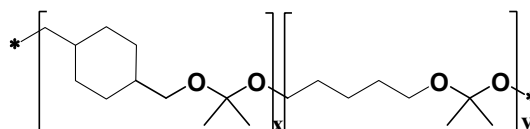
The influence of hydrophobicity on the hydrolysis kinetics of polyketal copolymers was investigated. Two sets of copolymers were synthesized and their hydrolysis rates were investigated. First, a series of copolymers, using varying ratios of the monomers 1,4-cyclohexanedimethanol and 1,5-pentanediol, were synthesized (Table 3.2). PK1, PK2, and PK3 are copolymers synthesized from 1,4-cyclohexanedimethanol and 1,5-pentanediol; their hydrophilicity scales with the amount of 1,5-pentanediol incorporated into the copolymer. This is due to the large difference in hydrophilicity between 1,5-pentanediol and 1,4-cyclohexanedimethanol, as evidenced by their respective log P values of 0.27 and 1.46. Figure 3.18 demonstrates that 1,5-pentanediol dramatically accelerates the pH 4.5 hydrolysis kinetics of 1,4-cyclohexanedimethanol-based polyketals. For example, the hydrolysis half-life of PCADK, a homo-polyketal synthesized from 1,4-cyclohexanedimethanol, is 24 days at pH 4.5 (Lee, Yang et al. 2007). In contrast, PK3, a copolymer that incorporated 13% 1,5-pentanediol and 87% 1,4-cyclohexanedimethanol, had a hydrolysis half-life of 2 days at pH 4.5 and was 100% hydrolyzed after 5 days. PK2, a PCADK derived copolymer with 7.5% of 1,5-



pentanediol incorporated, had a hydrolysis half-life of 3 days, which is faster than PCADK but slower than PK3. For all three polyketals, less than 15% of the polymers were hydrolyzed in pH 7.4 within the duration of the experiments of 10 days. Collectively, these results demonstrate that the hydrolysis kinetics of PK1 to PK3 scale with the amount of 1,5-pentanediol incorporated in their backbone, suggesting that the hydrolysis of polyketals is governed by their hydrophilicity. Similar copolymers with higher incorporation of 1,5-pentanediol were also generated; however those copolymers were viscous liquids, which are not suitable for formulation into microparticles for drug delivery. Therefore we only focused our hydrolysis analysis on the solid polyketal copolymers, PK1, PK2, and PK3.

Table 3.2. Polyketal copolymers composed of 1,4-cyclohexanedimethanol and 1,5-pentanediol.

Polymer ID	X	Y
PCADK	100%	0
PK 1	98%	2%
PK 2	92%	8%
PK 3	87%	13%



Chemical Structures of PK1, PK2, and PK3.

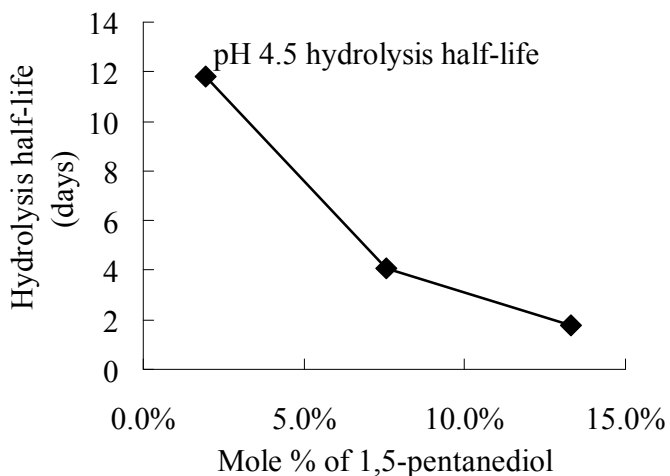
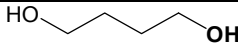
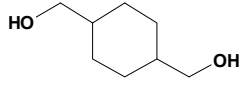
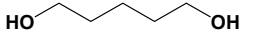
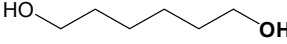
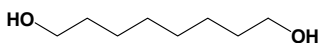


Figure 3.18. Hydrolysis half-lives of polyketal copolymers PK1, PK2, and PK3 at pH 4.5.

To determine if diols other than 1,5-pentanediol could similarly influence the hydrolysis kinetics of PCADK-derived copolymers, the hydrolysis kinetics of PK4, PK5, and PK6 were also investigated. These polyketals are PCADK-derived copolymers synthesized from 1,4-cyclohexanedimethanol and either 1,4-butanediol, 1,6-hexanediol, or 1,8-octanediol. Table 3.3 demonstrates that this set of copolymers also has an inverse relationship between hydrophobicity and hydrolysis kinetics. For example, PK4, a copolymer synthesized from 1,4-cyclohexanedimethanol and 1,4-butanediol, has the fastest hydrolysis kinetics of all the polyketal copolymers, with a hydrolysis half-life of 1 day at pH 4.5. This is predicted based on the more hydrophilic nature of 1,4-butanediol in comparison to the other diols. On the other hand, PK6, a copolymer composed of 1,4-cyclohexanedimethanol and 1,8-octanediol, had a pH 4.5 hydrolysis half-life of 18.6 days. In summary, these data demonstrate that the hydrolysis kinetics of polyketals can be tuned by varying their hydrophilicity and further support the hypothesis that diffusion of water into the polyketals is the rate-determining step governing their hydrolysis. Importantly, the hydrolysis kinetics of all the polyketal copolymers, PK 1-6, was pH-sensitive; in general they hydrolyzed at least one order of magnitude faster at pH 4.5 than at pH 7.4.

Table 3.3. Hydrolysis half-lives of polyketal copolymers at pH 4.5 and pH 7.4 at 37 °C.

Polymer composition					
Diol A	Percent diol A	Diol B	Percent diol B	Half life at pH 4.5	Log P of diol B
	97%	 1,4-butanediol	3%	1.0 day	-0.83
 1,4-cyclohexane dimethanol	87%	 1,5-pentanediol	13%	1.8 days	0.27
	85%	 1,6-hexanediol	15%	4.4 days	0.76
	87%	 1,8-octanediol	13%	18.6 days	1.75

\* log P is the logarithm of the water/octanol partition coefficient; the log P data were obtained from the Syracuse Research Corporation's PhysProp Database.

### Delivery of an NFκB inhibitor for treating ALF

We chose PK3 for further investigation as a drug carrier for the treatment of acute inflammatory diseases because of its suitable hydrolysis kinetics and biocompatible degradation products. The copolymer PK4 has faster hydrolysis kinetics than PK3; however it degrades into 1,4-butanediol, which is converted into  $\gamma$ -hydroxybutyrate *in vivo*, and subsequently causes toxicity to the central nervous system (Zvosec, Smith et al. 2001).

PK3 microparticles were used to enhance the delivery of imatinib in treating acute liver failure. Imatinib is a kinase inhibitor that inhibits NF- $\kappa$ B activation and has great potential for treating acute inflammatory diseases (Deininger and Druker 2003; Wolf, Wolf et al. 2005). The activation of NF- $\kappa$ B in Kupffer cells plays a central role in

causing acute liver failure by mediating the production and secretion of inflammatory molecules such as TNF- $\alpha$ , IL-1, IFN- $\gamma$ , and IL-12, which cause extensive tissue damage in the liver and significantly contribute to the pathology of acute liver failure (Pahl 1999; Higuchi, Kawakami et al. 2006). These cytokines regulate the phenotype of Kupffer cells themselves as well as the neighboring cells, such as hepatocytes and endothelial cells (Bilzer, Roggel et al. 2006). Several studies have demonstrated that inhibition of NF- $\kappa$ B activation in Kupffer cells offers great therapeutic potential for treating liver injuries (Zhou, Wang et al. 2004; Liu and Malik 2006; Higuchi, Kawakami et al. 2007).

Although imatinib has shown promise for treating acute inflammatory diseases in mouse models, there are also numerous side effects associated with imatinib, including heart failure and hepatic toxicity (Kerkela, Grazette et al. 2006; Yeon Hee, Hae Jeong et al. 2006). Our experiments demonstrated that imatinib-loaded PK3 microparticles significantly enhanced the therapeutic efficacy of imatinib by targeting it to macrophages, thereby increasing its concentration at the target site, and also by reducing the toxic side effects of imatinib on the heart and liver. For example, a dose of 500  $\mu$ g/kg of free imatinib resulted in an ALT value of approximately 2,000 U, whereas 500  $\mu$ g/kg of imatinib encapsulated in PK3 microparticles reduced the ALT values to baseline levels of only 50 U. The therapeutic efficacy of 15  $\mu$ g/kg of imatinib loaded in PK3 microparticles was similar to that of 500  $\mu$ g/kg of free imatinib. No noticeable toxicity was observed by injection of empty PK3 microparticles (11 mg suspended in 200  $\mu$ L of saline).

## CHAPTER 4

### DEVELOPMENT OF AN SOD DELIVERY SYSTEM FOR TREATING ACUTE LIVER FAILURE

#### 4.1 Abstract

Acute liver failure (ALF) can be characterized by destruction of metabolic capacity of the liver and is responsible for thousands of deaths each year. Oxidative stress produced by Kupffer cells, the resident macrophages in the liver, plays a critical role on mediating liver injury by inducing production of inflammatory cytokines such as tumor necrosis factor- $\alpha$  (TNF- $\alpha$ ). In this Chapter, the anti-oxidant protein, superoxide dismutase (SOD), was encapsulated in PK3 microparticles, which have suitable chemical and physical properties for drug delivery applications treating ALF. PK3 microparticles can passively accumulate in the liver, target Kupffer cells through phagocytosis, and release the encapsulated drug rapidly. Cell culture experiments demonstrated that PK3 microparticles can be taken up by macrophages. *In vivo* studies confirmed that PK3 microparticles target and preferentially accumulate the liver. SOD-loaded in PK3 microparticles was effective in reducing liver damage and systemic inflammation in mice that suffered from LPS-induced acute liver injury, as evidenced by decreased serum level of alanine aminotransferase and TNF- $\alpha$ . Based on our results, we anticipate numerous applications of polyketals microparticles for treating acute inflammatory diseases given their biocompatible degradation products, ability to target macrophages, and rapid release of encapsulated drugs.

## 4.2 Introduction

Acute liver failure (ALF) can be characterized by destruction of metabolic capacity of the liver and is responsible for thousands of deaths each year. Several pathologic conditions, including bacterial infection-induced sepsis, hemorrhagic viral infections, alcohol-induced liver toxicity, hepatic ischemia and reperfusion injury, and drug overdose, contribute to the pathology of ALF. Oxidative stress produced by Kupffer cells, the resident macrophages in the liver, plays a critical role on mediating liver injury by inducing production of inflammatory cytokines such as tumor necrosis factor- $\alpha$  (TNF- $\alpha$ ) (Decker, Lohmann-Matthes et al. 1989; Wheeler, Kono et al. 2001; Droge 2002; Kamata, Honda et al. 2005). Therefore inhibition of oxidative stress in the liver has great potential in treating ALF. Superoxide dismutase (SOD) is an enzyme that scavenges reactive oxygen species and has great potential to treat inflammatory diseases by suppressing ROS production by macrophages (Kinnula and Crapo 2003; Cuzzocrea, Thiernemann et al. 2004; Landis and Tower 2005). Numerous SOD delivery approaches for medical applications have been proposed; however, strategies for delivering SOD to the liver for treating ALF have been unsuccessful, primary because none of the existing SOD delivery strategies have the properties needed to treat ALF, which requires targeting SOD to the liver, releasing SOD within 1 – 2 days, serum stability, and good storage properties. Liposomes have potential for SOD delivery to treat ALF because of their ability to target and rapidly release SOD to the liver (Nakae, Yamamoto et al. 1990; Higuchi, Kawakami et al. 2006; Higuchi, Kawakami et al. 2007). However, liposomes are not sufficiently stable in serum and also have poor storage properties, which hinder their use for clinical applications treating ALF.

Microparticles based on biodegradable polymers have considerable potential for improving the efficacy of SOD, due to their excellent biocompatibility, long shelf life, and ability to efficiently target macrophages (Giovagnoli, Luca et al. 2005; Kohane, Tse et al. 2006). However, polymeric microparticles are predominantly formulated from polyesters, which can be problematic for the treatment of inflammatory diseases due to their acidic degradation products and slow hydrolysis kinetics.(Dailey, Jekel et al. 2006). Polyketals are a new class of polymers that are also being investigated for the delivery of SOD, and have several unique properties that make them suitable delivery vehicles for treating ALF (Lee, Yang et al. 2007; Yang, Bhide et al. 2008). First, polyketals degrade into alcohols and ketones and may avoid the inflammatory problems associated with the acidic degradation products of polyesters (Fu, Pack et al. 2000). Second, polyketals can be used to formulate microparticles, which can encapsulate and target SOD to phagocytic cells. For example, microparticles formulated from the aliphatic PCADK, encapsulating SOD, demonstrated improved efficacy of SOD in reducing the production of ROS by macrophages *in vitro* (Lee, Yang et al. 2007). We have also previously demonstrated that a polyketal obtained by copolymerizing 1,4-cyclohexanedimethanol and 1,5-pentenediol, termed PK3, has the desired properties for drug delivery applications treating ALF, due to its ability to target the liver and rapid hydrolysis at phagolysosomal pH. PK3 was used to encapsulate the anti-inflammatory drug, imatinib, an inhibitor of the transcription factor, NF $\kappa$ B, which is responsible for production of pro-inflammatory cytokines such as TNF- $\alpha$ . Our studies showed that PK3 microparticles significantly enhanced the therapeutic efficacy of imatinib in treating Con A-induced ALF in mice (Yang, Bhide et al. 2008). Even though polyketals have great promise for delivering SOD to treat ALF,

low encapsulation efficiency and loss of enzymatic activities of SOD in polyketal microparticle still remain a major challenge. In this Chapter, I demonstrate that improved encapsulation of SOD and retaining of enzymatic activities were achieved by using an improved strategy, solid-in-oil-in-water double emulsion method, to formulate PK3 microparticles. Cell culture experiments demonstrated that PK3 microparticles significantly enhanced the delivery of SOD to macrophages. *In vivo* studies demonstrated that PK3 microparticles significantly reduced liver necrosis and systemic inflammation in mice after ALF was induced by the endotoxin LPS, as evidenced by significantly reduce levels of ALT and TNF- $\alpha$  in their serum. Based on our findings, we anticipate numerous applications of polyketals for protein delivery treating acute inflammatory diseases given their biocompatible degradation products, ability to target macrophages, and rapid release of encapsulated drugs.



### 4.3 Experimental Methods

#### **Materials.**

All chemicals were purchased from Sigma-Aldrich (St. Louis, MO) and were used as received unless otherwise specified. TNF- $\alpha$  ELISA kit was purchased from eBioscience (San Diego, CA). ALT assay kit was purchased from Point Scientific (Canton, MI).

#### **Animals.**

Female Balb/C mice were purchased from Jackson Laboratory (Bar Harbor, ME). All animal experiments were approved by the Institutional Animal Care and Use Committee (IACUC) of the Georgia Institute of Technology.

#### **Formulation of SOD-loaded microparticles with water/oil/water emulsion**

SOD-loaded microparticles were formulated from polyketal copolymers using a water/oil/water emulsion method. Briefly, 50  $\mu$ L of an aqueous SOD solution (10 mg/mL) was added to 500  $\mu$ L of methylene chloride, which contained 50 mg of PK3 dissolved in it. The resulting mixture was sonicated briefly at 40 Watts (Branson Sonifier 250) and transferred to a 5 mL pH 7.4 buffer solution (100 mM sodium phosphate) containing 8% w/v poly(vinyl alcohol) (PVA, 31–50 kDa). The new mixture was emulsified using a homogenizer (Fisher Scientific Powergen 500 with a flat-bottom generator) and subsequently added to 30 mL of a 1% w/v PVA solution and stirred for at least 3 hours to evaporate the solvent. The resulting particles were washed 3 times by centrifugation, then re-suspended and freeze-dried.

### **Protein lyophilization**

SOD was dissolved in ultra pure de-ionized water (10 mg/mL). PEG ( $M_w$  5000) was co-dissolved in a four-to-one mass ratio to SOD. The solution was quickly frozen in liquid nitrogen, which was then lyophilized for 24-48 hours to obtain an SOD-PEG mixture.

### **Formulation of SOD-loaded microparticles with solid/oil/water emulsion**

The SOW method used was based on the techniques of Castellanos, *et al.* (Castellanos, Carrasquillo et al. 2001). Briefly, 5 mg of lyophilized protein and 50 mg of PCADK ( $M_n = 2277$ ) were mixed in 500  $\mu$ L of DCM through short vortexing (3000 RPM), bath sonication (approximately 15 minutes), and finally sonicated with a Branson Sonifier 250 (VWR Scientific, West Chester, PA) until a smooth dispersion was visible. This suspension was added to a 5% (w/v) PVA solution (25 mL) and was either homogenized at 6500 RPM for 2 minutes. The final emulsion was placed under vacuum in a rotary evaporator for quick removal of the DCM. The particles were washed and lyophilized using the same method as the W/O/W method.

### **Scanning Electron Microscopy.**

SEM images were taken to analyze the morphology of the polyketal microparticles. Briefly, SEM samples were prepared by attaching lyophilized particles onto 12.7 mm diameter aluminum sample mounting stubs (Electron Microscopy Sciences, Hatfield, PA), using conductive double sided carbon discs (SPI Supplies, West Chester, PA). The samples were coated with a gold sputter coater (International

Scientific Instruments, Prahran, Australia) for 2 minutes under an argon atmosphere. The SEM samples were subsequently analyzed using a Hitachi S-800 scanning electron microscope (Tokyo, Japan).

### **Determination of SOD encapsulation efficiency**

A Micro-BCA protein assay kit (Pierce 23235) was used to determine protein loading. Briefly, protein was isolated from the particles by dissolving a few milligrams of microparticles in 1 mL of SDS/HCl (0.25% w/v, 0.02 M) solution. BCA reagent (150  $\mu$ L) was mixed into microplate wells with 30  $\mu$ L of dissolved protein SDS/HCl solution and 120  $\mu$ L of PBS (100 mM) solution. The microplate was placed in a shaker (100 RPM) for approximately 30 seconds and then incubated for 2 hours at 37°C. The microplate was cooled to room temperature, and the absorbance at 562 nm was read by a plate reader. A protein calibration curve was made by preparing known concentrations of SOD solutions.

### **Determination of SOD activity**

A SOD assay activity kit (Fluka 19160) was used to determine the percent activity of SOD encapsulated in S/O/W and W/O/W microparticles. Briefly, approximately 2 mg of microparticles were dissolved in 500  $\mu$ L of DCM in a small vial. The vial was then placed in a 60°C oil bath, allowing the DCM to slowly evaporate, leaving solid polymer and SOD, which was then mixed in 1 mL of dilution buffer provided by the SOD assay kit. The dissolved SOD and suspended polymer were placed in a small centrifugation tube and centrifuged at 5000 G for 1 minute to separate the insoluble polymer from the

SOD solution. A kinetic study was then performed on the SOD solution and a set of prepared standards by measuring the absorbance (450 nm) as the SOD reacted with the SOD assay kit reagents over the course of ten minutes.

### **Cell Culture**

RAW 264.7 macrophage (ATCC number: TIB-71) from the American Type Culture Collection (ATCC) (Manassas, VA) were maintained at 37 °C under a humidified atmosphere of 5 % CO<sub>2</sub> in Dulbecco's modified eagle's medium (DMEM) containing 10% (v/v) fetal bovine serum (FBS), supplemented with penicillin (100 units/ml) and streptomycin (100 µg/ml). IC-21 macrophages (TIB-186) from ATCC were also maintained under the same conditions as TIB-71 with RPMI-1640 cell culture medium containing 10% FBS.

### **Efficacy of SOD-loaded PK3 microparticles *in vivo* and liver histology.**

Six to eight-week-old female BALB/c mice were obtained from the Jackson Laboratory (Bar Harbor, Maine). They were maintained under controlled conditions and had free access to standard chow and water. The efficacy of the PK3 microparticles encapsulating SOD was evaluated in an *in vivo* mouse model of acute liver injury. All reagents were injected in a total volume of 100 µL per BALB/c mouse for either intravenous (IV) or intraperitoneal (IP) injections. For statistical analysis, all experiments were performed using 6 mice per group unless otherwise specified. SOD-loaded PK3 microparticles (60 U/mg, 1 mg/mL) were injected into the blood stream of mice through a jugular vein, immediately followed by an IP injection of LPS (2.50

$\mu\text{g/kg}$ ) from *E.coli* 0111:B4 with 700 mg/kg of Galactosamine (GalN). After 24 h, blood was collected from the mice by cardiac puncture and centrifuged at 4,000 RPM for 15 minutes. Plasma alanine aminotransferase (ALT) level was measured for liver function analysis using an ALT assay kit (Pointe Scientific Inc., Canton, MI). Plasma TNF- $\alpha$  level was also measured by using an enzyme-linked immunosorbent assay (ELISA) kit. Significance of results was determined via the paired t test with  $p < 0.05$ .

### **Histological analysis of liver**

For liver histology, livers were collected and frozen in optimal cutting temperature (OCT). OCT embedded livers were sliced with 10 $\mu\text{m}$  sections using Microm Cryo-Star HM 560MV Cryostat and liver sections were stained with haematoxylin and eosin.

### **Bio-distribution of fluorescein-loaded PK3 microparticles *in vivo*.**

Fluorescein-loaded PK3 microparticles were used for a bio-distribution study of PK3 microparticles. Fluorescein-loaded PK3 microparticles were injected to 3 mice through their jugular vein. The mice were sacrificed 2 hours after the IV injection, and perfusion was performed using PBS (150 mM, pH 7.4). All organs were collected and placed in 5 mL of 20% (v/v) triton x-100 and 80% (v/v) PBS (150 mM, pH 7.4). The organs were homogenized at 12,000 RPM for 2 minutes and centrifuged at 5,000 RPM for 5 minutes. Fluorescence of fluorescein in clear supernatant was measured with 494 nm excitation and 510 nm emission.

**Bio-distribution of pentacene-loaded PK3 microparticles *in vivo*.**

Pentacene-loaded PK3 microparticles were used for a bio-distribution study of PK3 microparticles. Pentacene-loaded PK3 microparticles were injected to 3 mice through their jugular vein. The mice were anesthetized 2 hours after the injection and observed with a Xenogen IVIS Lumina *in vivo* imaging machine (Caliper Life Sciences, Hopkinton, MA).

## 4.4 Results

### Formulation of SOD-loaded PK3 microparticles

A water/oil/water double emulsion procedure and a solid/oil/water procedure were developed to encapsulate FITC-SOD, based on procedures developed for encapsulating SOD in PLGA microparticles (Perez, Castellanos et al. 2002; Castellanos, Crespo et al. 2003; Giovagnoli, Blasi et al. 2004). Figure 4.1A shows an SEM image of FITC-SOD-loaded microparticles, formulated from PK3, and demonstrates that their size ranges from 1 micron to 5 microns, which is suitable for intracellular delivery to phagocytic cells. The FITC-SOD-loaded microparticles could also be easily dispersed into an aqueous solution, after freeze drying, as demonstrated by the fluorescence microscope image in Figure 4.1B.

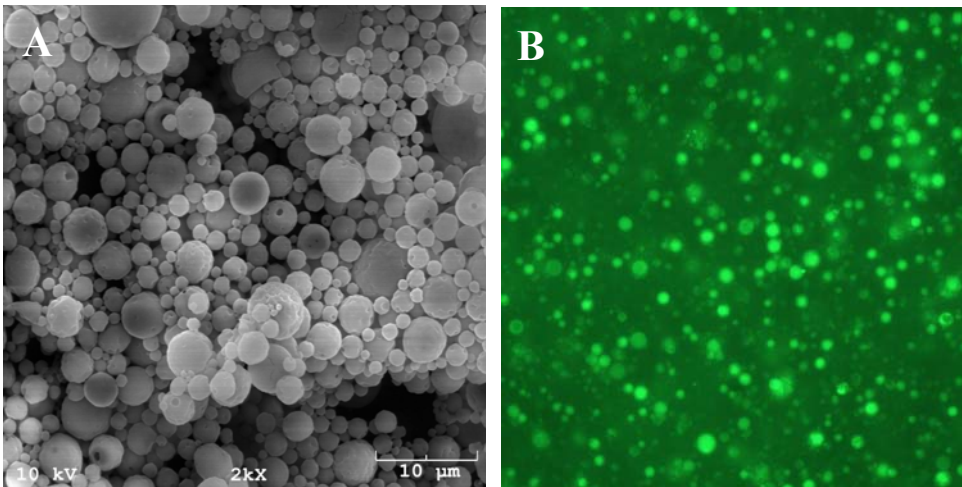


Figure 4.1. SEM image and fluorescence microscopy image of SOD-loaded PK3 microparticles. (A) SEM image of FITC-SOD-loaded microparticles formulated from PK3. (B) 10 X fluorescence microscopy image of the FITC-SOD-loaded particles in aqueous buffer.

### **Loading and enzymatic activity of SOD in PK3 microparticles**

The biological activity of SOD was determined through a kinetics study comparing encapsulated SOD to SOD solutions of known concentrations. The rate of reaction was determined by calculating the initial linear slopes of the absorbance versus time data of the standards and microparticles. A calibration curve was created by graphing these slopes of the standards versus the concentration of units of activity of each standard (Figure 4.2). From this calibration curve, the concentration of units of activity of the S/O/W and W/O/W microparticles was calculated. The activity of encapsulated SOD was determined by multiplying the amount of SOD encapsulated with the activity of SOD encapsulated. Dividing the concentration of units of activity of the S/O/W and W/O/W microparticles by their theoretical activity gives the amount of biological activity preserved (Table 4.1). Loading of SOD from S/O/W was calculated to be 60 units of active SOD/ mg of PK3 microparticles.

Table 4.1. SOD loading, encapsulation efficiency, and enzymatic activity in PK3 microparticles from S/O/W and W/O/W emulsion methods.

Double Emulsion Method	SOD Loading by weight	Encapsulation Efficiency	SOD Enzymatic Activity
S/O/W	4.0%	42.4%	29.9%
W/O/W	1.2%	11.8%	2.7%



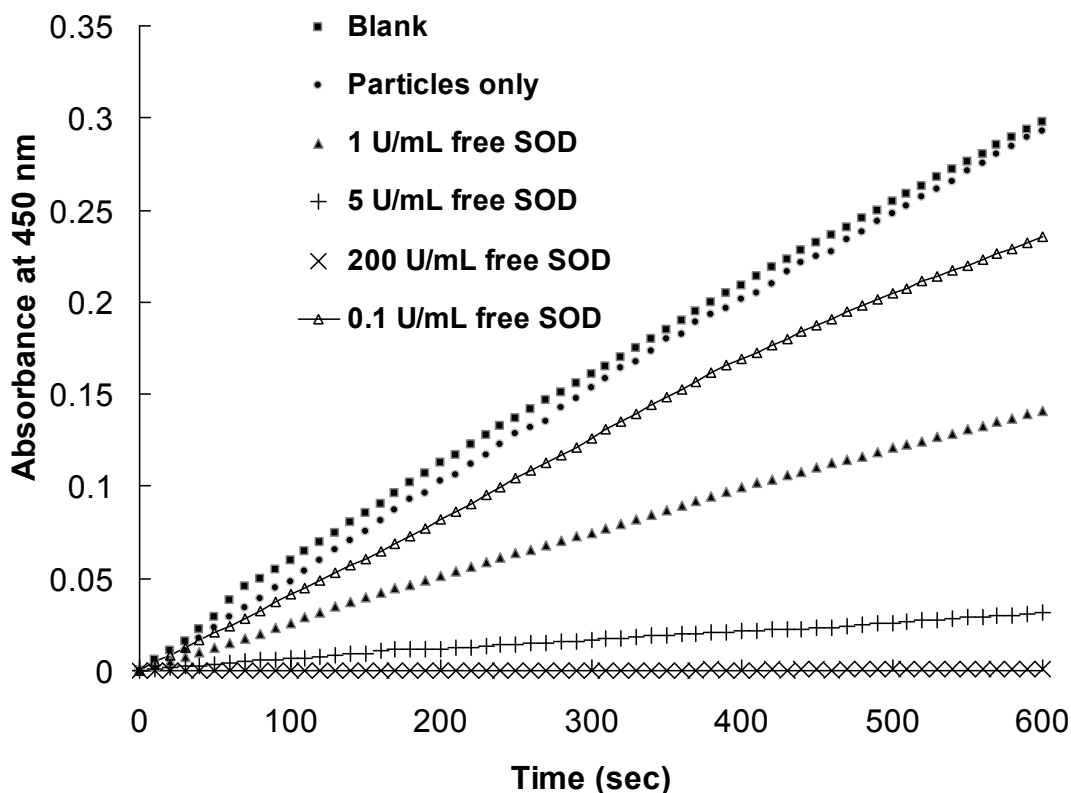


Figure 4.2. Enzymatic activities of SOD were determined by establishing a calibration curve. The activity of SOD was determined using an SOD assay kit (Fluka, SOD determination kit 19160, St Louis, MO). Superoxide causes the substrate used in the kit to have absorbance at 450 nm, which can be inhibited by active SOD; therefore declining slopes corresponds to increasing SOD activity.

### **Uptake of SOD loaded PK3 microparticles to macrophage cells**

We incubated the FITC-SOD loaded PK3 microparticles with TIB186 macrophage cells for 1 hour. Cells were subsequently washed extensively and observed under phase contrast and fluorescence microscope. Figure 4.3 shows phase contrast and fluorescence images of the same population and their overlay composite. The composite image clearly shows that the fluorescence activity was occurring inside the macrophage

cells, indicating that FITC-SOD particles were effectively taken up by macrophage cells within 1 hour of co-incubation of the particles with the cells.

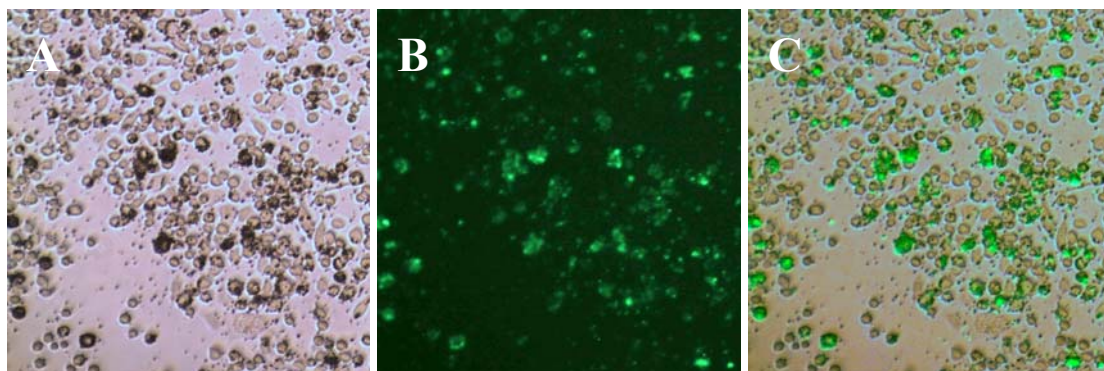


Figure 4.3. Macrophage uptake study of SOD-loaded PK3 microparticles. (A) Image of TIB186 macrophage cells incubated with FITC-SOD particles from 10X phase contrast microscope. (B) Image of the same population of cells as A from 10X fluorescence microscope. (C) Overlay image of A and B.

An uptake study using flow-cytometry was performed with FITC-SOD loaded PK3 microparticles. Macrophages were incubated with equal amounts of either FITC-SOD or FITC-SOD encapsulated within PK3 microparticles, for 24 hours, and analyzed by flow cytometry. Figure 4.4 demonstrates that PK3 microparticles dramatically increased the uptake of FITC-SOD. For example, FITC-SOD, dissolved in PBS buffer, is not efficiently taken up by macrophages, generating fluorescence levels that are comparable to untreated cells. In contrast, the fluorescence levels of macrophages treated with PK3 microparticles, containing FITC-SOD, is substantially higher than control cells, presumably due to efficient phagocytosis of the PK3 microparticles.

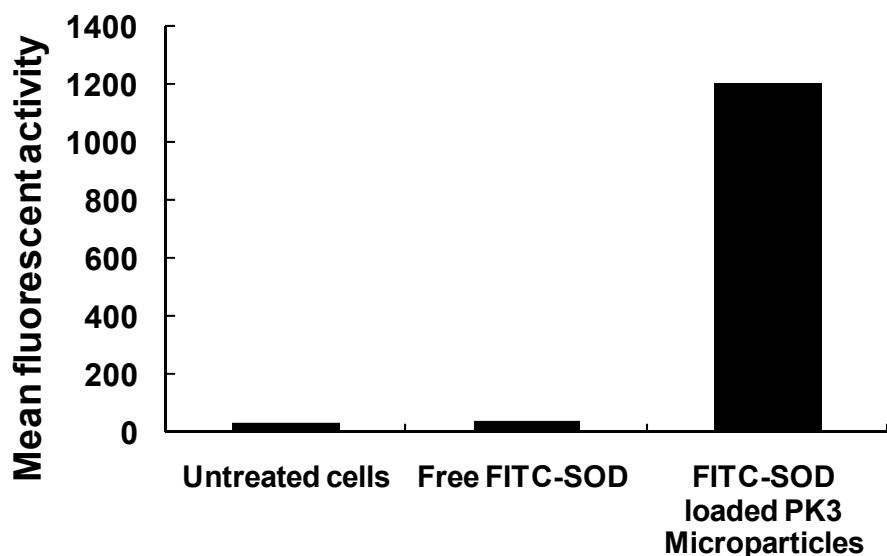


Figure 4.4. PK3 Microparticles enhance the delivery of SOD to macrophages. TIB-186 Macrophages were treated with either 1  $\mu\text{g}/\text{mL}$  free FITC-SOD or 1  $\mu\text{g}/\text{mL}$  FITC-SOD encapsulated within PK3 microparticles for 24 hours, extensively washed, and analyzed by flow cytometry (BD LSR II Flow Cytometer, San Jose, CA).

#### ***In vivo* delivery of polyketal microparticles to Kupffer cells**

In collaboration with Dr. Robert Pierce at the University of Rochester, polyketal microparticles formulated from PPADK containing 1% fluorescein by weight were administered intravenously to mice, and liver was isolated one hour post-injection for histological analysis. Fluorescent microscopy of the liver sections indicates that the polyketal microparticles are abundantly present throughout the liver. Anti-fluorescein immunohistochemistry confirms the presence of fluorescein-loaded microparticles within the cytoplasm of a Kupffer cell lining a liver sinusoid (Figure 4.5). Although PK3 was not used in this experiment, based on the similarities in physical properties among all polyketals, the results presented suggest that microparticles formulated from polyketals can target Kupffer cells *in vivo*.

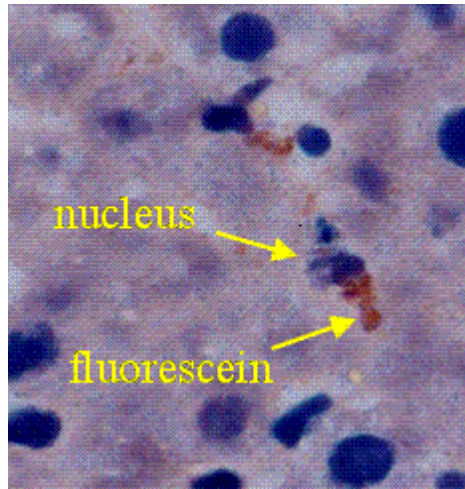


Figure 4.5. Release of fluorescein from PPADK microparticles. Dark red = anti-FITC staining; Blue = DAPI staining (nuclei).

#### ***In vivo* delivery of PK3 microparticles to the liver**

A biodistribution study was conducted to verify that PK3 microparticles could passively target the liver and accumulate in the liver. Fluorescein was encapsulated in PK3 microparticles (1% by weight), which were intravenously administered to mice. 2 hours after the IV injections, blood was collected from the mice, which were subsequently perfused to remove any residual blood. Five organs (lung, liver, kidney, spleen, and heart) were then isolated, homogenized, and centrifuged to give a supernatant, which was analyzed for their fluorescein concentrations. Figure 4.6 demonstrates that the fluorescein level found in the liver was significantly higher than the levels found in other organs, indicating that PK3 microparticles preferentially accumulated in the liver. Empty PK3 microparticles were also injected into mice to prove that there is no auto-fluorescence generated by the administration of microparticles

due to activation of immune cells (Figure 4.6). Interestingly, there was a small level of fluorescein detected in the blood, possibly because there was a small amount of fluorescein released in the blood due to degradation of the PK3 microparticles.

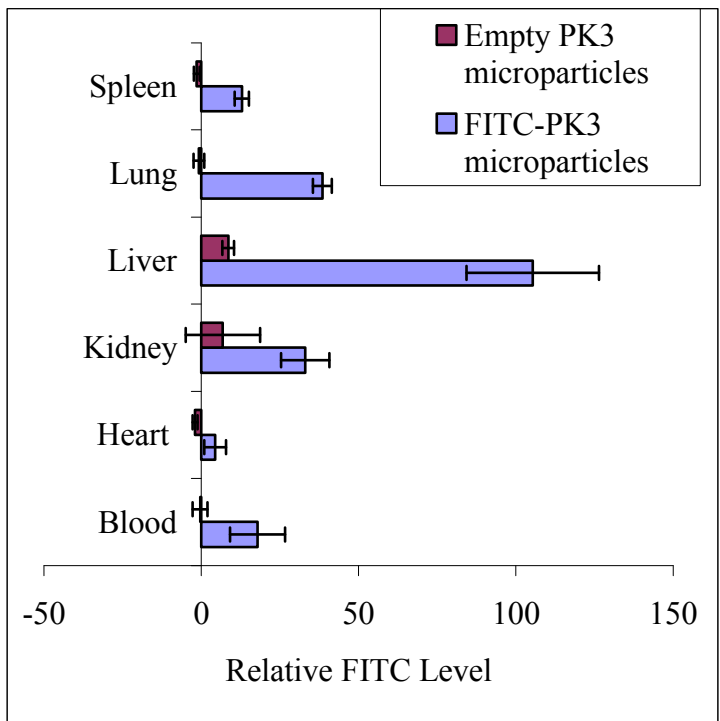


Figure 4.6. Biodistribution study using PK3 microparticles (0.1 mg/mouse) encapsulating fluorescein (1% by weight). Organs were collected 2 hours after fluorescein-PK3 microparticles were injected IV. Data presented as means  $\pm$  standard error of the mean (SEM), n = 3.

To visually verify that PK3 microparticles can passively target the liver, PK3 microparticles encapsulating a pentacene dye were also administered into mice via IV injections. Pentacene was chosen for this experiment because it has an emission wavelength of 710 nm, which is necessary for real-time *in vivo* imaging because long wavelength signals can penetrate the tissue and skin around those the organs. 2 hour after the IV injections, those mice were observed in a Xenogen *in vivo* imaging machine for the distribution of pentacene. The results demonstrate that the dye-loaded PK3 microparticles could only be found in the abdominal region of the mice. The intensity of

emission from pentacene is the strongest around the area where the liver resides in the mice (Figure 4.7). In combination with the quantitative data from the fluorescein-loaded PK3 microparticles, these results strongly suggest that PK3 microparticles passively target the liver.

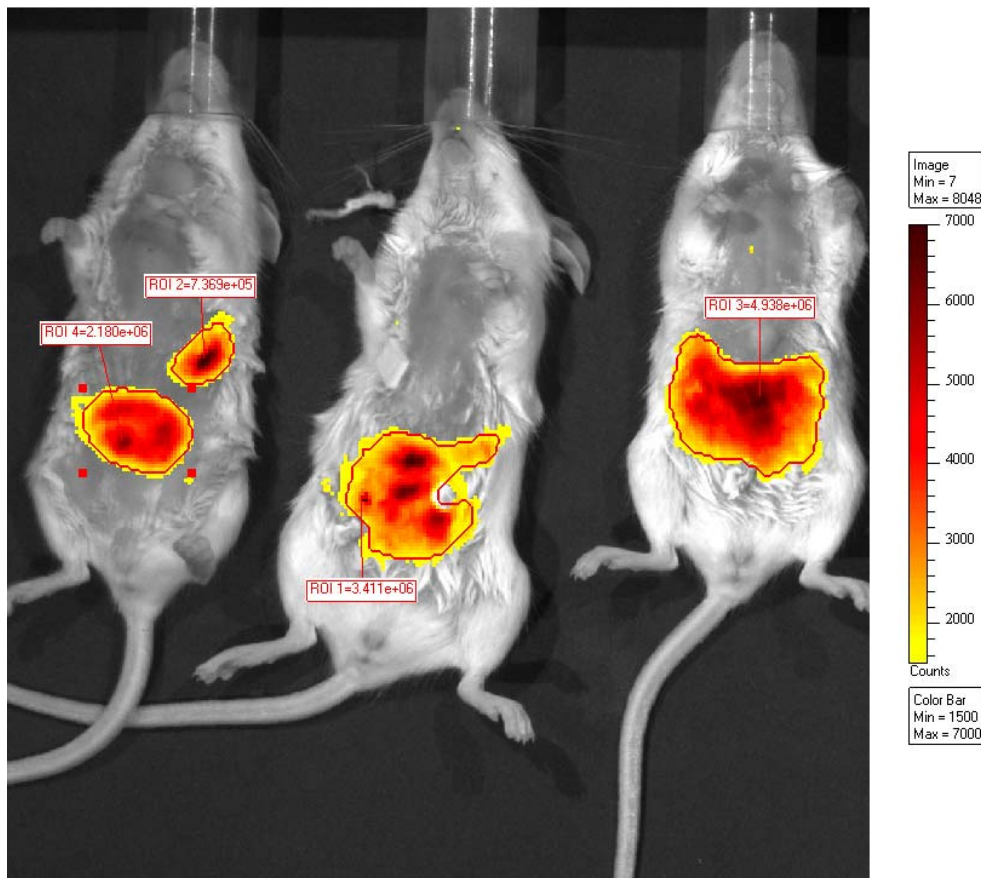
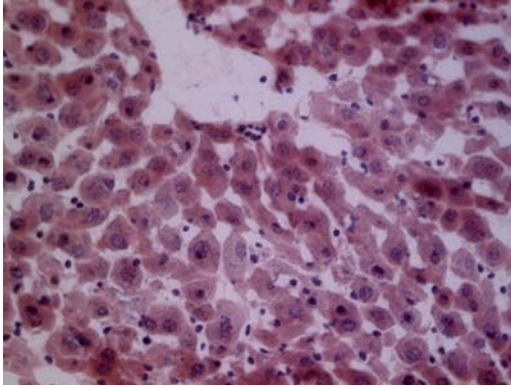


Figure 4.7. Biodistribution study using PK3 microparticles (0.1 mg/mouse) encapsulating pentacene (0.2% by weight). Images were taken 2 hours after pentacene-PK3 microparticles were injected IV. Data presented as mean  $\pm$  standard error of the mean (SEM),  $n = 3$ . Excitation wavelength = 670 nm, Emission wavelength = 710 nm.

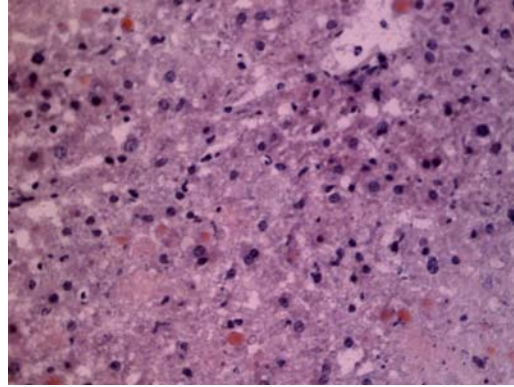
### **SOD-loaded PK3 microparticles for treating LPS-induced acute liver failure**

BALB/c mice were administered with either SOD-PK3 microparticles (SOD-PKM) (6 U of SOD/mouse), free SOD (6 U of SOD/mouse), saline, or empty PK3

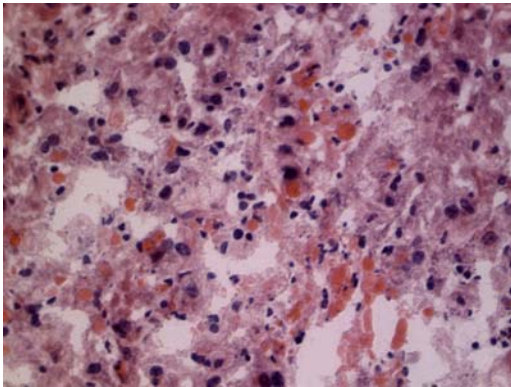
microparticles (PKM) through IV injections. LPS was immediately administered via IP injections to induce acute liver injury. 24 hours later, blood and the liver were collected from the mice. The severity of damage in the liver was assessed by histological analysis of the liver and quantified by measuring the serum levels of ALT and TNF- $\alpha$ . Figure 4.8 shows the histological analysis of sections from the liver of mice that received various treatments. Liver samples were frozen in OTC, cut into 10  $\mu\text{m}$  slices, mounted on glass slides, and stained with hematoxylin and eosin for morphological analysis. Liver slides from the negative group (saline IP + saline IV) show healthy cell structures with defined boundaries. Liver slides from mice that received free SOD, empty PKM, and saline through IV injections and LPS via IP injections show significant fusion of hepatocytes which no longer have clear boundaries for individual cells, indicating necrosis of hepatocytes. In addition, there is also presence of red blood cells in these liver slides as evidenced by red dots on the histology images, indicating that there was bleeding within the sinusoidal space of the liver in those mice. Sinusoidal bleeding is indicative of hepatocellular necrosis and extensive liver damage. On the other hand, liver slides from mice that received SOD-PKM and LPS do not have any red blood cells, and the boundaries of hepatocytes in these slides are much more defined than liver slides from mice that received free SOD, empty PKM, or saline. However there is still fusion among hepatocytes, indicating that there was necrosis in the liver for mice that received SOD-PKM, although the damage was not as great as the mice that received free SOD, empty PKM, or saline.



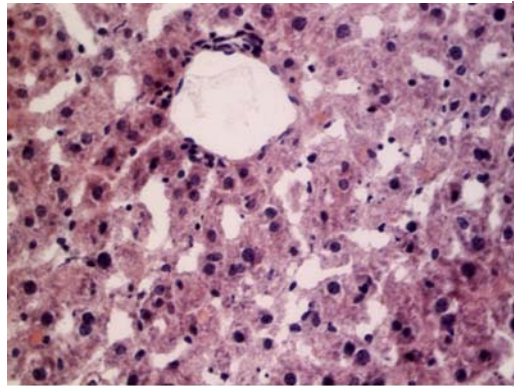
Saline IP + Saline IV



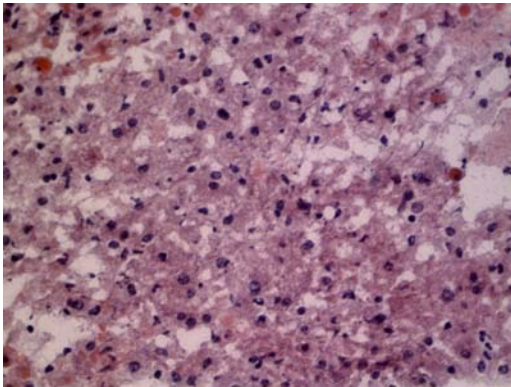
LPS IP + Saline IV



LPS IP + Empty PKM IV



LPS IP + SOD PKM IV



LPS + Free SOD IV

Figure 4.8. Liver histology study using hematoxylin and eosin (H&E) staining (tissue thickness sliced: 10um, magnification: x40)



The extent of liver damage in mice that received either SOD-PKM, free SOD, empty PKM, or saline was also quantified by measuring their serum ALT levels 24 hours after the treatment. Figure 4.9 demonstrates that mice that received free SOD, empty PKM, and saline before they were treated with LPS showed extremely high level of ALT in their serum, indicating that their livers were severely compromised, with extensive hepatocellular necrosis taking place in their livers. The mice that received SOD-PKM treatment and LPS showed a significantly lower level of ALT in their blood, suggesting that the hepatocellular necrosis was substantially less than mice that received free SOD, empty PKM, and saline. Interestingly, mice that received free SOD did not show any reduction in their serum ALT values. To verify that empty PKM does not cause significant liver damage, empty PKMs were injected IV into mice before they received saline through IP injections. The serum ALT values in those mice were not significantly increased.

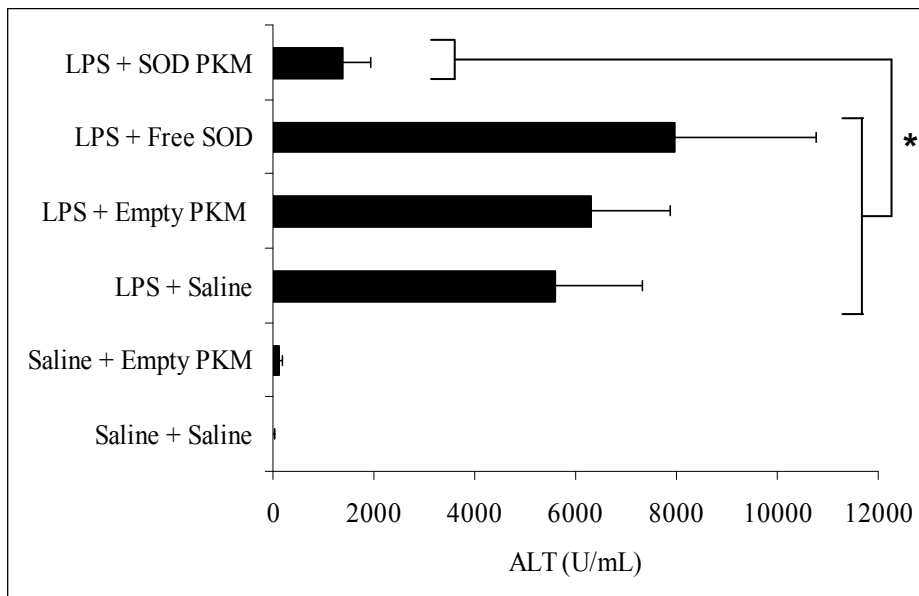


Figure 4.9. Alanine aminotransferase (ALT) assay; liver damage was measured by the amount of ALT enzyme in the plasma. Data presented as means  $\pm$  SEM, n = 6. Significance of results was determined via the paired t test with  $p < 0.05$  (95% confidence interval). \* indicates that the differences are statistically significant.

The levels of systemic inflammatory response was also quantified in mice that received either SOD-PKM, free SOD, empty PKM, or saline, by measuring their serum TNF- $\alpha$  levels. Figure 4.10 demonstrates that SOD-PKM was able to return the TNF- $\alpha$  levels back to the baseline level after the mice were treated with LPS. On the other hand, mice that received free SOD, empty PKM, or saline had elevated TNF- $\alpha$  levels in their blood after LPS treatment, presumably due to activation of NF $\kappa$ B in the Kupffer cells, which produce higher level of TNF- $\alpha$ .

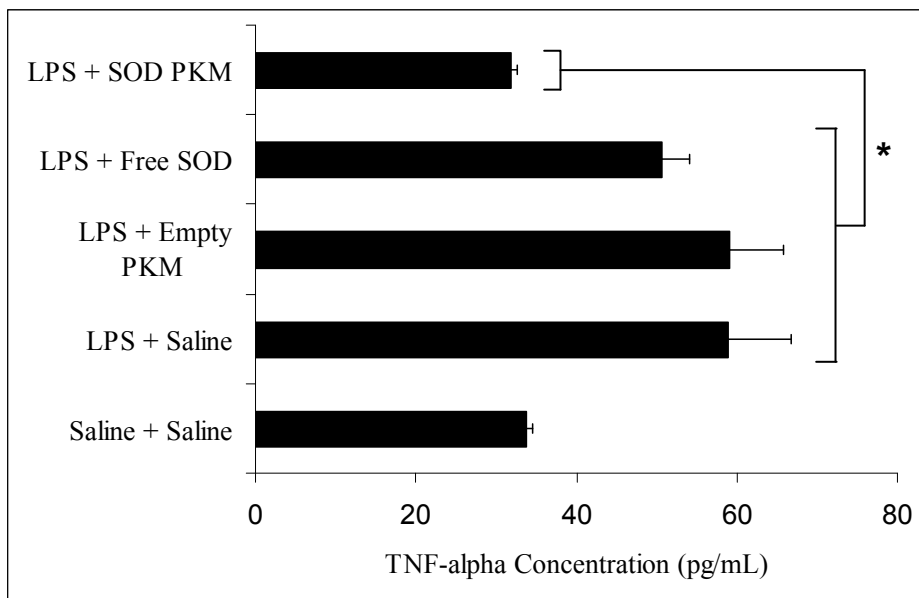


Figure 4.10. ELISA assay; the concentration of TNF- $\alpha$  in plasma collected at 24 h after the treatment of sample and LPS. Data presented as means  $\pm$  SEM, n = 6. Significance of results was determined via the paired t test with  $p < 0.05$  (95% confidence interval). \* indicates that the differences are statistically significant.

## 4.5 Discussion

### Formulation of PK3 microparticles encapsulating SOD

The polyketal PK3 was investigated for microparticle formulation because of its suitable hydrolysis kinetics and biocompatible degradation products, which are 1,5-pentanediol, 1,4-cyclohexanedimethanol, and acetone. The most common method for encapsulating hydrophilic molecules like oligopeptides and proteins within a hydrophobic polymer is the water-in-oil-in-water (W/O/W) double emulsion method. This method entails dissolving the polymer in an organic solvent, dissolving the protein in a small amount of water, and forming an emulsion of these two phases using high intensity mixing. This forms the first water-in-oil emulsion. This first emulsion is thermodynamically unstable, resulting in separation between the water and oil phases. Therefore, a second oil-in-water emulsification, with an stabilizer dissolved in the outer water phase, is necessary to disperse the first emulsion (Patrick J. Ginty 2006).

The W/O/W method has a few limitations. First, some of the hydrophilic protein may not remain encapsulated in the first W/O emulsion and can diffuse into the outer water phase. This results in low encapsulation efficiency, which is problematic when the protein loading is too low to effectively produce the desired therapeutic benefits. Second, this W/O/W method can destabilize proteins. Proteins can adsorb to the water-oil interface causing the protein to unfold due to simultaneous interactions between a thermodynamically favorable water phase and unfavorable organic phase (Sah 1999). One potential solution to these problems is using a different double emulsion method known as the solid-in-oil-in-water (S/O/W) double emulsion method.

The S/O/W method replaces the first emulsion of the W/O/W method with solid protein suspended in an organic solvent. Although organic solvents are thermodynamically unfavorable to proteins, the protein experiences a kinetic trap, which prevents unfolding and strongly reduces reactivity (Schwendeman 2002). This kinetic trap inhibits some of the primary causes of protein degradation including deamidation, oxidation, aggregation, hydrolysis, and shear stress caused by the emulsion process (Wright 2000). Furthermore, since the protein is not in solution throughout the entire process, less protein is lost through solvation into the aqueous phase, resulting in a greater encapsulation efficiency (Putney and Burke 1998).

The S/O/W method works most efficiently when the protein can be dispersed into particles are at least ten times smaller than the polymeric particle (Maa and Hsu 1997). Costantino developed a method of nebulizing protein particles using a spray freeze drying method (Costantino, Firouzabadian et al. 2000). However, this method is complicated and can be potentially damaging to proteins due to physical stresses. A simpler method of freeze drying the protein in a solution of polyethylene glycol (PEG) was developed, which results in PEG forming a matrix around the protein particles (Morita, Sakamura et al. 2000). This is hypothesized to take place through the aqueous phase-separation phenomena, where two different macromolecules in an aqueous solution spontaneously separate into a continuous phase and micro-sized droplets. This process is advantageous because it can control protein particle size, creates spherical protein particles, and results in a high yield of protein particles. Furthermore, since PEG is amphiphilic, it can readily be removed in an organic solvent without disturbing the protein particles (Morita, Sakamura et al. 2000). It was found that bovine serum albumin (BSA) co-lyophilized

with PEG forms far less aggregates when released from PLGA particles than when not lyophilized with a stabilizing excipient (Carrasquillo, Stanley et al. 2001; Al-Azzam, Pastrana et al. 2002).

Our previous attempts at encapsulating protein inside polyketal microparticles using the W/O/W method resulted in 1.2% protein loading of SOD in particles that were 10 – 20 microns in diameter (Lee, Yang et al. 2007). This value is relatively low and indicates a 65% loss of protein during the encapsulation process. Moreover, it is much more challenging to encapsulate SOD in microparticles with small diameters (1-5 microns), which are suitable for phagocytosis by macrophages. In this Chapter, I demonstrate that the S/O/W method was used to formulate polyketal microparticles (1-5 microns in diameter) which encapsulate SOD with higher loading efficiencies and greater preservation of SOD enzymatic activities than W/O/W method. Specifically, the S/O/W method results in 37 times greater loading of active SOD than the W/O/W method. This confirms that the S/O/W is not only superior to the W/O/W method for protein loading but also for preserving biological activity.

### **Biodistribution of PK3 microparticles**

One essential requirement for delivering SOD to treat acute liver failure is the ability to target SOD to the liver, particularly Kupffer cells, which are the primary sources of oxidative stress during liver injury. SOD by itself does not have affinity towards the liver. The distribution of SOD in the blood is 13 times higher than that in the liver 3 hours after SOD is administered to mice via IV injections (Nakaoka, Tabata et al. 1997). Our studies of fluorescein and pentacene-loaded PK3 microparticles

quantitatively and qualitatively demonstrated that PK3 microparticles 1- 5 microns in size can passively target and accumulate in the liver. Pentacene-loaded PK3 microparticles were preferentially accumulated in the abdominal region of mice where the liver resides only 2 hours after the particles were intravenously injected into the mice. There were no detectable levels of pentacene in other organs such as the heart, lung or blood. Since kidneys are located in the back of the liver, Figure 4.7 can not differentiate PK3 microparticle distribution between the liver and the kidneys. Therefore fluorescein was also encapsulated in PK3 microparticles to enable quantification of PK3 microparticle distribution *in vivo*. The distribution of fluorescein-loaded PK3 microparticles was 3 times higher in the liver than in the lung and kidneys. Importantly, the distribution of PK3 microparticles was 6 times higher in the liver than in the blood. This organ distribution of polyketal microparticles is consistent with that of PLGA microparticles of similar size where the liver distribution of PLGA microparticles is 10 times higher than in the blood 3 hours post IV injection (Dunn, Coombes et al. 1997). Based on these results, one can speculate that when SOD is loaded in PK3 microparticles, SOD will also preferentially accumulate in the liver. Therefore, PK3 microparticles can effectively target SOD to the liver to achieve a therapeutic effect, whereas the distribution of free SOD in the blood was much higher than in the liver. In combination with our previous study which showed that polyketal microparticles were only observed in the Kupffer cells, we can speculate that PK3 microparticles have great potential for delivering SOD to the liver, particularly Kupffer cells, to reduce oxidative stress in the liver during acute liver injury.

### ***In vivo* efficacy of SOD-loaded PK3 microparticles for treating ALF**

The *in vivo* efficacy of SOD-loaded PK3 microparticles was tested in a mice model of LPS-induced acute liver injury. The severity of damage in the liver was assessed by histological analysis of the liver and quantified by measuring the serum levels of ALT and TNF- $\alpha$ . ALT is an enzyme normally present within hepatocytes. During an acute liver injury event, hepatocytes are damaged and leak ALT into the blood, dramatically raising the serum ALT levels. The level of inflammatory responses in the liver was also assessed by measuring the serum TNF- $\alpha$  level, which corresponds to the secretion of pro-inflammatory cytokines due to activation of the transcription factor, NF $\kappa$ B, in the Kupffer cells.

For mice that received SOD-loaded PK3 microparticles, their liver histology slides do not show presence of red blood cells, suggesting that there was no significant sinusoidal bleeding. However, there was hepatocyte damage as evidenced by cell boundaries fusing among hepatocytes. The histological analysis of liver tissue from this group indicates that the hepatocytes were damaged to a certain extent, but not severely enough to cause sinusoidal bleeding as observed in the group of mice that did not receive any treatment. Serum ALT level from this group was also significantly lower than the positive control group but higher than the negative control group, indicating that the damage to hepatocytes was substantially less than mice that did not receive any treatment but significantly more than mice that did not have liver injury. Serum TNF- $\alpha$  level from this group was also returned back to the baseline level, indicating that the inflammatory response was diminished due to the target delivery of SOD to the liver. Interestingly, for the SOD-PKM treated group, serum ALT level was reduced but still significantly higher

than the baseline level, whereas TNF- $\alpha$  level was reduced to the baseline level. This could be attributed to targeting of PK3-microparticles to Kupffer cells, where intracellular superoxide was reduced to baseline level, resulting in normal expression of TNF- $\alpha$  because NF $\kappa$ B was not significantly activated. However, there was still extracellular superoxide that could cause hepatocyte necrosis and liver injury. Importantly, the same dosage of SOD injected intravenously did not show any reduction in liver injury or systemic inflammation as compared to the positive control. This is most likely due to lack of targeting SOD to the liver. Take together, these results prove that PK3 microparticles significantly improved the efficacy of SOD in treating LPS-induced acute liver injury.



## CHAPTER 5

### CONCLUSIONS AND FUTURE DIRECTIONS

#### 5.1 Conclusions

By completing the research described in this thesis, I have demonstrated the development of a new family of aliphatic polyketals for the delivery of SOD to treat acute liver failure. An aliphatic polyketal, PCADK, was designed to hydrolyze in the acidic environment of the phagolysosomes and enhance the delivery of therapeutics to phagocytic cells such as macrophages. Key attributes of PCADK are its well-characterized, neutral degradation products, and straightforward synthesis. PCADK was synthesized on a multi-gram scale in one step, and hydrolyzes into acetone and 1,4-cyclohexanedimethanol, both of which are non-acidic and have low toxicity. The hydrolysis of PCADK is pH-sensitive, having a hydrolysis half-life of 24.1 days at pH 4.5 and an estimated half-life of over 4 years at pH 7.4. We also demonstrated that the hydrolysis rate of PCADK could be accelerated by varying its hydrophilicity. Using this strategy, an aliphatic polyketal copolymer, PK3, was synthesized, which is suitable for drug delivery application treating acute liver failure, having a hydrolysis half-life of 2 days at pH 4.5, but was stable for several weeks at pH 7.4. Microparticles were formulated from PK3, which can passively target the liver and preferentially accumulate in the liver. PK3 microparticles, encapsulated the anti-inflammatory enzyme SOD, significantly improved the efficacy of SOD in treating LPS-induced acute liver damage *in vivo*, as evidenced by decreased serum levels of ALT and TNF- $\alpha$ . In summary, this thesis research demonstrated the ability of polyketal-based drug delivery systems for

treating acute inflammatory diseases and created a potential therapy for enhancing the treatment of acute liver failure. Based on our findings, we anticipate numerous applications of drug delivery systems based on aliphatic polyketals for treating inflammatory diseases, given their ability to target macrophages, rapid and tunable release kinetics, and biocompatible degradation products.

## 5.2 Future Directions

### **Synthesis of high molecular weight polyketals with new synthetic approaches**

The molecular weights of polyketals currently synthesized are relatively low, with a typical  $M_n$  being between 2000 and 4000 Da. We speculate that this is due to the step-growth nature of the polymerization, which makes the molecular weight very sensitive to the stoichiometry of the reactants. Although the diols and ketal were initially mixed at a 1 to 1 ratio, this reaction has to be performed at 100 °C, because of the need to remove the reaction byproduct methanol. However, 2,2-dimethoxypropane has a boiling point of 83 °C and was also removed at this temperature, thereby altering the 1 to 1 ratio of the reactants. The use of an alternative ketal, 2,2-diethoxypropane, for this acetal-exchange reaction will alleviate the removal of the reactants. 2,2-diethoxypropane has a boiling point of 132.2 °C, as opposed to the boiling point of 83 °C for 2,2-dimethoxypropane. Therefore the reactants in this alternative synthesis approach will not be removed under the reaction temperature, allowing the stoichiometry ratio of the reaction to be kept at 1:1. The precise control of the stoichiometry ratio of a step-growth polymerization will result in high conversion of the monomers and high molecular weight of polymers (Figure 5.1).

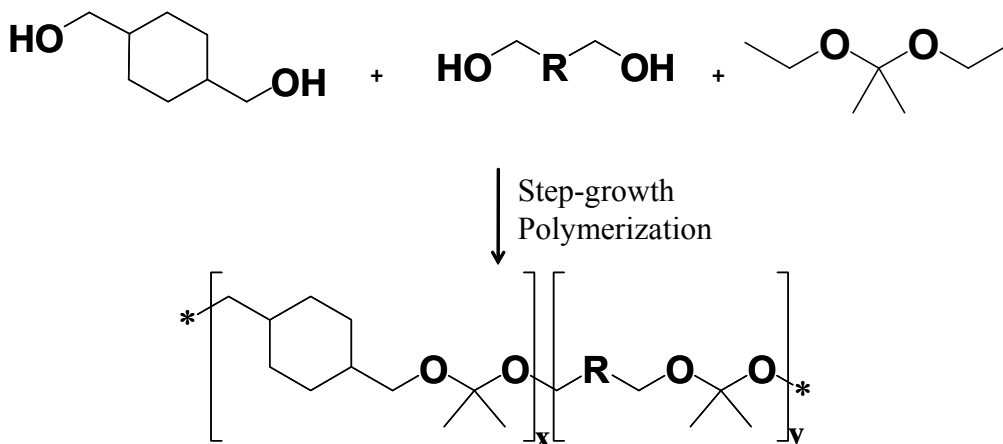


Figure 5.1. Synthesis of polyketals with diols and 2,2-diethoxypropane to yield high molecular weight polymers.

### Load SOD mimetic in PK3 microparticles to treat ALF

PK3 microparticles enhanced the delivery of SOD to the liver and reduced liver damage and inflammation in mice that suffered from LPS-induced acute liver injury. The level of serum TNF- $\alpha$  in those mice were similar to the baseline level of TNF- $\alpha$ . These results suggest that activation of NF $\kappa$ B in Kupffer cells in mice that received SOD-loaded PK3 microparticles was at baseline level due to delivery of SOD intracellularly to Kupffer cells. On the other hand, the ALT level in those mice ( $\sim$ 1000 U/mL) was still significantly higher than the baseline level ( $<$ 50 U/mL). This can be attributed to two reasons. First, the dosage of SOD delivered to the liver is only enough to reduce oxidative stress in the Kupffer cells but not in the hepatocytes and extracellular space of the liver. Second, SOD is not membrane permeable, and therefore can not diffuse out of the cell membrane. Once SOD-loaded PK3 microparticles are phagocytosed into Kupffer cells, the released SOD can not diffuse out of those Kupffer cells and scavenge extracellular SOD.

A potential solution is the use of hydrophobic mimetic of SOD, which has been extensively investigated for reducing oxidative stress in inflammatory diseases such as splanchnic artery occlusion and reperfusion, lung injury, ischemia/reperfusion injury, doxorubicin-induced cardiotoxicity, and acute liver failure (Kilgore, Friedrichs et al. 1994; Konorev, Kennedy et al. 1999; Cuzzocrea, Mazzon et al. 2001; Malassagne, Ferret et al. 2001; Vujaskovic, Batinic-Haberle et al. 2002). There are two major advantages in using SOD mimetic in combination with SOD for treating ALF. First, most SOD mimetic is hydrophobic and can therefore be encapsulated in PK3 microparticles with significantly higher loading efficiency than SOD. Second, SOD mimetic is membrane-permeable and therefore can diffuse out from Kupffer cells and into hepatocytes. This allows the SOD mimetic to scavenge superoxide residing in the extracellular space and in hepatocytes. Therefore, encapsulating both SOD and a SOD mimetic in PK3 microparticles has the potential to reduce oxidative stress in Kupffer cells, hepatocytes, and extracellular space in the liver, better protecting liver from oxidative stress during ALF than SOD-loaded PK3 microparticles alone.

#### **Further characterize SOD-loaded PK3 microparticles *in vivo***

We have shown that SOD-loaded PK3 microparticles can reduce inflammatory response and tissue damage in the liver. However, it remains unclear whether or not this reduction in ALT and TNF- $\alpha$  level is sufficient to increase the survival time of mice during ALF. Therefore, a survival study is recommended for assessing the ability of SOD-loaded PK3 microparticles in increasing the survival rate of mice suffering from ALF. During our preliminary studies in developing a mice model of ALF, it was

observed that in general, death occurred between 24 hours and 48 hours following an IP injection of LPS (2.50 µg/kg) with GalN (700 mg/kg). If a decrease in ALT and TNF- $\alpha$  levels leads to increased survival time, then mice treated with SOD-loaded PK3 microparticles will likely survive for a longer time than 48 hours after the initial LPS injection.

Furthermore, LPS/GalN model is one of the most commonly used models of lethal and nonlethal liver injury in mice (Lehmann, Freudenberg et al. 1987; Barton and Jackson 1993; Liu, Zhang et al. 2008). Rodents are constitutively resistant to LPS-induced liver toxicity; therefore, GalN is used to sensitize the liver by depleting hepatic uridine level, which leads to inhibition of protein synthesis in the liver (Mignon, Rouquet et al. 1999; Coen, Hong et al. 2007). However, this LPS/GalN model may not represent the pathology of acute liver injury in human. Therefore, a different model of acute liver injury in mice is also recommended for assessing the efficacy of SOD-loaded PK3 microparticles. For example, rodent model of acetaminophen (APAP)-induced acute liver injury has been extensively used as model for studying acute liver failure (Ferret, Hammoud et al. 2001; Reilly, Brady et al. 2001; Limaye, Apte et al. 2003). APAP induces acute liver injury by depleting glutathione in the liver and is not specific to rodents (Jones 1998). Therefore, APAP-induced ALF is potentially a better model for studying SOD delivery than LPS/GalN model of ALF.

### **Delivery of NF- $\kappa$ B inhibitors using PK3 microparticles for treating ALF**

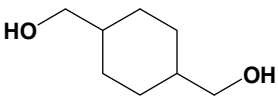
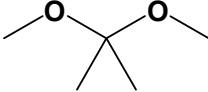
The activation of NF- $\kappa$ B in Kupffer cells also plays a central role in mediating acute liver failure. Therefore, therapeutic strategies that can inhibit NF- $\kappa$ B activation in

Kupffer cells also have great clinical potential. For example, Wolf *et al* showed that systemic injection of imatinib, which inhibits NF- $\kappa$ B activation, lowered the plasma TNF- $\alpha$  level (Wolf, Wolf et al. 2005). Our preliminary studies described in Chapter 3 also demonstrated that PK3 microparticles significantly enhanced efficacy of imatinib in treating Con A-induced acute liver failure, due to its inhibition of NF- $\kappa$ B activation in Kupffer cells and subsequent reduction in inflammatory response generated in the liver (Yang, Bhide et al. 2008). Therefore, drug delivery systems that can target NF- $\kappa$ B inhibitors to Kupffer cells have great potential in treating ALF. There have been close to 800 inhibitors of NF- $\kappa$ B identified, including antioxidants, peptides, small RNA/DNA, oligodeoxynucleotides, microbial/viral proteins, and small synthetic molecules (Pande and Ramos 2005; Gilmore and Herscovitch 2006). Among the potential targets for inhibiting NF- $\kappa$ B, I $\kappa$ B kinase (IKK) has been an important target for the development of clinically relevant NF- $\kappa$ B inhibitors. This is because IKK plays a critical role in the NF- $\kappa$ B signaling pathways from upstream signals. In particular, 6-Amino-4-(4-phenoxyphenylethylamino) quinazoline (APPEAQ) has been shown to be a highly potent inhibitor of NF- $\kappa$ B transcriptional activation ( $IC_{50}$  = 11 nM in Jurkat cells) and LPS-induced TNF- $\alpha$  production ( $IC_{50}$  = 7 nM in murine splenocytes) (Tobe, Isobe et al. 2003). APPEAQ is a hydrophobic molecule and can be easily encapsulated in polyketal microparticles via single emulsion procedures with high loading efficiency. Our preliminary studies show that APPEAQ was effective in inhibiting NF- $\kappa$ B activations in cultures of macrophages. Therefore, delivery of APPEAQ with PK3 microparticles offers another therapeutic approach for treating ALF.

## APPENDIX A

### EXPERIMENTAL PROTOCOLS

#### A.1. Synthesis of PCADK as an example of aliphatic polyketal

Materials	CDM 	DMP 	PTSA
<b>CAS #</b>	105-08-8	77-76-9	
<b>Mol. Wt</b>	144.21	104.15	190.22
<b>Formula</b>	$C_8H_{16}O_2$	$(CH_3)_2C(OCH_3)_2$	$CH_3C_6H_4SO_3 \cdot H_2O$
<b>Moles</b>	0.03467	0.03467	
<b>Amount</b>	5 g	4.26 mL	2 mL of 1 mg/mL in ethyl acetate
<b>b.p.</b>	283°C	83 °C	221 °C
<b>Density</b>	1.02 g/mL	0.847 g/mL	1.07 g/mL

1. Distill DMP and benzene; make 1 mg/mL PTSA solution in ethyl acetate.
2. Set up apparatus with distillation glassware and three-neck flask in oil bath.
3. Add 20 mL of distilled benzene to flask and heat the oil bath to 100°C.
4. Add CDM (5 g) to flask.
5. Add PTSA (2 mL) and DMP (4.26 mL) to flask to start reaction
6. Use meter funnel to add additional benzene (5 mL) and DMP (2 mL) to reaction every hour for 5 hours.
7. Let reaction run overnight.
8. Put triethylamine (1 mL) to stop reaction and pour mixture to cold hexane.
9. Put mixture in the freezer and vacuum filter after 2 hours.

### A.2. Synthesis of PK3 as an example of polyketal copolymer

Materials	CDM 80 mol%	Pentanediol 20 mol%	DMP	PTSA
CAS #	105-08-8	111-29-5	77-76-9	
Mol. Wt	144.21	104.15	104.15	190.22
Formula	C <sub>8</sub> H <sub>16</sub> O <sub>2</sub>	HO(CH <sub>2</sub> ) <sub>5</sub> OH	(CH <sub>3</sub> ) <sub>2</sub> C(OCH <sub>3</sub> ) <sub>2</sub>	CH <sub>3</sub> C <sub>6</sub> H <sub>4</sub> SO <sub>3</sub> ·H <sub>2</sub> O
Mol Ratio	80%	20%	100%	
Moles	0.03467	0.00867	0.04334	
Amount	5 g	0.908 mL	5.33 mL	2 mL of 1 mg/mL in ethyl acetate
b.p.	283°C	242 °C	83 °C	221 °C
Density	1.02 g/mL	0.994 g/mL	0.847 g/mL	1.07 g/mL

1. Distill DMP and benzene, make 1 mg/mL PTSA solution in ethyl acetate.
2. Set up apparatus with a distillation glassware and three-neck flask in oil bath.
3. Add 30 mL of distilled benzene to flask and heat the oil bath to 100°C.
4. Add CDM (5 g) and pentanediol (0.908 mL) to flask.
5. Add PTSA (3.5 mL) and DMP (5.33 mL) to flask to start reaction.
6. Use meter funnel to add additional benzene (5 mL) and DMP (2.5 mL) to reaction every hour for 6 hours.
7. Let reaction run overnight.
8. Put triethylamine (2 mL) to stop reaction and pour mixture to cold hexane.
9. Put in the freezer and filter after 2 hours.

### A.3. Formulation of polyketal microparticles encapsulating a hydrophobic drug

1. Make 5% PVA solution.
2. Dissolve 50 mg of polyketal in 0.5 mL of CH<sub>2</sub>Cl<sub>2</sub>.



3. Add 10 mg of the drug to DCM containing PCADK.
4. Add DCM solution to 5 mL of 5% PVA solution.
5. Homogenize with Powergen 500 for 1 minute at speed level 4.
6. Add the mixture to 15 mL of 1% PVA.
7. Stir for 4 hours at room temperature for solvent evaporation.
8. Transfer to a 50 mL centrifuge tube.
9. Centrifuge at 6000 g for 12 minutes.
10. Repeat washing two times.
11. Resuspend in 5 mL of DI water and freeze dry.
12. Freeze dry for 24 hours to give solid particles.

#### **A.4. Formulate SOD PK3 microparticles using water-in-oil-in-water method**

1. Make 5%, 2%, and 1% PVA solution.
2. Prepare 25 ml of 1% PVA solution in a flask with a stir bar placed in the flask.
3. Dissolve 100 mg of PK3 in 1 mL of  $\text{CH}_2\text{Cl}_2$ .
4. Dissolve 10 mg of SOD in 100  $\mu\text{L}$  of 2% PVA solution
5. Add 50  $\mu\text{L}$  of SOD solution (100mg/mL) to 500  $\mu\text{L}$  of  $\text{CH}_2\text{Cl}_2$  polyketal solution.
6. Homogenize at level 6 with Powergen 500 homogenizer for 30 seconds.
7. Add first emulsion to 5 mL of 5% PVA solution.
8. Homogenize at level 4 for 1 minute.
9. Add mixture to 25 mL 1% PVA solution and stir for 4 hours to evaporate organic solvent.

10. Transfer to 50 mL centrifuge tube and centrifuge at 5000 g for 15 minutes.
11. Discard supernatant and resuspend in 10 mL of DI water.
12. Centrifuge at 5000 g for 10 minutes.
13. Repeat washing once more.
14. Resuspend in 5 ml of DI water and freeze.
15. Freeze dry for 24 hours to give solid particles.

#### **A.5. Formulate SOD PK3 microparticles using solid-in-oil-in-water method**

1. Mix SOD with PEG in the weight ratio of 1:4.
2. Add as little DI water as possible to dissolve the mixture.
3. Quickly freeze the SOD/PEG solution in liquid nitrogen.
4. Put frozen mixture in a freezer dryer and freeze dry for 24 hours or until all water is removed.
5. Dissolve freeze-dried SOD/PEG in DI water.
6. Add 50  $\mu\text{L}$  of SOD/PEG solution (250 mg/mL) to 500 mg of polyketal dissolved in 500  $\mu\text{L}$  of  $\text{CH}_2\text{Cl}_2$  solution.
7. Homogenize at level 6 or sonicate at low power for 30 seconds to make a suspension of SOD/PEG particles in the organic solvent.
8. Add first solid-in-oil emulsion to 5 mL of 5% PVA solution.
9. Homogenize at level 4 for 1 minute.
10. Add mixture to 25 mL 1% PVA solution and stir for 4 hours to evaporate organic solvent.
11. Transfer to 50 mL centrifuge tube and centrifuge at 5000 g for 15 minutes.

12. Discard supernatant and resuspend in 10 mL of DI water.
13. Centrifuge at 5000 g for 10 minutes.
14. Repeat washing once more.
15. Resuspend in 5 ml of DI water and freeze.
16. Freeze dry for 24 hours to give solid particles.

#### **A.6. SOD loading and activities assays for SOD-loaded PK3 microparticles**

1. Make SOD standards using SOD stock and dilution buffer.

200 U/mL	50 U/mL	5 U/mL	1 U/mL	0.1 U/mL	Blank	SOD PKM (2mg/mL)
----------	---------	--------	--------	----------	-------	---------------------

2. Weight 2 mg of SOD-loaded PK3 microparticles and dissolve in 500  $\mu$ L of DCM in a small vial.
3. Place the vial in 60°C oil bath and allow DCM to evaporate
4. Add mixture to 1 mL of dilution buffer provided in the SOD kit
5. Place content in a centrifugation tube and centrifuge at 5000 g for 1 minute to separate the polymer from SOD.
6. Preparation of BCA working reagent (WR)
  - a. (10 unknowns) \* (150  $\mu$ L of WR per sample) = 1.5 mL, so make 2 mL of WR
7. Prepare fresh WR by mixing 25 parts of Micro BCA reagent MA and 24 parts reagent MB with 1 part of reagent MC, so combine 1 mL of MA and 0.96 mL of MB and 0.04 mL of MC.
8. Pipette 150  $\mu$ L of unknown sample in to a 96-well cell culture plate.

9. Add 150  $\mu\text{L}$  of the WR to each well and mix plate thoroughly on a plate shaker for 30 seconds.
10. Cover plate and incubate at 37  $^{\circ}\text{C}$  for 2 hours.
11. Cool plate to room temperature.
12. Measure the absorbance at or near 562 nm on a plate reader.
13. Subtract the average 562 nm absorbance reading of the blank standard replicates from the 562 nm reading of all other individual standard and unknown samples.
14. For measuring activities of SOD in the standards and unknown samples, add 20  $\mu\text{L}$  of sample solutions to a well in a 96-well cell culture plate.
15. Add 200  $\mu\text{L}$  of WST and 20  $\mu\text{L}$  of enzyme working solution to each well.
16. Read absorbance at 450 nm using a micro-plate reader for 10 minutes (60 readings) on kinetic mode.

#### **A.7. *In vivo* studies with SOD-loaded PK3 microparticles**

1. Place order for mice.
2. Label each cage (3 mice/cage) and tag the mice.
3. Set up anesthesia and surgical equipment.
4. Anesthetize mice one at a time.
5. Prepare the mice one at a time for jugular vein injection by removing hair in the chest area and cleaning the area with ethanol.
6. Inject 100  $\mu\text{L}$  of SOD-loaded PK3 microparticles (1mg/mL), free SOD, empty particles, or saline, into the jugular vein.
7. Inject 100  $\mu\text{L}$  LPS/GalN
8. Put mice back to cage and let them recover

9. Put cages back to the mice room and observe the mice regularly.
10. After 24 hours, check the mice and prepare for blood collection.
11. Prepare the needle by washing it in histamine solution.
12. Anesthetize mice one at a time.
13. Insert a needle from underneath the rib cage.
14. Thrust the needle towards the chest in a swift motion.
15. Try drawing blood while slowly withdrawing the needle.
16. Once the needle is in the heart, blood will come out and fill the syringe.
17. Once enough blood is collected ( $>400 \mu\text{L}$ ), put the blood in a heparin/gel treated blood collection tube.
18. Shake the tube to prevent coagulation.
19. After 5-10 minutes, centrifuge the tube at 4,000 RPM for 15 minutes.
20. Store the sample in fridge for ALT analysis.
21. Analyze ALT level using a ALT reagent set (Pointe Scientific).
22. Isolate the liver and put in OCT for histological analysis.

#### **A.8. Procedures for ALT measurements using ALT kit from Point Scientific.**

1. Prepare working reagent. For each sample to be measured, prepare a separate tube of working reagent. The total volume of the reagent should be 1mL and the composition of the working reagent should be as follows:
  - a. 5 parts reagent 1  $\Rightarrow$  833 $\mu\text{L}$
  - b. 1 part reagent 2  $\Rightarrow$  166 $\mu\text{L}$
2. Incubate working reagent solution and serum in 37°C bath for 10-15 minutes.
3. Turn on spectrophotometer. Zero the meter with water at 340nm.

4. Transfer 50 $\mu$ L of serum into the first tube of reagent.
5. Vortex mixture of serum and reagent for 5-10 seconds.
6. Transfer mixture into cuvette and measure absorbance at 340 nm over 90 seconds.
7. Select the most linear portion of the curve should be towards the beginning) and perform the following calculations with that data to determine ALT.
8. Repeat steps 4-7 for the rest of the samples.
9. Calculate ALT value using the following equation

$$\text{ALT (U/L)} = \Delta\text{ABS/Minute} \times 3536$$

#### **A.9. Procedure for TNF- $\alpha$ measurement using ELISA kit from eBiosciences**

1. Using Assay diluent, dilute standards.
2. Add 25  $\mu$ L/well of serum and 75 $\mu$ L of Assay Diluent to the wells.
3. Cover and seal the plate and incubate at room temp for 2 hours or overnight at 4 $^{\circ}$ C.
4. Aspirate wells and wash 5 times with >250  $\mu$ L/well of Wash Buffer that are diluted to 1X. Allow at least 1 min for soaking during each wash step. Blot plate on absorbent pad to remove any residual buffer.
5. Add 100 $\mu$ L/well of detection antibody diluted in 1X assay Diluent (as noted on Certificate of Analysis). Seal the plate and incubate at room temperature for 1 hour
6. Aspirate and wash for 5 times as in step 5.
7. Add 100  $\mu$ L/well of Avidin-HRP diluted in 1X Assay Diluent (noted in C of A). Seal the plate and incubate at room temp for 30 min.

8. Aspirate and wash as in step 5. In this wash step, soak wells in Wash Buffer for 1 to 2 minutes prior to aspiration. Repeat for 7 times.
9. Add 100  $\mu\text{L}$ /well of substrate solution to each well. Incubate for 15 min at room temp.
10. Add 50  $\mu\text{L}$ /well of Stop Solution to each well.
11. Read plate at 450 nm, subtract 570 nm reading from 450 nm reading and analyze data.

#### **A.10. Biodistribution studies of PK3 microparticles in mice.**

1. Place order for mice.
2. Re-suspend the PK3 microparticles in saline at concentration of 1 mg/mL
3. Set up anesthesia and surgical equipment.
4. Anesthetize mice one at a time
5. Prepare the mice one at a time for jugular vein injection by removing hair in the chest area and cleaning the area with ethanol.
6. Inject 100  $\mu\text{L}$  of fluorescein-loaded PK3 microparticles (1mg/mL), pentacene-loaded PK3 microparticles, empty particles, or saline, into the jugular vein.
7. Put mice back to cage and let them recover
8. Put cages back to the mice room and observe the mice regularly.
9. After 2 hours, anesthetize the mice injected with pentacene-loaded PK3 microparticles and image with Xenogen imaging machine.
10. For mice injected with fluorescein-loaded PK3 microparticles, empty microparticles, or saline, check the mice and prepare for blood collection

11. Prepare the needle by washing it in histamine solution.
12. Anesthetize mice one at a time
13. Insert a needle from underneath the rib cage
14. Thrust the needle towards the chest in a swift motion
15. Try draw blood while slowly withdrawing the needle
16. Once the needle is in the heart, blood will come out and fill the syringe
17. Once enough blood is collected ( $>400 \mu\text{L}$ ), put the blood in a heparin/gel treated blood collection tube.
18. Shake the tube to prevent coagulation.
19. After 5-10 minutes, centrifuge the tube at 4,000 rpm for 15 minutes.
20. Perfuse with PBS and isolate the heart, liver, spleen, kidney, and lung for analysis.
21. Weigh the organs, and place them in 1 mL of Triton X100 + 4 mL of PBS.
22. Homogenize at level 3 with Powergen 500 homogenizer.
23. Centrifuge at 10000 X g for 10 minutes.
24. Add 1 mL of homogenate to 2 mL of PBS and measure emission from 505 – 550 nm (excitation = 495 nm).
25. Record data and use 518 nm emission to determine FITC concentration.



## REFERENCES

- 1 Adachi, Y., B. U. Bradford, et al. (1994) Inactivation of Kupffer cells prevents early alcohol-induced liver injury. *Hepatology* 20, 453-60.
- 2 Al-Azzam, W., E. A. Pastrana, et al. (2002) Co-lyophilization of bovine serum albumin (BSA) with poly(ethylene glycol) improves efficiency of BSA encapsulation and stability in polyester microspheres by a solid-in-oil-in-oil technique. *Biotechnology Letters* 24, 1367-1374.
- 3 Anderson, J. M. and M. S. Shive. (1997) Biodegradation and biocompatibility of PLA and PLGA microspheres. *Advanced Drug Delivery Reviews* 28, 5.
- 4 Ando, S., D. Putnam, et al. (1999) PLGA microspheres containing plasmid DNA: preservation of supercoiled DNA via cryopreparation and carbohydrate stabilization. *J Pharm Sci* 88, 126-30.
- 5 Angus, D. C., W. T. Linde-Zwirble, et al. (2001) Epidemiology of severe sepsis in the United States: Analysis of incidence, outcome, and associated costs of care. *Critical Care Medicine* 29, 1303-1310.
- 6 Barton, B. E. and J. V. Jackson. (1993) Protective role of interleukin 6 in the lipopolysaccharide-galactosamine septic shock model. *Infect Immun* 61, 1496-9.
- 7 Bedda, S., A. Laurent, et al. (2003) Mangafodipir prevents liver injury induced by acetaminophen in the mouse. *J Hepatol* 39, 765-72.
- 8 Bilir, B. M., D. Guinette, et al. (2000) Hepatocyte transplantation in acute liver failure. *Liver Transpl* 6, 32-40.
- 9 Bilzer, M., F. Roggel, et al. (2006) Role of Kupffer cells in host defense and liver disease. *Liver International* 26, 1175-1186.
- 10 Briscoe, P., I. Caniggia, et al. (1995) Delivery of superoxide dismutase to pulmonary epithelium via pH-sensitive liposomes. *Am J Physiol* 268, L374-80.
- 11 Cadee, J. A., L. A. Brouwer, et al. (2001) A comparative biocompatibility study of microspheres based on crosslinked dextran or poly(lactic-co-glycolic)acid after subcutaneous injection in rats. *J Biomed Mater Res* 56, 600-9.
- 12 Capancioni, S., K. Schwach-Abdellaoui, et al. (2003) In Vitro Monitoring of Poly(ortho ester) Degradation by Electron Paramagnetic Resonance Imaging. *Macromolecules* 36, 6135-6141.

- 13 Carrasquillo, K. G., A. M. Stanley, et al. (2001) Non-aqueous encapsulation of excipient-stabilized spray-freeze dried BSA into poly(lactide-co-glycolide) microspheres results in release of native protein. *J Control Release* 76, 199-208.
- 14 Castellanos, I. J., K. G. Carrasquillo, et al. (2001) Encapsulation of bovine serum albumin in poly(lactide-co-glycolide) microspheres by the solid-in-oil-in-water technique. *Journal of Pharmacy and Pharmacology* 53, 167-178.
- 15 Castellanos, I. J., R. Crespo, et al. (2003) Poly(ethylene glycol) as stabilizer and emulsifying agent: a novel stabilization approach preventing aggregation and inactivation of proteins upon encapsulation in bioerodible polyester microspheres. *J Control Release* 88, 135-45.
- 16 Celik, O. and J. Akbuga. (2007) Preparation of superoxide dismutase loaded chitosan microspheres: characterization and release studies. *Eur J Pharm Biopharm* 66, 42-7.
- 17 Coen, M., Y. S. Hong, et al. (2007) The mechanism of galactosamine toxicity revisited; a metabonomic study. *J Proteome Res* 6, 2711-9.
- 18 Coombes, A. G., S. Tasker, et al. (1997) Biodegradable polymeric microparticles for drug delivery and vaccine formulation: the surface attachment of hydrophilic species using the concept of poly(ethylene glycol) anchoring segments. *Biomaterials* 18, 1153-61.
- 19 Cordes, E. H. and H. Bull. (1974) Mechanism and catalysis for hydrolysis of acetals, ketals, and ortho esters. *Chemical Reviews* 74, 581.
- 20 Costantino, H. R., L. Firouzabadian, et al. (2000) Protein spray-freeze drying. Effect of atomization conditions on particle size and stability. *Pharmaceutical Research* 17, 1374-1383.
- 21 Crofton, R. W., M. M. Diesselhoff-den Dulk, et al. (1978) The origin, kinetics, and characteristics of the Kupffer cells in the normal steady state. *J Exp Med* 148, 1-17.
- 22 Cuzzocrea, S., E. Mazzon, et al. (2001) Protective effects of a new stable, highly active SOD mimetic, M40401 in splanchnic artery occlusion and reperfusion. *Br J Pharmacol* 132, 19-29.
- 23 Cuzzocrea, S., C. Thiemermann, et al. (2004) Potential therapeutic effect of antioxidant therapy in shock and inflammation. *Curr Med Chem* 11, 1147-62.
- 24 Dailey, L. A., N. Jekel, et al. (2006) Investigation of the proinflammatory potential of biodegradable nanoparticle drug delivery systems in the lung. *Toxicol Appl Pharmacol* 215, 100-8.

- 25 Dang, W., T. Daviau, et al. (1996) Morphological Characterization of Polyanhydride Biodegradable Implant Gliadel® During in Vitro and in Vivo Erosion Using Scanning Electron Microscopy. *Pharmaceutical Research* 13, 683-691.
- 26 Decker, K. (1990) Biologically active products of stimulated liver macrophages (Kupffer cells). *Eur J Biochem* 192, 245-61.
- 27 Decker, T., M. L. Lohmann-Matthes, et al. (1989) Comparative study of cytotoxicity, tumor necrosis factor, and prostaglandin release after stimulation of rat Kupffer cells, murine Kupffer cells, and murine inflammatory liver macrophages. *J Leukoc Biol* 45, 139-46.
- 28 Deininger, M. W. N. and B. J. Druker. (2003) Specific Targeted Therapy of Chronic Myelogenous Leukemia with Imatinib. *Pharmacol Rev* 55, 401-423.
- 29 Diesselhoff-den Dulk, M. M., R. W. Crofton, et al. (1979) Origin and kinetics of Kupffer cells during an acute inflammatory response. *Immunology* 37, 7-14.
- 30 DiVincenzo, G. D. and D. A. Ziegler. (1980) Metabolic fate of 1,4-cyclo[14C]hexanedimethanol in rats. *Toxicol Appl Pharmacol* 52, 10-5.
- 31 Droge, W. (2002) Free radicals in the physiological control of cell function. *Physiol Rev* 82, 47-95.
- 32 Dunn, S. E., A. G. A. Coombes, et al. (1997) In vitro cell interaction and in vivo biodistribution of poly(lactide-co-glycolide) nanospheres surface modified by poloxamer and poloxamine copolymers. *Journal of Controlled Release* 44, 65-76.
- 33 Dunne, M., I. Corrigan, et al. (2000) Influence of particle size and dissolution conditions on the degradation properties of polylactide-co-glycolide particles. *Biomaterials* 21, 1659-68.
- 34 Feng, S. S., G. Ruan, et al. (2004) Fabrication and characterizations of a novel drug delivery device liposomes-in-microsphere (LIM). *Biomaterials* 25, 5181-9.
- 35 Ferret, P. J., R. Hammoud, et al. (2001) Detoxification of reactive oxygen species by a nonpeptidyl mimic of superoxide dismutase cures acetaminophen-induced acute liver failure in the mouse. *Hepatology* 33, 1173-80.
- 36 Freed, L. E., G. Vunjak-Novakovic, et al. (1994) Biodegradable polymer scaffolds for tissue engineering. *Biotechnology (N Y)* 12, 689-93.
- 37 Frein, D., S. Schildknecht, et al. (2005) Redox regulation: a new challenge for pharmacology. *Biochem Pharmacol* 70, 811-23.

- 38 Fu, K., D. W. Pack, et al. (2000) Visual Evidence of Acidic Environment Within Degrading Poly(lactic-co-glycolic acid) (PLGA) Microspheres. *Pharmaceutical Research* 17, 100.
- 39 Fujiwara, N. and K. Kobayashi. (2005) Macrophages in Inflammation. *Current Drug Targets - Inflammation & Allergy* 4, 281-286.
- 40 Gilmore, T. D. and M. Herscovitch. (2006) Inhibitors of NF-kappaB signaling: 785 and counting. *Oncogene* 25, 6887-99.
- 41 Giovagnoli, S., P. Blasi, et al. (2004) Biodegradable microspheres as carriers for native superoxide dismutase and catalase delivery. *AAPS PharmSciTech* 5, e51.
- 42 Giovagnoli, S., G. Luca, et al. (2005) Long-term delivery of superoxide dismutase and catalase entrapped in poly(lactide-co-glycolide) microspheres: In vitro effects on isolated neonatal porcine pancreatic cell clusters. *Journal of Controlled Release* 107, 65-77.
- 43 Goodman, R. B., J. Pugin, et al. (2003) Cytokine-mediated inflammation in acute lung injury. *Cytokine & Growth Factor Reviews* 14, 523-535.
- 44 Gopferich, A. (1996) Mechanisms of polymer degradation and erosion. *Biomaterials* 17, 103.
- 45 Gopferich, A. and J. Tessmar. (2002) Polyanhydride degradation and erosion. *Advanced Drug Delivery Reviews* 54, 911.
- 46 Gref, R., Y. Minamitake, et al. (1994) Biodegradable long-circulating polymeric nanospheres. *Science* 263, 1600-3.
- 47 Heffernan, M. J. and N. Murthy. (2005) Polyketal Nanoparticles: A New pH-Sensitive Biodegradable Drug Delivery Vehicle. *Bioconjugate Chem.* 16, 1340-1342.
- 48 Heller, J. (1984) Biodegradable polymers in controlled drug delivery. *Crit Rev Ther Drug Carrier Syst* 1, 39-90.
- 49 Heller, J. and J. Barr. (2004) Poly(ortho esters)--from concept to reality. *Biomacromolecules* 5, 1625-32.
- 50 Heller, J., J. Barr, et al. (2002) Poly(ortho esters): synthesis, characterization, properties and uses. *Adv Drug Deliv Rev* 54, 1015-39.
- 51 Higuchi, Y., S. Kawakami, et al. (2006) Intravenous administration of mannosylated cationic liposome/NFkappaB decoy complexes effectively prevent

- LPS-induced cytokine production in a murine liver failure model. *FEBS Lett* 580, 3706-14.
- 52 Higuchi, Y., S. Kawakami, et al. (2007) The potential role of fucosylated cationic liposome/NF[ $\kappa$ ]B decoy complexes in the treatment of cytokine-related liver disease. *Biomaterials* 28, 532-539.
- 53 Hirai, K., R. Hattori, et al. (1999). Image-forming method. Application: EP EP, (Konica Corporation, Japan; Konishiroku Photo Ind.). 64 pp.
- 54 Hitchon, C. A. and H. S. El-Gabalawy. (2004) Oxidation in rheumatoid arthritis. *Arthritis Res Ther* 6, 265-78.
- 55 Hoek, J. B. and J. G. Pastorino. (2002) Ethanol, oxidative stress, and cytokine-induced liver cell injury. *Alcohol* 27, 63-8.
- 56 Hudson, L. D. and K. P. Steinberg. (1999) Epidemiology of Acute Lung Injury and ARDS. *Chest* 116, 74S-a-82.
- 57 Ignatius, A. A. and L. E. Claes. (1996) In vitro biocompatibility of bioresorbable polymers: poly(L, DL-lactide) and poly(L-lactide-co-glycolide). *Biomaterials* 17, 831-9.
- 58 Itoh, Y., M. Matsusaki, et al. (2006) Enzyme-responsive release of encapsulated proteins from biodegradable hollow capsules. *Biomacromolecules* 7, 2715-8.
- 59 Jaeschke, H., G. J. Gores, et al. (2002) Mechanisms of hepatotoxicity. *Toxicol Sci* 65, 166-76.
- 60 Jain, R., S. M. Standley, et al. (2007) Synthesis and Degradation of pH-Sensitive Linear Poly(amidoamine)s. *Macromolecules* 40, 452-457.
- 61 Jian Wu, L. L. R. D. Y. A. C. M. H. N. M. A. Z. (2004) Liposome-mediated extracellular superoxide dismutase gene delivery protects against acute liver injury in mice. *Hepatology* 40, 195-204.
- 62 Jones, A. L. (1998) Mechanism of action and value of N-acetylcysteine in the treatment of early and late acetaminophen poisoning: a critical review. *J Toxicol Clin Toxicol* 36, 277-85.
- 63 Kamata, H., S. Honda, et al. (2005) Reactive oxygen species promote TNF $\alpha$ -induced death and sustained JNK activation by inhibiting MAP kinase phosphatases. *Cell* 120, 649-61.
- 64 Kerkela, R., L. Grazette, et al. (2006) Cardiotoxicity of the cancer therapeutic agent imatinib mesylate. *Nat Med* 12, 908-916.

- 65 Kilgore, K. S., G. S. Friedrichs, et al. (1994) Protective effects of the SOD-mimetic SC-52608 against ischemia/reperfusion damage in the rabbit isolated heart. *J Mol Cell Cardiol* 26, 995-1006.
- 66 Kinnula, V. L. and J. D. Crapo. (2003) Superoxide dismutases in the lung and human lung diseases. *Am J Respir Crit Care Med* 167, 1600-19.
- 67 Kohane, D. S., J. Y. Tse, et al. (2006) Biodegradable polymeric microspheres and nanospheres for drug delivery in the peritoneum. *J Biomed Mater Res A* 77, 351-61.
- 68 Kono, H., I. Rusyn, et al. (2001) Diphenyleneiodonium sulfate, an NADPH oxidase inhibitor, prevents early alcohol-induced liver injury in the rat. *Am J Physiol Gastrointest Liver Physiol* 280, G1005-12.
- 69 Kono, H., I. Rusyn, et al. (2000) NADPH oxidase-derived free radicals are key oxidants in alcohol-induced liver disease. *J Clin Invest* 106, 867-72.
- 70 Konorev, E. A., M. C. Kennedy, et al. (1999) Cell-permeable superoxide dismutase and glutathione peroxidase mimetics afford superior protection against doxorubicin-induced cardiotoxicity: the role of reactive oxygen and nitrogen intermediates. *Arch Biochem Biophys* 368, 421-8.
- 71 Kumar, N., R. S. Langer, et al. (2002) Polyanhydrides: an overview. *Advanced Drug Delivery Reviews* 54, 889.
- 72 Kumar, T. R., K. Soppimath, et al. (2006) Novel delivery technologies for protein and peptide therapeutics. *Curr Pharm Biotechnol* 7, 261-76.
- 73 Kwon, Y. J., E. James, et al. (2005) In vivo targeting of dendritic cells for activation of cellular immunity using vaccine carriers based on pH-responsive microparticles. *Proc Natl Acad Sci U S A* 102, 18264-8.
- 74 Kwon, Y. J., S. M. Standley, et al. (2005) Directed Antigen Presentation Using Polymeric Microparticulate Carriers Degradable at Lysosomal pH for Controlled Immune Responses. *Mol. Pharmaceutics* 2, 83-91.
- 75 Landis, G. N. and J. Tower. (2005) Superoxide dismutase evolution and life span regulation. *Mech Ageing Dev* 126, 365-79.
- 76 Landmann, R., F. Scherer, et al. (1995) LPS directly induces oxygen radical production in human monocytes via LPS binding protein and CD14. *J Leukoc Biol* 57, 440-9.
- 77 Langer, R. (1998) Drug delivery and targeting. *Nature* 392, 5-10.

- 78 Laursen, J. B., S. Rajagopalan, et al. (1997) Role of superoxide in angiotensin II-induced but not catecholamine-induced hypertension. *Circulation* 95, 588-93.
- 79 Lee, S., S. C. Yang, et al. (2007) Polyketal Microparticles: A New Delivery Vehicle for Superoxide Dismutase. *Bioconjugate Chem.* 18, 4-7.
- 80 Lehmann, T. G., M. D. Wheeler, et al. (2003) Effects of three superoxide dismutase genes delivered with an adenovirus on graft function after transplantation of fatty livers in the rat. *Transplantation* 76, 28-37.
- 81 Lehmann, V., M. A. Freudenberg, et al. (1987) Lethal toxicity of lipopolysaccharide and tumor necrosis factor in normal and D-galactosamine-treated mice. *J Exp Med* 165, 657-63.
- 82 Li, N. and M. Karin. (1999) Is NF-kappaB the sensor of oxidative stress? *FASEB J* 13, 1137-43.
- 83 Lieber, A., C. Y. He, et al. (1997) The role of Kupffer cell activation and viral gene expression in early liver toxicity after infusion of recombinant adenovirus vectors. *J Virol* 71, 8798-807.
- 84 Limaye, P. B., U. M. Apte, et al. (2003) Calpain released from dying hepatocytes mediates progression of acute liver injury induced by model hepatotoxicants. *Toxicol Appl Pharmacol* 191, 211-26.
- 85 Liu, L., Y. Ge, et al. (2003) Stability of rhCu, Zn-SOD encapsulated in poly(lactide-co-glycolide) microspheres. *Zhongguo Yaoxue Zazhi (Beijing, China)* 38, 190-193.
- 86 Liu, L. M., J. X. Zhang, et al. (2008) A role of cell apoptosis in lipopolysaccharide (LPS)-induced nonlethal liver injury in D-galactosamine (D-GalN)-sensitized rats. *Dig Dis Sci* 53, 1316-24.
- 87 Liu, P., Y. Hu, et al. (2001) Effects of salviainolic acid A (SA-A) on liver injury: SA-A action on hepatic peroxidation. *Liver* 21, 384-90.
- 88 Liu, S. F. and A. B. Malik. (2006) NF-kappa B activation as a pathological mechanism of septic shock and inflammation. *Am J Physiol Lung Cell Mol Physiol* 290, L622-L645.
- 89 Luisa Corvo, M., J. C. Jorge, et al. (2002) Superoxide dismutase entrapped in long-circulating liposomes: formulation design and therapeutic activity in rat adjuvant arthritis. *Biochim Biophys Acta* 1564, 227-36.

- 90 Maa, Y. F. and C. C. Hsu. (1997) Effect of primary emulsions on microsphere size and protein-loading in the double emulsion process. *Journal of Microencapsulation* 14, 225-241.
- 91 Malassagne, B., P. J. Ferret, et al. (2001) The superoxide dismutase mimetic MnTBAP prevents Fas-induced acute liver failure in the mouse. *Gastroenterology* 121, 1451-9.
- 92 Michael, S. L., N. R. Pumford, et al. (1999) Pretreatment of mice with macrophage inactivators decreases acetaminophen hepatotoxicity and the formation of reactive oxygen and nitrogen species. *Hepatology* 30, 186-95.
- 93 Middleton, J. C. and A. J. Tipton. (2000) Synthetic biodegradable polymers as orthopedic devices. *Biomaterials* 21, 2335-46.
- 94 Mignon, A., N. Rouquet, et al. (1999) LPS challenge in D-galactosamine-sensitized mice accounts for caspase-dependent fulminant hepatitis, not for septic shock. *Am J Respir Crit Care Med* 159, 1308-15.
- 95 Morita, T., Y. Sakamura, et al. (2000) Protein encapsulation into biodegradable microspheres by a novel S/O/W emulsion method using poly(ethylene glycol) as a protein micronization adjuvant. *Journal of Controlled Release* 69, 435-444.
- 96 Murthy, N., J. Campbell, et al. (2003) Design and synthesis of pH-responsive polymeric carriers that target uptake and enhance the intracellular delivery of oligonucleotides. *J Control Release* 89, 365-74.
- 97 Nakae, D., K. Yamamoto, et al. (1990) Liposome-encapsulated superoxide dismutase prevents liver necrosis induced by acetaminophen. *Am J Pathol* 136, 787-95.
- 98 Nakaoka, R., Y. Tabata, et al. (1997) Prolongation of the serum half-life period of superoxide dismutase by poly(ethylene glycol) modification. *Journal of Controlled Release* 46, 253-261.
- 99 O'Grady, J. G. and S. W. Schalm. (1993) Acute liver failure: Redefining the syndromes. *Lancet* 342, 273.
- 100 Ogushi, I., Y. Iimuro, et al. (2003) Nuclear factor  $\kappa$ B decoy oligodeoxynucleotides prevent endotoxin-induced fatal liver failure in a murine model. *Hepatology* 38, 335-344.
- 101 Okado-Matsumoto, A. and I. Fridovich. (2001) Subcellular distribution of superoxide dismutases (SOD) in rat liver: Cu,Zn-SOD in mitochondria. *J Biol Chem* 276, 38388-93.



- 102 Ozden, T. A., H. Uzun, et al. (2004) The effects of hyperbaric oxygen treatment on oxidant and antioxidants levels during liver regeneration in rats. *Tohoku J Exp Med* 203, 253-65.
- 103 Pagliara, P., E. C. Carla, et al. (2003) Kupffer cells promote lead nitrate-induced hepatocyte apoptosis via oxidative stress. *Comp Hepatol* 2, 8.
- 104 Pahl, H. L. (1999) Activators and target genes of Rel/NF-kappaB transcription factors. *Oncogene* 18, 6853-66.
- 105 Palmer, L. A., A. Doctor, et al. (2007) S-nitrosothiols signal hypoxia-mimetic vascular pathology. *J Clin Invest* 117, 2592-601.
- 106 Pande, V. and M. J. Ramos. (2005) NF-kappaB in human disease: current inhibitors and prospects for de novo structure based design of inhibitors. *Curr Med Chem* 12, 357-74.
- 107 Papisov, M. I. (2001) Acyclic polyacetals from polysaccharides: biomimetic biomedical "stealth" polymers. *ACS Symposium Series* 786, 301-314.
- 108 Patrick J. Ginty, S. M. H., Felicity R.A.J. Rose, Kevin M. Shakesheff (2006). An Assessment of the Role of Polymers for Drug Delivery in Tissue Engineering. Polymers in Drug Delivery. A. S. Ijeoma Uchegbu. Boca Raton, CRC Press: 63-75.
- 109 Perez, C., I. J. Castellanos, et al. (2002) Recent trends in stabilizing protein structure upon encapsulation and release from bioerodible polymers. *J Pharm Pharmacol* 54, 301-13.
- 110 Polson, J. and W. M. Lee. (2005) AASLD position paper: the management of acute liver failure. *Hepatology* 41, 1179-97.
- 111 Putney, S. D. and P. A. Burke. (1998) Improving protein therapeutics with sustained-release formulations. *Nature Biotechnology* 16, 153-157.
- 112 Reilly, T. P., J. N. Brady, et al. (2001) A protective role for cyclooxygenase-2 in drug-induced liver injury in mice. *Chem Res Toxicol* 14, 1620-8.
- 113 Rosen, H. B., J. Chang, et al. (1983) Bioerodible polyanhydrides for controlled drug delivery. *Biomaterials* 4, 131-3.
- 114 Roux, E., M. Francis, et al. (2002) Polymer based pH-sensitive carriers as a means to improve the cytoplasmic delivery of drugs. *Int J Pharm* 242, 25-36.
- 115 Sah, H. (1999) Protein behavior at the water/methylene chloride interface. *Journal of Pharmaceutical Sciences* 88, 1320-1325.

- 116 Sasada, M., M. J. Pabst, et al. (1983) Activation of mouse peritoneal macrophages by lipopolysaccharide alters the kinetic parameters of the superoxide-producing NADPH oxidase. *J Biol Chem* 258, 9631-5.
- 117 Schumann, J., D. Wolf, et al. (2000) Importance of Kupffer cells for T-cell-dependent liver injury in mice. *Am J Pathol* 157, 1671-83.
- 118 Schwendeman, S. P. (2002) Recent advances in the stabilization of proteins encapsulated in injectable PLGA delivery systems. *Critical Reviews in Therapeutic Drug Carrier Systems* 19, 73-98.
- 119 Sheff, D. (2004) Endosomes as a route for drug delivery in the real world. *Adv Drug Deliv Rev* 56, 927-30.
- 120 Soppimath, K. S., T. M. Aminabhavi, et al. (2001) Biodegradable polymeric nanoparticles as drug delivery devices. *Journal of Controlled Release* 70, 1-20.
- 121 Spenlehauer, G., M. Vert, et al. (1989) In vitro and in vivo degradation of poly(D,L lactide/glycolide) type microspheres made by solvent evaporation method. *Biomaterials* 10, 557-63.
- 122 Su, G. L. (2002) Lipopolysaccharides in liver injury: molecular mechanisms of Kupffer cell activation. *Am J Physiol Gastrointest Liver Physiol* 283, G256-65.
- 123 Tabata, Y., S. Gutta, et al. (1993) Controlled Delivery Systems for Proteins Using Polyanhydride Microspheres. *Pharmaceutical Research* 10, 487-496.
- 124 Tamada, J. and R. Langer. (1992) The development of polyanhydrides for drug delivery applications. *J Biomater Sci Polym Ed* 3, 315-53.
- 125 Tamada, J. A. and R. Langer. (1993) Erosion kinetics of hydrolytically degradable polymers. *Proc Natl Acad Sci U S A* 90, 552-6.
- 126 Tamber, H., P. Johansen, et al. (2005) Formulation aspects of biodegradable polymeric microspheres for antigen delivery. *Adv Drug Deliv Rev* 57, 357-76.
- 127 Tansey, W., S. Ke, et al. (2004) Synthesis and characterization of branched poly(L-glutamic acid) as a biodegradable drug carrier. *J Control Release* 94, 39-51.
- 128 Thiele, L., B. Rothen-Rutishauser, et al. (2001) Evaluation of particle uptake in human blood monocyte-derived cells in vitro. Does phagocytosis activity of dendritic cells measure up with macrophages? *J Control Release* 76, 59-71.

- 129 Thurman, R. G. (1998) II. Alcoholic liver injury involves activation of Kupffer cells by endotoxin. *Am J Physiol Gastrointest Liver Physiol* 275, G605-611.
- 130 Tilg, H., A. Kaser, et al. (2006) How to modulate inflammatory cytokines in liver diseases. *Liver International* 26, 1029-1039.
- 131 Tobe, M., Y. Isobe, et al. (2003) A novel structural class of potent inhibitors of NF-kappa B activation: structure-activity relationships and biological effects of 6-aminoquinazoline derivatives. *Bioorg Med Chem* 11, 3869-78.
- 132 Tomlinson, R., J. Heller, et al. (2003) Polyacetal-doxorubicin conjugates designed for pH-dependent degradation. *Bioconjug Chem* 14, 1096-106.
- 133 Tomlinson, R., M. Klee, et al. (2002) Pendent Chain Functionalized Polyacetals That Display pH-Dependent Degradation: A Platform for the Development of Novel Polymer Therapeutics. *Macromolecules* 35, 473-480.
- 134 Uchikura, K., T. Wada, et al. (2004) Lipopolysaccharides induced increases in Fas ligand expression by Kupffer cells via mechanisms dependent on reactive oxygen species. *Am J Physiol Gastrointest Liver Physiol* 287, G620-6.
- 135 Valdivia, A., Y. Perez, et al. (2005) Improved anti-inflammatory and pharmacokinetic properties for superoxide dismutase by chemical glycosidation with carboxymethylchitin. *Macromol Biosci* 5, 118-23.
- 136 van de Weert, M., W. E. Hennink, et al. (2000) Protein instability in poly(lactic-co-glycolic acid) microparticles. *Pharm Res* 17, 1159-67.
- 137 van Dijkhuizen-Radersma, R., S. C. Hesselting, et al. (2002) Biocompatibility and degradation of poly(ether-ester) microspheres: in vitro and in vivo evaluation. *Biomaterials* 23, 4719-29.
- 138 Victor, V. M., M. Rocha, et al. (2005) Role of free radicals in sepsis: antioxidant therapy. *Curr Pharm Des* 11, 3141-58.
- 139 Voter, K. Z., J. C. Whitin, et al. (2001) Ozone exposure and the production of reactive oxygen species by bronchoalveolar cells in humans. *Inhal Toxicol* 13, 465-83.
- 140 Vujaskovic, Z., I. Batinic-Haberle, et al. (2002) A small molecular weight catalytic metalloporphyrin antioxidant with superoxide dismutase (SOD) mimetic properties protects lungs from radiation-induced injury. *Free Radic Biol Med* 33, 857-63.

- 141 Wake, K. (1980) Perisinusoidal stellate cells (fat-storing cells, interstitial cells, lipocytes), their related structure in and around the liver sinusoids, and vitamin A-storing cells in extrahepatic organs. *Int Rev Cytol* 66, 303-53.
- 142 Wang, C., Q. Ge, et al. (2004) Molecularly engineered poly(ortho ester) microspheres for enhanced delivery of DNA vaccines. *Nat Mater* 3, 190-6.
- 143 Wang, Y., J. Q. Gao, et al. (2006) Biodegradable and complexed microspheres used for sustained delivery and activity protection of SOD. *J Biomed Mater Res B Appl Biomater* 79, 74-8.
- 144 Watson, P., A. T. Jones, et al. (2005) Intracellular trafficking pathways and drug delivery: fluorescence imaging of living and fixed cells. *Adv Drug Deliv Rev* 57, 43-61.
- 145 Wheeler, M. D., M. Katuna, et al. (2001) Comparison of the effect of adenoviral delivery of three superoxide dismutase genes against hepatic ischemia-reperfusion injury. *Hum Gene Ther* 12, 2167-77.
- 146 Wheeler, M. D., H. Kono, et al. (2001) The role of Kupffer cell oxidant production in early ethanol-induced liver disease. *Free Radic Biol Med* 31, 1544-9.
- 147 Wheeler, M. D., H. Kono, et al. (2001) Delivery of the Cu/Zn-superoxide dismutase gene with adenovirus reduces early alcohol-induced liver injury in rats. *Gastroenterology* 120, 1241-50.
- 148 White, C. R., T. A. Brock, et al. (1994) Superoxide and peroxynitrite in atherosclerosis. *Proc Natl Acad Sci U S A* 91, 1044-8.
- 149 Wolf, A. M., D. Wolf, et al. (2005) The kinase inhibitor imatinib mesylate inhibits TNF- $\alpha$  production in vitro and prevents TNF-dependent acute hepatic inflammation. *PNAS* 102, 13622-13627.
- 150 Wright, J. (2000). Overview of Protein Formulation and Delivery. Protein Formulation and Delivery. E. J. McNally. New York, Marcel Dekker: 1-4.
- 151 Wu, J., L. Liu, et al. (2004) Liposome-mediated extracellular superoxide dismutase gene delivery protects against acute liver injury in mice. *Hepatology* 40, 195-204.
- 152 Wullaert, A., G. van Loo, et al. (2007) Hepatic Tumor Necrosis Factor Signaling and Nuclear Factor- $\kappa$ B: Effects on Liver Homeostasis and Beyond. *Endocr Rev*, er.2006-0031.

- 153 Yabe, Y., N. Kobayashi, et al. (2001) Prevention of Neutrophil-Mediated Hepatic Ischemia/Reperfusion Injury by Superoxide Dismutase and Catalase Derivatives. *J Pharmacol Exp Ther* 298, 894-899.
- 154 Yang, S. C., M. Bhide, et al. (2008) Polyketal copolymers: a new acid-sensitive delivery vehicle for treating acute inflammatory diseases. *Bioconjug Chem* 19, 1164-9.
- 155 Yeon Hee, P., P. Hae Jeong, et al. (2006) BNP as a marker of the heart failure in the treatment of imatinib mesylate. *Cancer letters* 243, 16-22.
- 156 Yih, T. C. and M. Al-Fandi. (2006) Engineered nanoparticles as precise drug delivery systems. *J Cell Biochem* 97, 1184-90.
- 157 Zender, L., S. Hutker, et al. (2003) Caspase 8 small interfering RNA prevents acute liver failure in mice. *PNAS* 100, 7797-7802.
- 158 Zhou, Z., L. Wang, et al. (2003) A critical involvement of oxidative stress in acute alcohol-induced hepatic TNF-alpha production. *Am J Pathol* 163, 1137-46.
- 159 Zhou, Z., L. Wang, et al. (2004) Abrogation of nuclear factor-kappaB activation is involved in zinc inhibition of lipopolysaccharide-induced tumor necrosis factor-alpha production and liver injury. *Am J Pathol* 164, 1547-56.
- 160 Zima, T. and M. Kalousova. (2005) Oxidative stress and signal transduction pathways in alcoholic liver disease. *Alcohol Clin Exp Res* 29, 110S-115S.
- 161 Zvosec, D. L., S. W. Smith, et al. (2001) Adverse Events, Including Death, Associated with the Use of 1,4-Butanediol. *N Engl J Med* 344, 87-94.
- 162 Zwacka, R. M., W. Zhou, et al. (1998) Redox gene therapy for ischemia/reperfusion injury of the liver reduces AP1 and NF-kappaB activation. *Nat Med* 4, 698-704.